Blocking myeloid cell activation with ART and adjunctive methylglyoxal-bis-guanylhydrazone (MGBG) decreases SIV-associated cardiovascular pathology.

Kevin Suresh White

A thesis

submitted to the Faculty of

the department of Biology

in partial fulfillment

of the requirements for the degree of

Master of Science

Boston College

Morrissey College of Arts and Sciences
Graduate School

April 2024

Blocking myeloid cell activation with ART and adjunctive methylglyoxal-bis-guanylhydrazone (MGBG) decreases SIV-associated cardiovascular pathology.

Kevin Suresh White

Advisor: Kenneth Williams, Ph.D.

HIV-associated comorbidities including neurological disorders (HAND) and cardiovascular diseases (CVD) persist in people living with HIV (PLWH) regardless of adherence to antiretroviral therapies (ART). The development of these comorbidities correlates with increased monocyte/macrophages activation and accumulation. Studies report that the development of CVD and HAND are connected in PLWH, but few studies have examined the roles that monocyte/macrophages activation have in their co-development. We first asked how frequently CD8+ T lymphocyte depleted, SIV-infected rhesus macaques with AIDS co-developed cardiac pathology and SIV encephalitis (SIVE) compared to animals that developed CVD or SIVE alone, and animals with no significant cardiac pathology (NSF) and SIV with no encephalitis (SIVnoE) (Chapter 2). We sought to determine whether animals with concomitant CVD and SIVE had more monocyte activation, cardiac macrophages accumulation, and productively infected SIV-RNA+ and SIV- gp41+ cells in the heart and brain compared to animals with CVD or SIVE alone, and animals with NSF and SIVnoE. We found that animals with AIDS co-developed CVD and SIVE more frequently than animals developed CVD or SIVE alone, and NSF and SIVnoE. Animals with CVD and SIVE had increased biomarkers of monocyte activation, cardiac

macrophages inflammation, and productively infected macrophages in the brain. We found that the quantity of SIV-RNA+ cells in the heart was sparse compared to the brain. When detected, cardiac SIV-RNA+ cells are CD68+ and CD206+ cardiac macrophages. Levels of plasma soluble CD163 (sCD163) correlated with plasma galectin-3 (Gal-3), galectin-9, and interleukin-18 (IL-18), more so than plasma viral load. We then assessed cardiac tissues from PWLH with HIV encephalitis (HIVE) and HIV no encephalitis (HIVnoE). We found that PLWH with HIVE had more cardiac inflammation and fibrosis than PLWH with HIVnoE. These findings indicate that CVD and HAND pathogenesis are connected, and that the level of myeloid cell activation correlates with the development and severity of concomitant CVD and HAND. The findings from this study emphasize the importance that macrophages accumulation has in developing AIDS-related comorbidities. Our findings highlight the importance of targeting monocyte/macrophages activation and accumulation in future HIV therapies.

The persistence of CVD in the post-ART era suggests that ART successfully inhibits AIDS pathogenesis and HIV replication, but fails to block monocyte activation and macrophages accumulation correlated with CVD pathogenesis. We hypothesize that the optimal therapeutic approach for HIV- infection includes blocking AIDS pathogenesis and viral replication, and inhibiting monocyte/macrophages activation. Methylglyoxal-bis-guanylhydrazone (MGBG) is a polyamine biosynthesis inhibitor selectively taken up by monocytes and macrophages. MGBG treatment blocks monocyte/macrophages activation in vitro, AIDS pathogenesis, and decreases inflammation in cardiac and brain tissues of SIV-infected rhesus macaques. We asked whether animals treated with ART and adjunct

MGBG (ART+MGBG) had an additive decrease in monocyte activation and turnover, cardiac macrophages inflammation and collagen deposition compared to animals on ART, and untreated animals (Chapter 3). We found that animals on ART+MGBG had lower percentages of cardiac collagen deposition than animals on ART. Animals on ART, and ART+MGBG did not develop AIDS, and had decreased cardiac inflammation and collagen, and monocyte activation and turnover compared to untreated animals. Finally, we identified two populations of Gal-3 expressing (Gal-3+) cells in the heart, CD163+ Gal-3+ cardiac macrophages and CD163- Gal-3+ cells. Animals on ART, and ART+MGBG had decreased numbers of CD163+ Gal-3+ cardiac macrophages compared to untreated animals. All animals had similar numbers of CD163- Gal-3+ cells, and low frequencies of SIV-RNA+ cardiac macrophages regardless of treatment. These data suggests that blocking AIDS pathogenesis with ART, and ART+MGBG correlates with decreased monocyte activation and cardiac inflammation and collagen deposition. Overall, we did not find an additive effect in animals on ART+MGBG compared to animals on ART. Our findings show how targeting monocyte/macrophages activation with ART+MGBG blocks AIDS pathogenesis and decreases cardiac macrophages inflammation. This study demonstrates the advantages of therapeutic strategies blocking myeloid cell activation in conjunction with ART.

Table of Contents

List of Tables

List of Figures

Acknowledgments

Firstly, I would like to acknowledge my supervisor Dr. Kenneth Williams for his patience and funding which made this work possible. Secondly, I want to thank the members of my thesis committee, Dr. Welkin Johnson and Dr. Ismael Ben Fofana for their support throughout the completion of this thesis. Thanks to Dr. Andrew Miller, Dr. Woong-Ki Kim, Dr. Marco Salemi, Dr. Tricia Burdo, and the staff at the Tulane National Primate Research Center for their continued collaboration and scientific input. I am grateful to my colleagues (past and present) in Dr. William's lab, Boston College's Biology department faculty, and fellow graduate students for their engaging conversations and time.

Thanks to Arsenal Football Club and every geopolitical/history podcast available, for the near- endless entertainment and sanity checks over the years. COYG! Most importantly, I would like to extend a special thanks to my wonderful and supportive parents, Ronnie and Vasugi White, my partner Chai, my brother Ali, and the rest of my friends and family for their endless support and understanding during my time at Boston College. I am extremely thankful for each and every one of you!

List of Abbreviations

AIDS	Acquired Immunodeficiency Syndrome
ANI	Asymptomatic Neurocognitive Impairment
ANOVA	Analysis of Variance
ART	Antiretroviral Therapy
ART+MGBG	Antiretroviral therapy with adjunctive methylglyoxal-bis-guanylhydrazone
BrdU	5-bromo-2'-deoxyuridine
CCL2	C-C motif chemokine Ligand 2
CCR2	C-C motif chemokine Receptor 2
CCR5	C-C motif chemokine Receptor 5
CNS	Central Nervous System
CSF	Cerebrospinal Fluid
CVD	Cardiovascular Diseases
CXCR4	C-X-C motif chemokine Receptor 4
DAB	3,3' -diaminobenzidine tetrahydrochloride
DMF	Dimethyl Fumarate
dpi	Days' Post-Infection
ECMV	Encephalomyocarditis Virus
G-CSF	Granulocyte-Colony Stimulating Factor
Gal-3	Galectin-3
HAD	HIV-associated Dementia
HAND	HIV-associated Neurocognitive Disorder
H & E	Hematoxylin and Eosin
HIV	Human Immunodeficiency Virus
HIVE	Human Immunodeficiency Virus Encephalitis

HIVnoE	Human Immunodeficiency Virus with no Encephalitis
IFN-α	Interferon alpha
IFN-γ	Interferon gamma
IL-18	Interleukin-18
i.v.	Intravenous
LPS	Lipopolysaccharides
MCP-1	Monocyte Chemoattractant Protein-1
MGBG	Methylglyoxal-bis-guanylhydrazone
MGNC	Multinucleated Giant Cell
MHC II	Major Histocompatibility Complex class II
MND	Mild Neurocognitive Disorder
NSF	No Significant Findings (in cardiac tissues)
NT-proBNP	N-Terminal prohormone of Brain Natriuretic Peptide
OPN	Osteopontin
PLWH	People Living With HIV
RT	Reverse Transcription
sCD14	Soluble CD14
sCD163	Soluble CD163
SEM	Standard Error of the Mean
SIV	Simian Immunodeficiency Virus
SIVE	Simian Immunodeficiency Virus Encephalitis
SIVnoE	Simian Immunodeficiency Virus with no Encephalitis
subQ	Subcutaneously
TGF-β	Transforming Growth Factor-beta
TNF-α	Tumor Necrosis Factor alpha

1.0 Introduction

1.1 Epidemiology and clinical progression of HIV- infection

Human immunodeficiency virus (HIV-) infection is a leading cause of disease globally with approximately 37.7 million people living with HIV (PLWH). HIV-infection is characterized by the depletion of CD4+ T lymphocytes in the blood and gut, and the infection of cells co-expressing CD4 and chemokine receptors C-C motif chemokine Receptor 5 (CCR5) or C-X-C motif chemokine Receptor 4 (CXCR4) including, monocytes and macrophages[9, 10]. In the pre- antiretroviral therapy (ART) era, the progression of HIV-infection is best characterized in three phases: acute infection (0- 12 weeks), asymptomatic infection (1-7 years), and finally, acquired immunodeficiency syndrome (AIDS) (> 7 years)[8] **(Figure 1.1)**. During the acute phase of HIV-infection, plasma viral load increases drastically ($10^5 - 10^6$ HIV-RNA copies per mL), concurrent with CD4+ T lymphocyte depletion in the blood and gastrointestinal tract (>500 cells/mm^3). During the asymptomatic stage, HIV-1 specific CD8+ T cells decrease plasma viremia by 10^1 - 10^2 viral copies per mL, while HIV-mediated destruction of naïve CD4+ T cells continues [11]. The development of AIDS is characterized by a further decrease in CD4+ T lymphocytes (<200 cells/mm^3), the presence of opportunistic infections (*e.g. mycobacterium tuberculosis, candida albicans,* Epstein-Barr virus*, etc.*), and the development of diseases including AIDS lymphomas, Kaposi sarcoma, cardiovascular diseases (CVD), and HIV encephalopathy (HIVE) in the central nervous system (CNS)[8, 12]. During the development of AIDS, high levels of circulating lipopolysaccharides (LPS) indicate bacterial infection and microbial translocation from the intestinal lumen to the blood [13-16]. LPS increases as a result of HIV-mediated disruption of CD4+ T cells and development of a leaky gut, and

correlates with increased CD14+ monocyte and CD8+ T cell activation, and AIDS pathogenesis [15, 16]. In summary, AIDS pathogenesis is driven by the depletion of CD4+ T cells, innate and adaptive responses to viral replication, microbial translocation from the gut, opportunistic infections, and increased levels of myeloid cell activation in the blood, tissues, and cerebrospinal fluid (CSF) [15, 17, 18]. These findings indicate that the suppression of viral replication, reconstitution of CD4+ cells in the blood and gut, and abrogation of immune activation are key to blocking AIDS pathogenesis.
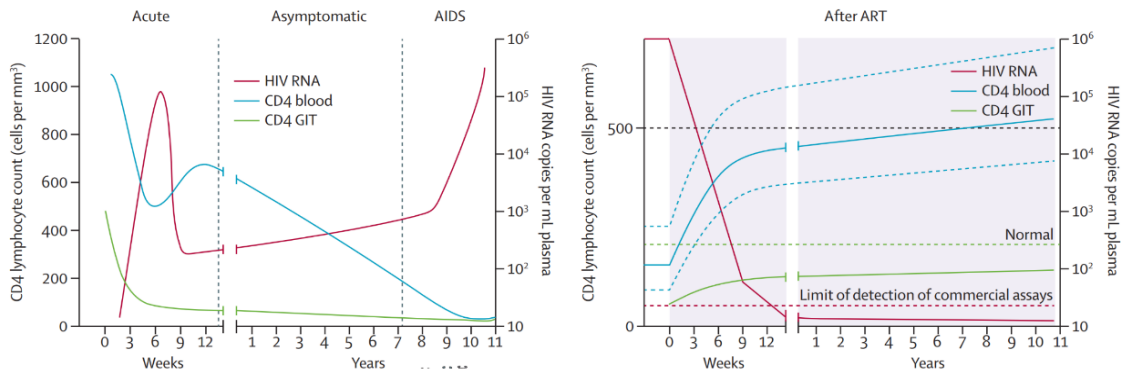
Figure 1.1. Clinical progression of HIV-1 infection pre-ART (left) and post-ART (right). In the pre-ART era, levels of plasma HIV-RNA follow a biphasic pattern, increasing during the acute phase of HIV- infection, decreasing during the asymptomatic phase, and increasing terminally with the development of AIDS. Numbers of CD4+ T lymphocytes in the blood and gut are gradually depleted with the development of AIDS. The initiation of ART decreases plasma viral load to undetectable levels, recovers CD4+ T cells in the blood and gut, and blocks AIDS pathogenesis[8]. Adapted from Maartens *et al.* (2014).

1.2 HIV life cycle, tropism, and genome

HIV-1 is an enveloped retrovirus with a capsid containing two copies of an RNA genome (approximately 9.2 kilobase pairs), and retroviral enzymes. The HIV-1 genome encodes structural Gag (matrix, capsid, and nucleocapsid), enzymatic Pol (protease, reverse transcriptase, and integrase), envelop Env (surface gp120 and transmembrane gp41 glycoproteins), accessory (Vif, Vpr, Vpu, and Nef), and regulatory (Tat and Rev) proteins[19]. HIV-1 infection begins with the attachment of HIV-1 envelope gp120 to susceptible target cells by binding the primary CD4 receptor and CCR5 or CXCR4 coreceptors. Conformational changes in HIV-1 gp41 facilitates irreversible virus-host membrane fusion [20]. Viral reverse transcription (RT) begins with the dissociation of the HIV capsid in the host cell's cytoplasm, continues with trafficking and import of the HIV-1 core into the nucleus, and subsequent completion of RT via HIV-1 reverse transcriptase [21-23]. The integration of HIV-DNA into the host genomes of CD4+ T cells and macrophages are facilitated by viral integrase and leads to the formation of the HIV provirus [24]. Establishment of the HIV provirus, and proviral transcription are mediated by viral hijacking of the host cell's RNA polymerase II, and export of viral mRNA from the nucleus to the cytosol [19, 25]. Following the translation of HIV-1 structural and accessory proteins, nascent viral proteins traffic to the virion assembly site at the host's plasma membrane, Gag proteins are assembled into immature viral particles, and viral budding and dissemination of immature viral progeny from the host plasma membrane occurs. HIV-1 accessory proteins facilitate the modification and progression of HIV-infection throughout the viral replication cycle. Maturation of viral progeny occurs outside of the initial host, and involves cleavage of the Gag-Pol polyprotein by HIV-protease[19].

1.3 HIV-associated comorbidities persist despite virus suppression with ART.

ART regimens suppress viral replication, block AIDS pathogenesis, and decrease the burden of AIDS mortality and morbidity by almost 50% compared to ART naïve PLWH [26]. The primary function of ART is the inhibition of HIV-replication by blocking a combination of viral entry, RT, HIV-DNA integration, and virion maturation **(Figure 1.2)**. Standard ART regimens are composed of a combination of two to three drugs including: non-nucleoside reverse transcriptase inhibitors, nucleoside reverse transcriptase inhibitors, protease inhibitors, and integrase inhibitors. Within two weeks of ART initiation, plasma viral suppression is achieved, with plasma viral load decreasing to low or undetectable levels (< 50 copies/ mL), and blood CD4+ cell counts recovering (>500 CD4+ cells/uL) [27]. Adherence to ART has substantially increased the life expectancy of PLWH to levels near the average expectancy observed in HIV-uninfected individuals. The introduction of ART has transformed HIV-infection from an acute disease to a manageable, chronic disease [28, 29]. The most impactful factors affecting life expectancy in PLWH on ART include CD4+ T cell count, early HIV diagnosis, time of ART initiation post-infection, and lifelong adherence to ART [28, 30, 31]. Concurrent with the suppression of plasma HIV-RNA and the reconstitution of CD4+ T cells completely in the blood and partially in the gut, ART treatment also decreases biomarkers of immune activation compared to ART naïve PLWH. Despite adherence to ART, biomarkers of monocyte and macrophages activation in the blood and tissues remain elevated, and the continued presence of circulating LPS and latently infected cells correlates with increased risk of

mortality and non-AIDS comorbidities including CVD, and HIV-associated neurocognitive disorders (HAND) [16, 31-33].
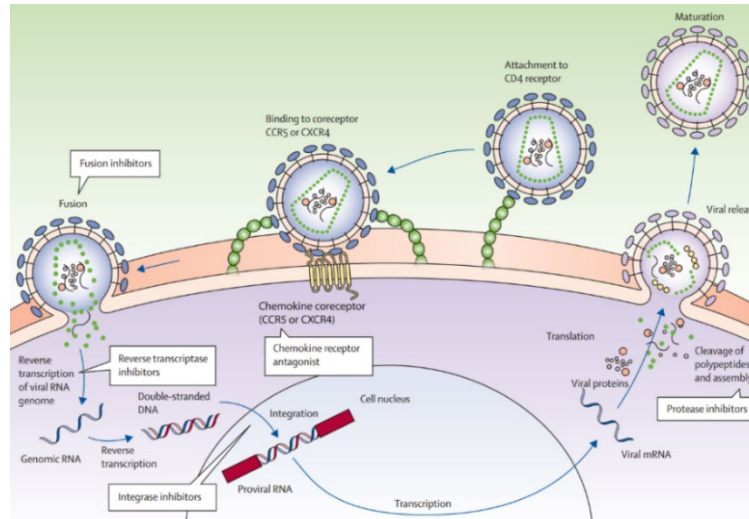
Figure 1.2. Diagram of the stages of HIV-1 replication and the antiretroviral drugs that target and block HIV (white boxes). HIV-1 infection begins by binding the primary CD4 receptor and CCR5 or CXCR4 co-receptors. Viral RT begins with the dissociation of the HIV capsid in the host cell's cytoplasm, trafficking and importation of the HIV-1 core into the nucleus, and completion of RT via HIV-1 reverse transcriptase. Subsequent trafficking of nascent viral mRNA and proteins to the host cell membrane, and viral budding and release of progeny into the extracellular space completes the replication cycle. ART regimens include non-nucleoside reverse transcriptase inhibitors, nucleoside reverse transcriptase inhibitors, protease inhibitors, and integrase inhibitors[8]. ART inhibits HIV-replication by blocking a combination of viral entry, RT, HIV-DNA integration, and virion maturation. Adapted from Maartens *et al.* (2014).

The prevalence of CVD and HAND in the post-ART era indicates that ART successfully blocks plasma virus and AIDS pathogenesis, but fails to inhibit myeloid cell activation and clear latent viral reservoirs associated with the development of non-AIDS comorbidities[27, 33, 34]. When ART is interrupted, plasma virus rebounds, immune activation increases, and the process of productive infection and viral dissemination in

tissues repeats [31, 35]. Rebounding plasma virus is driven by the reactivation of latently infected, SIV-DNA+ macrophages in gut and CNS tissues [9, 36, 37]. Using molecular clock analysis, Andrade *et al.* (2020) demonstrated that following ART interruption, recrudescent HIV in the blood is CD14+ macrophages-tropic, suggesting that recrudescent HIV is macrophage-derived and linked to continued myeloid cell activation[38]. Latently infected SIV-DNA+ CD4+ T cells and macrophages in the CNS harbor replication competent virus in SIV-infected nonhuman primates on ART [4, 36, 39], suggesting that ART has poor penetrance in tissues and macrophages, and fails to clear the latent viral reservoir. In summary, ART effectively blocks AIDS pathogenesis, suppresses plasma viral load, and prolongs the lifespans of PLWH, but fails to block myeloid cell activation and accumulation and clear tissue viral reservoirs[40]. For those reasons, the development of a functional cure for HIV-infection must block HIV replication, myeloid cell activation and accumulation, and prevent the establishment of latently infected viral reservoirs in tissues.

1.4 CD8+ T lymphocyte-depletion in nonhuman primates produces a model of rapid neuroAIDS pathogenesis.

SIV-infection in rhesus macaques follows a similar route of progression to HIV-infection in humans[41, 42]. The extended duration of time for SIV-infected macaques to develop AIDS, the varied frequencies of AIDS and SIVE pathogenesis, and the difficulty in obtaining post-mortem human tissues make it difficult for research into AIDS pathogenesis and AIDS-related comorbidities to progress. In rhesus macaque models of SIV-infection, AIDS pathogenesis can take up to 1-3 years to progress, and only a low percentage (approximately 25%) of animals develop SIVE encephalitis (SIVE) [43].

Nonhuman primate models of rapid AIDS and SIVE progression provide a model suitable for developing strategies to treat AIDS-related malignancies. Additional advantages of nonhuman primate models of rapid AIDS pathogenesis include, control of the viral clone or swarm used, control over the time and duration of SIV-inoculation, and control over the composition and usage of ART and/or additional therapies.

The two established models of inducing rapid neuroAIDS pathogenesis in nonhuman primates include the administration of lymphocyte-depleting antibodies, CD4R1 (CD4+ T lymphocyte-depleting antibody)[44] or cM-T807 (CD8+ T lymphocyte-depleting antibody)[43]. Both models result in increased levels of plasma SIV-RNA , monocyte activation and expansion, and accumulation of productively infected SIV-RNA+ macrophages [6, 44-46] . CD8+ T lymphocyte-depleted, SIV-infected macaques develop high plasma viral load, rapid AIDS pathogenesis (3-4 months), and have a higher incidence of SIVE compared to their non-depleted counterparts [42, 47]. To achieve severe AIDS and SIVE pathogenesis, animals are inoculated with the viral swarm, SIVmac251. The SIVmac251 swarm is a macrophage-tropic strain of SIV originally isolated from the rhesus macaque, Mm251-79, following inoculation with lymphocytic lymphoma tissue[48, 49]. Macaques inoculated with SIVmac251 have increased SIV viral loads in the blood and CSF, depleted CD4+ T cells in the blood, SIV-p17+ CNS macrophages accumulation, and develop SIVE[42, 50, 51]. Models of rapid AIDS pathogenesis provide a method for studying the dynamics of SIV- infection, myeloid cell activation, and AIDS/ SIVE pathogenesis in a timely manner.

1.5 Monocytes are a heterogenous population of mononuclear phagocytes.

Monocytes are mononuclear phagocytes that comprise 5-10% of the peripheral blood mononuclear cell population, and are derived from bone marrow precursors. Under healthy conditions, monocytes remain in circulation for a period of days before migrating to tissues and differentiating to macrophages where they maintain a steady state and tissue homeostasis[52, 53]. Broadly, monocyte functions include cytokine production, antigen presentation, and replenishment of tissue macrophages populations following injury[54]. In humans, monocytes are a heterogenous population in which monocyte subsets and functions are defined by the expression of the cell surface-markers CD14, LPS receptor, and CD16, FcγIII receptor[55]. Monocyte subsets are classified as classical (CD14+ CD16-), intermediate (CD14+ CD16+), and nonclassical (CD14- CD16+), with each subset demonstrating unique sets of gene expression profiles in the contexts of health and disease[55, 56]. In healthy individuals, classical monocytes express genes enriched for promoting tissue repair, angiogenesis, wound healing, and coagulation. Intermediate monocytes have potent antigen presentation capacities and express genes for α- and β-chains of the major histocompatibility complex class II (MHC II). Nonclassical monocytes are associated with immune surveillance and express genes associated with cytoskeleton remodeling and phagocytosis[56].
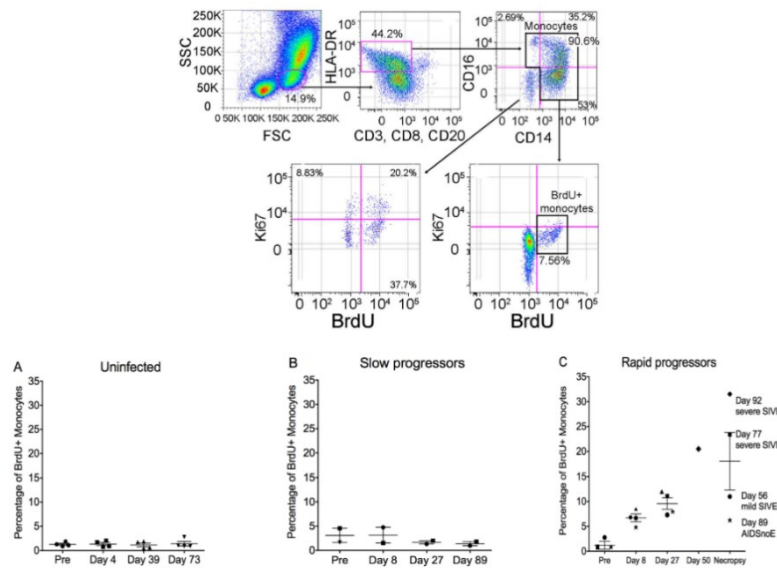
Figure 1.3. Gating schematic for BrdU+ monocytes in the blood isolated from SIV-infected, CD8+ T lymphocyte-depleted rhesus macaques (top). Increased percentages of BrdU+ monocytes (> 10-15%) early with infection (8 and 27 days' post infection) and terminally correlates with rapid progression to AIDS and SIVE (bottom)[7]. Adapted from Burdo *et al.* (2010).

1.6 Monocyte activation correlates with AIDS pathogenesis.

Chronic monocyte and macrophages activation are key determinants of AIDS pathogenesis, and predicts disease progression better than plasma viral load[57]. The majority subset of CD14+ CD16- monocytes observed in the healthy, HIV- uninfected population shifts to an expansion of CD14+ CD16+ and CD14- CD16+ monocyte subsets with HIV-/SIV- infection [58]. CD14+ CD16+ monocyte expansion correlates with the development of AIDS, CVD, and HAND [59-61]. CD14+ CD16+ monocytes are susceptible to productive HIV- and SIV- infection, and traffic to sites of inflammation and the CNS, where they are involved in further dissemination of virus [35, 62-64].

During untreated infection, rapid increases in the levels of inflammatory cytokines including monocyte chemoattractant protein-1 (MCP-1), soluble CD14 (sCD14), interferons alpha and gamma (IFNα and IFN-γ), and sCD163; CD14+ CD16+ and CD14-CD16+ monocyte activation and expansion; and 5-bromo-2'-deoxyuridine positive (BrdU+) monocyte turnover correlates with AIDS pathogenesis [7, 65-71]. BrdU is a thymidine analog incorporated into DNA during the S-phase, and is used to monitor monocyte kinetics from the bone marrow into the blood. Early and terminal proliferation of BrdU+ monocytes above 10-15%, is predictive of increased rates and severities of AIDS and SIVE pathogenesis **(Figure 1.3)** [7, 71]. At the transcriptomic level, Nowlin *et al.* (2018), demonstrated that early in SIV-infection, the monocyte transcriptional profile skews towards an upregulation of genes associated with interferon stimulation, monocyte trafficking, anti-viral responses[66]. This suggests that early after initial viral infection, changes in monocyte turnover, and increased CD14+ CD16+ monocyte activation function as important determinants of HIV-replication and AIDS progression and severity. With ART, the amount of productively infected monocytes and biomarkers of inflammation are decreased; with ART initiation following early HIV-diagnosis having a more potent inhibitory effect on immune activation than ART initiation later with HIV-diagnosis (> 1 year) **(Figure 1.4)** [1, 35]. This suggests that early inhibition of viral replication correlates with a stronger decrease in biomarkers of monocyte activation, viral infection, and improved overall survival.
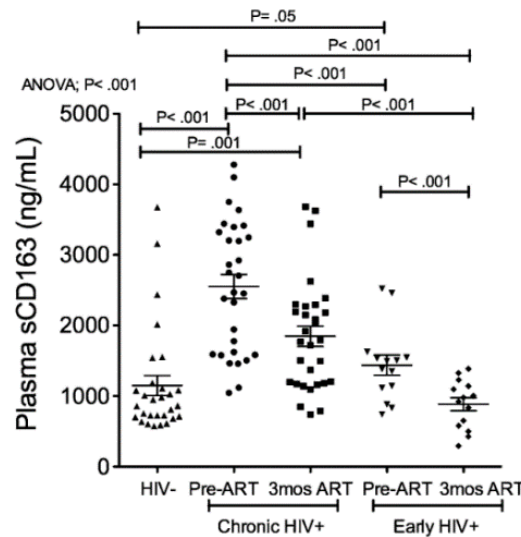
Figure 1.4. Plasma sCD163 levels in chronically (> 1 year) and acutely (<1 year) infected PLWH, pre-ART and 3 months post-ART[1]. ART initiation decreases sCD163 early with HIV-infection to levels similar to the HIV-uninfected population. ART initiation does not decrease sCD163 to HIV-uninfected level in chronically infected PLWH. Adapted from Burdo *et al.* (2011).

1.7 HAND persists in the post-ART era and correlates with myeloid cell activation.

HAND is a spectrum of disorders encompassing asymptomatic neurocognitive impairment (ANI), mild neurocognitive disorder (MND), and HIV associated dementia (HAD). HAND's clinical manifestations include behavioral, motor, and neurocognitive deficits, and increases mortality in PLWH [10, 30]. In the pre-ART era, PLWH had an estimated 16% risk of developing HAD, the most severe form of HAND [67]. ART administration has greatly reduced HAND-associated mortality and morbidity [12, 72]. In the post-ART era, the development of the more severe forms of HAND, HAD and HIVE, have decreased to less than 5% amongst PLWH. Despite plasma virus suppression and declining frequencies of HIVE and HAD in the post-ART era, milder forms of HAND persist in 50%

of ART treated PLWH [72]. Though the mechanisms of neuronal injury and death in PLWH with HAND are not well understood, high levels of HIV-RNA in the blood and CSF, low CD4+ T lymphocyte nadir, irreversible neurologic injury, and increased myeloid cell activation consistently correlate with HAND pathogenesis[10, 39, 73-75].

Using a model of SIV neuroAIDS, magnetic resonance spectroscopy data reveals that neuronal injury is inversely correlated with plasma SIV-replication, and CD14+ CD16+ and CD14- CD16+ monocytes expansion [43]. In the CSF, biomarkers correlated with monocyte activation and neuroinflammation including sCD14, MCP-1, IFNγ, soluble TNF receptor II (sTNFR-II), neopterin, neurofilament light chain (NFL), and S100 calcium-binding protein B (S100B), are increased in PLWH[18, 75-77]. Together, these findings suggest that HIV-associated neuronal injury is linked to SIV-replication and increased monocyte activation. The introduction of ART has decreased biomarkers of myeloid cell activation and neuroinflammation in the CSF[78], however the persistence of HAND in PLWH on ART suggests that inflammatory biomarkers in the CSF do not completely represent levels of myeloid cell activation in the CNS[17]. Studies assessing SIV-infected macaques treated with ART show that decreased viral loads in the blood and CSF and CD14+ CD16+ monocyte activation are inversely correlated with improved biomarkers of neuronal function [79]. Indeed, Burdo *et al.* (2014) found that levels of sCD163 in the plasma are more accurately correlated with neurological impairment in PLWH on ART than sCD163 in the CSF[74].

Galectin-9 is a carbohydrate-binding protein expressed and secreted by activated macrophages, that correlates with chronic inflammation and AIDS pathogenesis in PLWH [80-83]. Elahi *et al.* (2012) found that during HIV-infection, increased binding between galectin-9 and T-cell immunoglobulin and mucin-domain containing-3 (Tim3) correlates with decreased CD4+ T cell susceptibility to HIV-infection [84]. Recently, levels of plasma and CSF galectin-9 have been assessed for their utility as biomarkers of HAND and AIDS pathogenesis. Increased levels of galectin-9 in the blood correlates with acute HIV-infection[83, 85], plasma HIV viral load, and AIDS pathogenesis[81], while galectin-9 in the CSF correlates with neurocognitive impairment in PLWH [86]. Plasma galectin-9 remains elevated in PLWH on ART compared to the HIV-uninfected population and correlates with high risks of morbidity and HAND [81, 83, 85, 86]. These findings suggest that decreasing levels of galectin-9 in the blood and CSF may correlate with decreased macrophages activation and non-AIDS comorbidities.

HIV-/ SIV- infection of the CNS occurs during the acute phase of infection, and is correlated with increased CD14+ CD16+ monocyte activation and trafficking[64, 67], and CD206+[87] and CD163+ perivascular macrophages accumulation [88]. SIV-RNA is detected in the CNS during the acute phase, as early as 4 days' post-infection [89], remains dormant during the asymptomatic phase, and re-emerges terminally with AIDS [90]. The process by which monocyte- and macrophage- associated virus enters the CNS, is coined the Trojan Horse model. In this model, HIV-/ SIV- infected CD14+ CD16+ monocytes traffic past the blood brain barrier and enter the CNS via gradients of the migratory chemokine, monocyte chemoattractant protein-1 (MCP-1)/ C-C motif chemokine ligand 2

(CCL2) [63, 64]. Once in the CNS, virally infected "Trojan Horse" CD14+ CD16+ monocytes seed the brain with virus. HIV-/ SIV- seeding of the CNS also occurs via the accumulation of infected CD163+ macrophages in the perivascular cuffs of the CNS[88, 91-94]. During the acute phase, from 12 to 14 days' post infection, increased CD16+ CD68+ macrophages are observed in the choroid plexus and perivascular spaces of the CNS [88, 95]. CNS macrophages accumulation correlates with increased biomarkers of neuroinflammation in the CSF and blood, and with productively infected SIV-RNA+ macrophages in the brain[90].

Post-mortem analyses of HIVE and SIVE lesions in CNS cortical tissues reveal that productively infected, CD163+ perivascular macrophages and multinucleated giant cells (MNGCs) make up the bulk of encephalitic lesions [6, 95]. Using intracisternal injections of fluorescently-labeled Dextrans early (20 days' post-infection) and terminally, Nowlin *et al.* (2015) examined the cellular composition of SIVE lesions and found that lesions consist of early infiltrating CD163+ perivascular macrophages (Dextran-FITC+), and late arriving SIV-p28+ CD163+ perivascular macrophages terminally (Dextra-AF647+)[6] **(Figure 1.5)**. The MAC387 antibody recognizes myeloid related protein 14 (MRP14), and calprotectin, a heterodimer of MRP8/MRP14. MAC387+ macrophage accumulation in the CNS differentiates SIV-infected macaques that rapidly developed SIVE from chronically infected animals with little or no pathology[96]. Soulas *et al.* (2011) found BrdU+ MAC387+ CNS macrophages in SIVE lesions and in the brains of PLWH with AIDS and chronic disease[97]. MAC387+ CNS macrophages were also BrdU+, suggesting that MAC387+ macrophages represent a subset of early infiltrating CNS macrophages.

Combined, these findings reveal that early and terminal infiltrations of productively infected CD163+ macrophages and BrdU+ MAC387+ macrophages into the CNS correlates with SIVE pathogenesis.
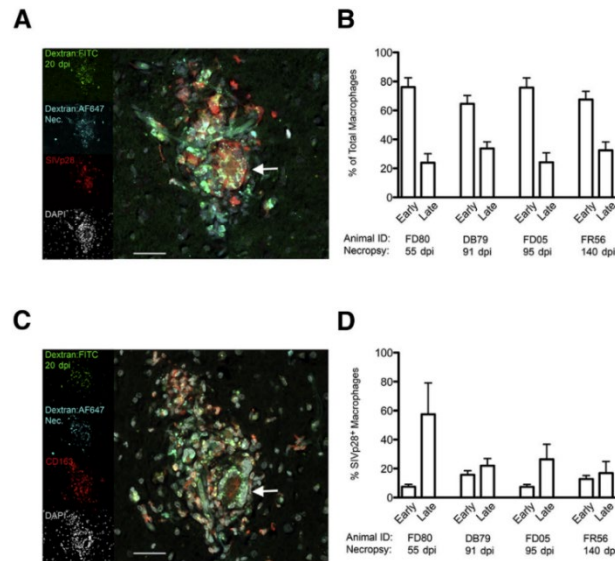
Figure 1.5. SIVE lesions contain CD163+ perivascular macrophages (Dextran-FITC+, green) that traffic to the CNS early and productively infected SIVp28+ CD163+ perivascular macrophages (Dextran-AF647+, red) that traffic to the CNS terminally [6]. Macrophages activation and accumulation occur early and terminally in SIV-infection and correlates with the severity of SIVE pathogenesis. Adapted from Nowlin *et al.* (2015).
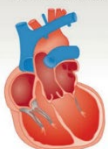
1.8 Excessive monocyte and macrophages activation drives the development of CVD in PLWH.

HIV-associated CVD encompasses a range of disorders including dilated cardiomyopathy, pericarditis, hypertension, coagulopathy, and vascular and coronary diseases [98-100]. In the pre-ART era, approximately 10-40% of PLWH were predicted to develop CVD [101]. During acute HIV-infection, increased levels of surrogate biomarkers of myocardial dysfunction and damage in the blood, N-terminal prohormone of brain

natriuretic peptide (NT-proBNP) and cardiac troponin T, correlates with subclinical, inflammatory cardiomyopathy [102], suggesting that the conditions needed to develop CVD in PLWH occurs early with infection. Traditional assessments for predicting CVD risk in the uninfected population such as the Framingham risk factors which include cigarette smoking, high blood pressure, and total cholesterol; plus levels of plasma D-dimer and C-reactive protein, do not consistently predict the risk of developing CVD in PLWH regardless of ART[103-106] **(Figure 1.6)**. This suggests that additional factors independent of lifestyle decisions and related to myeloid cell activation correlate with the development of CVD in PLWH. Despite decreased mortality and morbidity with ART, PLWH have a 1.5 - 2-fold increased risk of adverse cardiac events including myocardial infarction and cardiomyopathy compared to the age-matched, HIV-uninfected population [34, 103, 107, 108]. Studies measuring myocardial function with cardiac magnetic resonance imaging in both ART naïve and ART treated PLWH, reveals significant decreases in left ventricular ejection fraction, increased left ventricular mass and fibrosis, and an overall increased risk of adverse cardiac events with HIV, that are not present in the HIV-uninfected population[109-112], suggesting that chronic inflammatory conditions within the cardiovascular system are not targeted by ART and correlate with increased cardiac morbidity and mortality.

Excessive CD14+ CD16+ monocyte and macrophages activation are key to the development of atherosclerosis, myocardial fibrosis, heart failure, and cardiac pathogenesis in the HIV- uninfected population and PLWH[113-118]. Under healthy conditions, macrophages in the heart maintain cardiac homeostasis and function as key regulators of

fibrosis via their interactions with collagen-producing myofibroblasts, secretion of profibrotic mediators including transforming growth factor beta (TGF-β), antigen presentation, and immune surveillance [53, 119]. Cardiac collagen is necessary for wound-healing and tissue-remodeling however, excessive cardiac collagen deposition results in cardiac fibrosis, a pathological response to repeated tissue damage and inflammation resulting in increased cardiac muscle stiffness, left ventricular dysfunction, and eventually, CVD [119]. In the vasculature, cholesterol metabolism is mediated in-part by macrophages uptake of oxidized low-density lipids within the arterial intima. Adherence to unhealthy lifestyle habits including a high cholesterol diet, smoking, and lack of exercise leads to the development of atherosclerosis[113]. Atherosclerosis is characterized by the accumulation of foam cells, lipid-laden macrophages, in the arterial intima that develop as fatty streaks along the endothelium obstructing blood flow to tissues[120]. Together, monocytes and macrophages function as key regulators of cardiovascular homeostasis under healthy conditions, and CVD pathogenesis with disease.

	Pre-ART	First-generation ART regimens	Contemporary ART regimens	Optimized ART regimens	Curative therapies
				Future	
HIV treatment	No HIV-specific therapy	• PI • NRTI • NNRTI	• PI • NRTI • NNRTI • CCR5 antagonist • Integrase inhibitor	• Early ART initiation • Two-drug regimens • Injectable medications • New therapeutic targets	• Stem-cell-based therapies • Strategies to eliminate latency • Genome editing • Broadly neutralizing antibodies
Inflammatory and immunological status	• AIDS • Inflammation	• Immunodeficiency • Chronic inflammation	• Immunodeficiency • Chronic inflammation	Chronic inflammation	Eradication of HIV infection
Cardiovascular complications	• Pericardial effusion • Dilated cardiomyopathy	• Atherosclerosis • Myocardial infarction • Dilated cardiomyopathy • Stroke • Peripheral artery disease	• Heart failure • Atrial fibrillation • Sudden cardiac death • Coronary heart disease	• Increased risk of cardiovascular diseases	

Figure 1.6. Overview of CVDs in PLWH during the pre-ART and post-ART eras. Future treatments for HIV-associated CVD must eradicate HIV infection, inhibit AIDS pathogenesis, and block myeloid cell activation driving chronic inflammation [3-5]. Adapted from Hsue *et al.* (2019).

The conditions that lead to CVD in the post-ART era are driven by CD68+, CD163+, CD206+, and MAC387+ cardiac macrophages inflammation and fibrosis in PLWH and SIV-infected rhesus macaques [46, 121-124]. PLWH have higher levels of chronic inflammatory risk factors including, immune activation, viral replication, vascular and endothelial dysfunction, and dyslipidemia that serve as more reliable predictors of CVD compared to the HIV- uninfected population [109, 125-127]. Additionally, increased CD14+ CD16+ and CD14- CD16+ monocyte activation and accumulation in the arterial intima correlates with the development of atherosclerosis in PLWH [128-130]. Studies in nonhuman primate models of SIV- infection suggests that there are little to no SIV-RNA+ cells in the heart regardless of the presence of cardiac pathology and ART treatment, suggesting that productive infection in cardiac tissues has little impact on the rate of cardiac pathogenesis [2, 46, 131, 132]. When detected, cardiac SIV-RNA+ cells are co-localized to CD68+ CD206+ macrophages, suggesting that cardiac macrophages accumulation, not viral infection in the heart, correlates with cardiac pathogenesis [133]. CVD persistence in the post-ART era indicates that mechanisms of cardiac damage are multifactorial and are correlated with monocyte and macrophages activation more so than plasma and cardiac viral load.

Galectin-3 is a β-galactoside binding lectin expressed by activated macrophages, and associated with binding extracellular matrix proteins including laminin and fibronectin[134]. In the HIV- uninfected population, increased levels of plasma galectin-3 and myocardial galectin-3 expression correlates with cardiovascular inflammation, cardiac fibrosis, and heart failure [135-139]. Recent data among PLWH on ART, suggest that plasma

18

galectin-3 is inversely correlated with the development of noncalcified coronary plaque[114, 140, 141], suggesting that plasma galectin-3 may be a biomarker of cardiac macrophages activation and CVD in PLWH. Though studies regarding galectin-3's association with CVD in PLWH are limited, increased plasma and myocardial galectin-3 are possibly correlated with cardiac pathogenesis in SIV-infected animals. Identifying biomarkers of myeloid cell activation that reliably correlate with CVD in PLWH could lead to the discovery of potential targets driving CVD pathogenesis. Increased biomarkers of monocyte and macrophages activation in the blood including sCD14, sCD163, IL-18, and CCL2, correlate with the development of stable, calcified plaque; rupture prone, noncalcified plaque; and cardiac inflammation in PLWH and SIV-infected macaques[129, 142-147]. These data suggest that targeting and blocking factors correlated with monocyte and macrophages activation could decrease the rate and severity of CVD in PLWH.
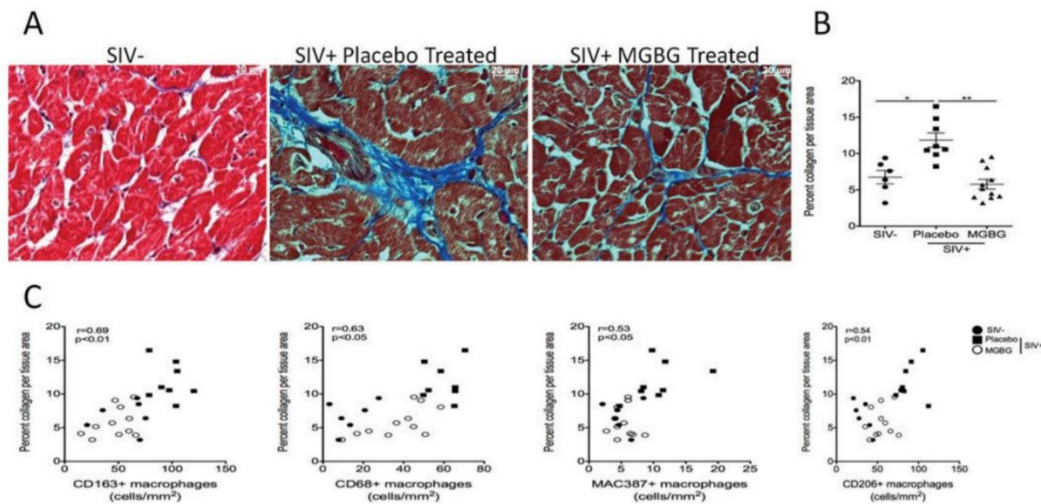
Figure 1.7. SIV-infected animals treated with methylglyoxal-bis guanylhydrazone (MGBG) had less severe cardiac inflammation and fibrosis compared to placebo controls[2]. Decreased cardiac macrophages inflammation correlates with cardiac collagen. Adapted from Walker *et al.* (2014).

1.9 Blocking myeloid cell activation decreases SIV-associated CVD and SIVE.

The persistence of comorbidities in the post-ART era, and their correlation to myeloid cell activation, suggests that the targeted inhibition of monocyte and macrophages activation will decrease the rate and severity of HIV- related comobidities. Campbell *et al.* (2011) demonstrated that SIV-infected macaques treated with the tetracycline antibiotic, Minocycline, had decreased CD14+ CD16+ and CD14- CD16+ monocytes activation and improved biomarkers of neuronal protection, suggesting that blocking monocyte activation correlates with improved CNS health [148]. Blocking monocyte and macrophages traffic with early (0 days' post-infection) and late (28 days' post-infection) anti-α4 antibody treatments, improved biomarkers of CNS protection, decreased macrophages inflammation in the heart and CNS, and limited the amount of SIV-p28+ and SIV-DNA+ cells in the CNS [132, 149]. These findings show that blocking monocyte and macrophages traffic to the CNS and heart correlates with decreased cardiac and CNS pathology. Recent data suggests that the polyamine biosynthesis inhibitor MGBG, is selectively taken up by monocytes and macrophages, decreases CD16 expression and BrdU incorporation, and blocks HIV infection in monocytes *in vitro* [150, 151]. Further, CD8+ T lymphocyte-depleted, SIV-infected macaques treated with an oral formulation of MGBG did not develop AIDS or SIVE, had decreased CD14+ CD16+ monocyte activation, and macrophages inflammation in the heart and CNS[2, 152] **(Figure 1.7)**. Together, these findings indicate that targeting monocyte and macrophages activation and accumulation correlates with decreased incidence and severity of SIV-associated comorbidities. For that reason, it is likely that the optimal therapeutic approach for HIV-infection involves the suppression of plasma

virus, inhibition of AIDS pathogenesis, and the targeted inhibition of myeloid cell activation .

1.10 Summary of studies in this thesis.

Biomarkers of monocyte and macrophages activation and accumulation correlates with the development of HIV-associated comorbidities in PLWH [7, 71, 87, 153]. We first asked how frequently SIV-infected macaques with AIDS developed concomitant CVD and SIVE compared to animals that developed CVD or SIVE alone, and no cardiac pathology (NSF) and SIV with no encephalitis (SIVnoE) (Chapter 2). We then asked whether animals with CVD and SIVE had more cardiac macrophages inflammation, CD14+ CD16+ monocyte activation, levels of plasma galectin-3, galectin-9, IL-18, and sCD163, and infected SIV-DNA+, SIV-RNA+, and SIV-gp41+ cells in brain and heart tissues compared to animals with CVD or SIVE alone, and NSF and SIVnoE animals. We found that concomitant CVD and SIVE developed more frequently in animals with AIDS than CVD or SIVE alone, and NSF and SIVnoE. We found that animals with CVD and SIVE had more cardiac inflammation and fibrosis, productively infected CNS macrophages, and early and terminal biomarkers of monocyte activation compared to animals with CVD or SIVE alone, and NSF and SIVnoE animals. We found that early (8 and 19 days' post infection) and terminal increases in CD14+ CD16+ monocytes correlated with the percentage of cardiac collagen deposition. We found little to no SIV-DNA+, SIV-RNA+, and SIV-gp41+ cells in the heart regardless of pathology. We also report that cardiac SIV-RNA+ cells are CD68+ CD206+ macrophages. We show that plasma galectin-3, galectin-9, and IL-18 correlated with plasma sCD163 but not with plasma viral load. We also show

that cardiac macrophages inflammation and fibrosis are increased in PLWH with HIVE compared to PLWH with HIVnoE. Our findings show that monocyte activation and macrophages accumulation, not productive viral infection in the heart, drives the development and severity of concomitant CVD and SIVE.

Despite viral suppression and AIDS inhibition with ART, increased CD14+ CD16+ monocyte activation and macrophages inflammation persist[1, 32, 114, 129], suggesting that ART alone is not sufficient for blocking myeloid cell activation associated with the development of comorbidities in PLWH. Previously, we and others demonstrated that targeting myeloid cell activation and accumulation correlates with the inhibition of AIDS, blocks SIV-infection, and decreases cardiac and CNS inflammation[2, 132, 149, 152]. We hypothesized that SIV-infected macaques treated with ART and adjunctive MGBG would block viral replication, AIDS pathogenesis, and monocyte and macrophage activation compared to animals on ART alone, or with no treatment. We asked whether SIV-infected macaques on ART plus adjunctive MGBG (ART+MGBG) had an additive decrease in cardiac macrophages inflammation, cardiac collagen, and biomarkers of monocyte activation and turnover in blood compared to animals on ART (Chapter 3). We found that animals on ART+MGBG had more of a decrease in cardiac collagen deposition than animals on ART. We also found that animals on ART, and ART+MGBG had decreased cardiac macrophages inflammation and collagen, levels of plasma galectin-3, galectin-9, IL-18, and sCD163, CD14+ CD16+ monocyte activation, and BrdU+ monocyte turnover, compared to untreated animals. Consistent with previous findings [2, 132], we found a positive correlation between the numbers of cardiac macrophages and collagen deposition

in all of the animals examined. We did not find a correlation between decreased cardiac inflammation and collagen based on ART, and ART+MGBG treatments. We also identified two populations of galectin-3 expressing cells (Gal-3+) in cardiac tissues: CD163+ Gal-3+ macrophages and CD163- Gal-3+ cells. We report that animals on ART, and ART+MGBG had fewer CD163+ Gal-3+ cardiac macrophages compared to untreated animals. There were similar levels of cardiac SIV-RNA+ macrophages and CD163- Gal-3+ cells, in all animals regardless of treatments. Our findings emphasize the importance of targeting monocyte and macrophages activation to block CVD pathogenesis.

1.11 Novel findings in this thesis

1.11.1 Chapter 2

1. Animals with AIDS develop concomitant CVD and SIVE more frequently than CVD or SIVE alone, and NSF and SIVnoE.

2. Animals with CVD and SIVE had more cardiac inflammation and fibrosis, and biomarkers of monocyte activation compared to animals with CVD or SIVE alone, and NSF and SIVnoE.

3. Animals with CVD and SIVE had more CD14+ CD16+ monocyte activation early with infection (8 and 19 dpi) and terminally compared to animals with CVD or SIVE alone, and NSF and SIVnoE.

4. Early (8 and 19 dpi) and terminal numbers of CD14+ CD16+ monocyte correlates with cardiac fibrosis in all animals examined.

5. There are more productively infected SIV-RNA+ and SIV-gp41+ cells in the CNS than in the hearts of all animals examined, regardless of pathology.

6. Despite their low abundance in the heart, cardiac SIV-RNA+ cells are CD68+ and CD206+ cardiac macrophages.

7. Animals with CVD and SIVE had more CNS SIV-RNA+ and CNS SIV-gp41+ cells compared to animals with CVD or SIVE alone, and NSF and SIVnoE.

8. There are little to no cardiac SIV-DNA+, cardiac SIV-RNA+ and cardiac SIV-gp41+ cells in all of the animals regardless of pathology.

9. PLWH that have HIVE have increased cardiac macrophages inflammation and fibrosis compared to PLWH with HIVnoE.

1.11.2 Chapter 3

1. There was an additive decrease in the percentage of cardiac collagen deposition in animals on ART+MGBG compared to animals on ART.

2. Animals on ART, and ART+MGBG, and untreated animals had similar frequencies of cardiac histopathology (inflammation, fibrosis, and cardiomyocyte degeneration).

3. Biomarkers of monocyte activation, BrdU+ monocyte turnover, SIV-RNA+ cardiac macrophages, cardiac macrophages inflammation and fibrosis were decreased in animals on ART, and ART+MGBG compared to untreated animals.

4. Two populations of Gal-3+ cells (CD163+ Gal-3+ macrophages and CD163- Gal-3+ cells) were identified in the cardiac tissues of SIV-infected rhesus macaques.

Figure 1. Gasson Hall, Boston College. Photo by Lee Pellegrini

2.0 Simian immunodeficiency virus- infected rhesus macaques with AIDS co-develop cardiovascular pathology and encephalitis.

Kevin S. White[1], Joshua A. Walker[1], John Wang[1], Patrick Autissier[1], Andrew D. Miller[2], Nadia N. Abuelezan[3], Rachel Burrack[4], Qingsheng Li[4], Woong-Ki Kim[5], Kenneth C. Williams[1*]

[1]Department of Biology, Boston College, Chestnut Hill, MA, USA;

[2]Department of Biomedical Sciences, Section of Anatomic Physiology, Cornell University College of Veterinary Medicine, Ithaca, NY, USA;

[3]Connel School of Nursing, Boston College, Chestnut Hill, MA, USA;

[4]Nebraska Center for Virology, School of Biological Sciences, University of Nebraska-Lincoln, Lincoln, NE, USA;

[5]Division of Microbiology, Tulane National Primate Research Center, Covington, LA, USA

[*]Corresponding author can be contacted at:

Department of Biology- Boston College

120 Commonwealth, Massachusetts, 02467 USA

Telephone Number: (617) 552-1168

E-mail: Kenneth.williams.3@bc.edu

Equal Contribution for Authorship: Kevin S. White and Joshua A. Walker share co-first authorship for this manuscript.

2.1 Abstract

Despite effective antiretroviral therapy, HIV co-morbidities remain where central nervous system (CNS) neurocognitive disorders and cardiovascular disease (CVD)-pathology that are linked with myeloid activation are most prevalent. Comorbidities such as neurocognitive dysfunction and cardiovascular disease (CVD) remain prevalent among people living with HIV. We sought to investigate if cardiac pathology (inflammation, fibrosis, cardiomyocyte damage) and CNS pathology (encephalitis) develop together during simian immunodeficiency virus (SIV) infection and if their co-development is linked with monocyte/macrophage activation. We used a cohort of SIV-infected rhesus macaques with rapid AIDS and demonstrated that SIV encephalitis (SIVE) and CVD pathology occur together more frequently than SIVE or CVD pathology alone. Their co-development correlated more strongly with activated myeloid cells, increased numbers of CD14+ CD16+ monocytes, plasma CD163 and interleukin-18 (IL-18) than did SIVE or CVD pathology alone, or no pathology. Animals with both SIVE and CVD pathology had greater numbers of cardiac macrophages and increased collagen and monocyte/macrophage accumulation, which were better correlates of CVD-pathology than SIV-RNA. Animals with SIVE alone had higher levels of activated macrophage biomarkers and cardiac macrophage accumulation than SIVnoE animals. These observations were confirmed in HIV infected individuals with HIV encephalitis (HIVE) that had greater numbers of cardiac macrophages and fibrosis than HIV-infected controls without HIVE. These results underscore the notion that CNS and CVD pathologies frequently occur together in HIV and SIV infection, and demonstrate an unmet need for adjunctive therapies targeting macrophages.

27

2.2 Introduction

HIV-associated comorbidities affect 20-50% of people living with HIV (PLWH) despite effective antiretroviral therapy (ART) [108, 154-158]. Of these, cardiovascular diseases (CVD) and HIV-associated neurocognitive disorders (HAND) are the most prevalent and are likely linked, although this has not been thoroughly documented [159-163]. Traditional biomarkers of CVD are insufficient for predicting CVD risk in HIV-infected individuals on ART, highlighting the necessity to further investigate the etiologies of HIV-associated CVD pathogenesis [108, 155, 164, 165]. Anecdotally, it appears that the incidence of cardiac and central nervous system (CNS) pathologies, and of CVD and neurocognitive dysfunction among HIV-uninfected individuals often are concomitant and are linked; likely through systemic inflammation and cardiovascular risk factors [166-173]. Importantly, both are associated with increased monocyte/macrophage activation and accumulation in tissues [10, 73, 174-176]. The development of pre-ART HIV encephalitis (HIVE) among HIV-infected adults and children is associated with myocardial dysfunction, underscoring the possible connection between cardiac and CNS pathogenesis with HIV-infection [177-179].

Central to CVD and CNS pathologies in PLWH and SIV-infected monkeys is myeloid cell activation. This has been demonstrated in many ways, including elevated plasma soluble CD14 (sCD14) and CD163 (sCD163), increased numbers of activated CD14+ CD16+ monocytes, and the accumulation of CD163+, CD206+, and MAC387+ macrophages [2, 58, 66, 121, 129, 153, 180-182]. Monocyte/macrophage activation and accumulation in the CNS also are correlated with neuroinflammation, encephalitis, and HAND with HIV and SIV infection [6, 10, 43, 58, 66, 74, 87, 95, 97, 181, 183, 184]. Whether such cardiac inflammation

and fibrosis, and HAND/HIVE and SIV encephalitis (SIVE) pathogenesis co-occur and correlate with higher levels of monocyte and macrophage activation have not been thoroughly addressed. We and others have shown that blocking monocyte traffic or inhibiting macrophage activation experimentally in SIV-infected macaques reduces cardiac inflammation and CNS pathology, highlighting the importance of monocytes and macrophages in the pathogenesis of both SIV comorbidities [132, 148, 149]. Plasma galectin-3 and -9, are β-galactoside- binding lectins secreted, in part, by activated macrophages [139, 185] and correlate with HIV comorbidities [137, 186]. Galectin-3 correlates with myocardial fibrosis and cardiac inflammation in HIV-uninfected and HIV-infected cohorts, and plasma and cerebrospinal fluid (CSF) galectin-9 correlates with acute HIV-1 infection and HAND [83, 85, 86, 139, 140, 187-189]. Plasma interleukin-18 (IL-18) is an inflammatory cytokine associated with macrophage activation and pyroptosis, plasma viral load, atherosclerosis, and CVD in symptomatic, HIV-infected patients and SIV-infected monkeys [145, 147, 190, 191]. In addition, sCD163 made solely by myeloid cells correlates with CVD and non-calcified plaque, HAND, and plasma virus in HIV-infected individuals on or off ART and SIV-infected monkeys [70, 74, 153, 180].

In this study, we asked whether SIV infected animals with AIDS co-developed CVD and SIVE, and whether animals that co-developed CVD pathology and SIVE had more monocyte and macrophage activation than animals with CVD pathology alone or SIVE alone, and animals with no significant cardiac pathology and SIV with no encephalitis (SIVnoE). Twenty-three CD8+ T lymphocyte-depleted, SIV-infected macaques with AIDS were examined for the prevalence of cardiac fibrosis, inflammation,

and cardiomyocyte degeneration, and SIVE. We assessed the numbers of cardiac macrophages, cardiac collagen, monocyte activation, productive infection in the heart and CNS, and plasma sCD163, IL-18, and galectin-3 and -9. Corollary, translational studies were done in PLWH with and without HAND, where significantly increased numbers of cardiac macrophages were found in HAND versus non HAND individuals.

2.3 Materials and Methods

2.3.1 Animals, SIV-infection, and CD8+ T-lymphocyte depletion

Twenty-three rhesus macaques were utilized in this study. Five were housed at Harvard University's New England Primate Research Center (NEPRC) and eighteen were housed at Tulane University's Tulane National Primate Research Center (TNPRC) in accordance with standards of the American Association for Accreditation of Laboratory Animal Care. This was a retrospective study using all male Rhesus macaques (Macaca mulatta). Animals were experimentally infected intravenously (i.v) by inoculation with bolus of SIVmac251 viral swarm (20 ng of SIV p28) provided by Ronald Desrosiers, over a 5 minute time-period. Animals were adults (3.6-12.6 years old). Animals with the Mamu B*08 and B*17 alleles were excluded. Blood samples were taken prior to, on the day of infection, and weekly thereafter. Animals underwent CD8+ T-lymphocyte depletion for rapid AIDS and consistent SIVE. CD8+ T-lymphocyte depletion was achieved with subcutaneous administration of human anti-CD8 antibody, cM-T807 (10 mg/kg) at day 6 post-infection, and i.v. administration (5 mg/kg) on days 8 and 12 post-infection. Simian AIDS was determined postmortem by the presence of opportunistic infections, tumors, and the development of SIV giant cell pneumonia, cytomegalovirus pneumonia, SIVE with giant cells, *pneumocystis jirovecii*, or lymphoma. With the presence of AIDS, animals were anesthetized with ketamine-HCl and euthanized with i.v. pentobarbital overdose and exsanguinated.

2.3.2 Plasma viral load

Plasma SIV-RNA was quantified using real-time PCR, as previously describe[41, 192, 193]. Five hundred µL of EDTA plasma was collected and SIV virions were pelleted by centrifugation at 20,000 g for 1 hour. The PCR assay targets conserved sequences of SIV-*gag*. The threshold sensitivity was 100 copy Eq/mL, with an average inter-assay coefficient variation of less than 25%. The CT cut off for SIV DNA is 39-40 cycles.

2.3.3 Assessment of inflammation and fibrosis in cardiac tissues and CNS SIVE

Following exsanguination, a standard necropsy was performed and lymph nodes and parenchymal organs including heart and brain, were fixed in 10% neutral buffered formalin. Tissues were paraffin embedded, sectioned at 5µm, and stained with hematoxylin and eosin. Sections of cardiac (left ventricle) and central nervous system (CNS) cortical tissues were analyzed blindly by a veterinary pathologist. Ten randomly selected images of cardiac and CNS cortical tissues were taken using an Olympus BX43 Light Microscopy (Evident, Tokyo, Japan) at 400x fields and graded subjectively and blindly by an ACVP certified Veterinary Pathologist, and categorized based on the degree of cardiac inflammation, cardiac fibrosis, and cardiomyocyte degeneration as having: A) no significant findings (NSF), B) mild, C) moderate, or D) severe pathology. SIVE was diagnosed based on the presence of MNGCs, accumulation of perivascular macrophages, and productive SIV infection [7, 194-196].

2.3.4 Single-label immunohistochemistry of cardiac tissues

Sections of formalin-fixed, paraffin-embedded cardiac tissues were immunohistochemically assessed for numbers of macrophages and CD3+ T-lymphocytes, as previously described [132]. Macrophages were identified using monoclonal antibodies against CD163 (clone EdHu-1, Serotec; Oxford, UK), CD68 (clone KP1, Dako; Glostrup, Denmark), Myeloid/Histiocyte Antigen (clone MAC387, Dako), and CD206 (clone 685645, R&D Systems; Minneapolis, MN); T-lymphocytes were identified using a polyclonal antibody against CD3 (Agilent- cat A0452, Dako, Santa Clara, CA). Data are presented as the mean positive number of cells/mm^2 from 20 non-overlapping fields of view plus or minus the standard error of the mean (SEM). SIV-productively infected cells in cardiac and CNS cortical tissues were immunohistochemically stained for SIV-gp41+ cells (clone: KK41, NIH AIDS Reagent Program; Germantown, MD). Quantitation of SIV-gp41+ cells/mm^2 was achieved by counting SIV-gp41+ cells from 20 random, non-overlapping images of brain and cardiac sections at 400x total magnification using the Zeiss Axio Imager.M1 microscope and AxioVision (Version 4.8, Zeiss; Oberkochen, Germany).

2.3.5 Measurement of myocardial fibrosis

Cardiac collagen deposition was measured using a modified Massons Trichrome stain, as previously described [132]. Tissue sections were imaged using a Zeiss Axio Imager M1 microscope with Plan-Apochromat x20/0.8 Korr objectives. The percent collagen per total tissue area was determined using ImageJ Analysis software from 20 non-overlapping 200x

microscopic fields (field area= 0.148mm^2) and data are presented as the percent collagen per total tissue area plus or minus the SEM.

2.3.6 Immunohistochemical analysis of samples from the Manhattan HIV Brain Bank cohort

Sections of cardiac tissues were examined post-mortem, from n=22 individuals from the Manhattan HIV Brain Bank (MHBB) cohort. All HIV infected individuals were ART naïve and matched with regard to age, race, and sex. All individuals examined were male. Eleven patients had HIV no encephalitis (HIVnoE) and eleven patients had HIV encephalitis (HIVE). HIVnoE patients had an average age of 44.7 ± 1.15 years, and HIVE patients had an average age of 43.5 ± 1.27 years. Four patients were white, ten were Hispanic, and eight were black. Nine HIVnoE patients, and ten HIVE patients had CD4+ T cell counts < 200 cells. Single-label immunohistochemistry was performed on formalin-fixed, paraffin-embedded sections of cardiac tissues. Macrophages were identified with monoclonal antibodies against CD68 (KP1, Bio-RaD), CD163 (EDHU, Bio-Rad), CD206 (MMR/CD206, RD Systems), and Myeloid/Histiocyte Antigen MAC387 (MAC387, Bio-Rad) cardiac macrophages. Cardiac T-lymphocytes were identified using the polyclonal antibody against CD3. Data are presented as the mean number of positive cells/mm^2 from 20 non-overlapping 200x fields of view plus or minus the SEM. Cardiac collagen deposition was measured using a modified Massons Trichrome stain. Tissue sections were imaged using a Zeiss Axio Imager M1 microscope with Plan-Apochromat x20/0.8 Korr objectives. The percent collagen per total tissue area was determined using ImageJ Analysis software from 20 non-overlapping 200x microscopic fields (field area =

0.148mm^2) and data are presented as the percent collagen per total tissue area plus or minus the SEM.

2.3.7 SIV-RNA and SIV-DNA detection using RNAscope and DNAscope

SIV-RNA was detected *in situ* using the RNAscope ® 2.5 HD Assay-Red (Advanced Cell Diagnostics [ACD]; Newark, CA) on formalin-fixed, paraffin-embedded, 5-µm thick sections of three CNS cortical and one cardiac tissue per animal, as previously described [197]. Sections were deparaffinized in xylenes and 100% ethanol and air dried. Antigen retrieval with boiling citrate buffer for 15 min and protease digestion at 40°C for 30 min was performed [197]. SIV-RNA-specific probes targeting SIVmac239 envelope (ACD), RNAscope® positive control Mmu-PPIB (ACD) or RNAscope® negative control DapB (ACD) were applied to sections. Quantitation of SIV-RNA+ cells/mm^2 in the CNS and heart were achieved by counting and averaging the numbers of SIV-RNA+ cells from 20 random, non-overlapping images taken from three CNS cortical sections and one cardiac section, respectively, at 400x total magnification using the Zeiss Axio Imager.M1 microscope and AxioVision. SIV-DNA was detected *in situ* using an SIV-DNA sense probe (ACD) for RNAscope® Assay on one cardiac section per animal. DNAscope was performed, as previously described [176, 198]. To reduce non-specific signal, heart tissues were pre-treated with 2N HCL for 30 min at room temperature. Following DNAscope, cardiac sections were scanned and digitized with Aperio CS2 Scanscope. SIV-DNA+ cells/mm^2 were quantified using a positive pixel count algorithm in Aperio's Spectrum Plus analysis program (version 9.1, Aperio ePathology Solutions, Leica Biosystems; Wetzlar, Germany), as previously described [199].

2.3.8 Plasma biomarker ELISAs

Plasma IL-18 (R & D Systems; Minneapolis, MN), galectin-3 (R & D Systems), galectin-9 (R & D Systems) and soluble CD163 (sCD163) (IQ Products; Groningen, Netherlands) concentrations were analyzed with ELISAs according to the manufacturer's protocol. Concentrations of galectin-3 and galectin-9 were measured using BioTek Powerwave 340 (BioTek; Winooski, VT) at a wavelength of 450 nm and a correction wavelength of 540 nm. Concentrations of plasma galectin-3 and -9, and sCD163 were presented as ng/mL. Concentrations of plasma IL-18 were presented as pg/mL.

2.3.9 Flow cytometry

Flow cytometric analysis was conducted on 100 μl aliquots of whole blood collected in EDTA-coated tubes. Blood samples were taken at 0, 8, 19 days post infection (dpi) and terminally. Samples from animals housed at the NERPC were shipped and analyzed the same day and samples from animals at the TNPRC were shipped overnight. Erythrocyte lysis was performed (ImmunoPrep Reagent System, Beckman Coulter; Brea, CA), followed by 2 washes with PBS, and incubation with fluorochrome-conjugated antibodies including anti-CD14-APC (clone: M5E2, BD Pharmingen; San Diego, CA), anti-CD16-PE (clone: 3G8, BD Pharmingen) anti-HLA-DR-PerCP-Cy5.5 (clone: L243, BD Pharmingen). All samples were fixed in 2% paraformaldehyde and results were acquired on a BD FACS Aria (BD Biosciences; San Jose, CA) and analyzed with Tree Star Flow Jo version 8.7. Monocytes were first selected based on size and granularity (FSC vs SSC)

followed by selection of HLA-DR$^+$ CD14$^+$ cells. From this acquisition gate the percentage of monocyte subsets expressing CD14 and/or CD16 could be determined. The absolute number of peripheral blood monocytes for each animal was calculated by multiplying the total white blood cell count by the total percentage of monocytes determined by flow cytometry.

2.3.10 Statistical analysis

Statistical analyses were done using Prism version 10 software (GraphPad Software, Inc.; San Diego, CA). Comparisons between animals with CVD and SIVE, animals with CVD or SIVE alone, and NSF and SIVnoE animals were made using a one-way analysis of variance (ANOVA) with Dunn's multiple comparisons. Comparisons between CVD only and NSF only, and SIVE only and SIVnoE only animals were made using a non-parametric Mann-Whitney t-test. A Spearman rank test was used for all correlations. Statistical significance was accepted at p< 0.05.

2.3.11 Study approval

Animals were housed at Harvard University's New England Regional Primate Research Center (NEPRC) or Tulane University's National Primate Center (TNPRC) and handled in strict accordance with Harvard University's and Tulane University's National Primate Research Center Institutional Animal Care and Use Committee (IACUC). Animal IACUC approval from NEPRC and TNPRC was granted for all procedures: The NERPC protocol number for this study was 04420 and the animal welfare assurance number was A3431-01.

The TNRPC the protocol number is 3497 and the animal welfare assurance number is A4499-01. All human cardiac tissues from the Manhattan HIV Brain Bank cohort were obtained and examined with the written informed consent of all individuals prior to participation in this study. These were de-identified post mortem tissue specimens and were therefore IRB exempt.

2.4 Results

2.4.1 A greater number of animals with AIDS co-develop CVD pathology and SIVE than CVD pathology or SIVE alone.

Of twenty-three animals sacrificed with AIDS defining criteria (weight loss, intractable diarrhea, recurrent secondary infections) **(Table 2.1)**, based on histopathology, 10 (43.5%) co-developed CVD pathology (macrophage accumulation, collagen deposition, cardiomyocyte degeneration) and SIVE [SIV-RNA, macrophage accumulation, multi-nucleated giant cells (MNGC)], 6 (26.1%) had CVD pathology or SIVE alone, and 7 (30.4%) had no significant histopathological findings (NSF) and SIV no encephalitis (SIVnoE). Of the sixteen animals with AIDS defining histopathology **(Table 2.1)**, 10 (62.5%) co-developed CVD pathology and SIVE, and 6 (37.5%) had CVD pathology or SIVE alone (Table 1). There were greater percentages of animals with a) cardiomyocyte degeneration [NSF and SIVnoE (0/7), CVD-pathology or SIVE alone (1/6) and CVD pathology and SIVE (5/10)]; b) degree of cardiac fibrosis [NSF or SIVnoE (0/7), CVD-pathology or SIVE alone (3/6; 1 severe), CVD pathology and SIVE (6/10; 2 severe)]; and c) cardiac inflammation [NSF and SIVnoE (0/7), CVD pathology or SIVE (3/6, 1 mild) and CVD pathology and SIVE (9/10; moderate-to-severe)] in animals that co-developed CVD pathology and SIVE. There were no significant differences in the average survival days post infection (dpi) among animals with CVD and SIVE (104.8 ± 9.4 dpi), CVD or SIVE alone (99.8 ± 10.9 dpi), and NSF and SIVnoE (168.6 ± 47.2 dpi) nor in age or weight among CVD pathology and SIVE (7.7 ± 0.9 years, 10 ± 0.8 kg), CVD pathology or SIVE alone (6.9 ± 0.7 years, 8.6 ± 1.6 kg), and NSF and SIVnoE (5.7 ± 1.5 years, 7.3 ± 1.2 kg) **(Supplementary Table 2.1).**

2.4.2 Animals with CVD pathology and SIVE had greater numbers of cardiac macrophages than animals with NSF and SIVnoE.

Animals with CVD and SIVE had increased numbers of CD68+ (2.5-fold), CD163+ (2.7-fold), CD206+ (2.5-fold), and MAC387+ (1.8-fold) cardiac macrophages, compared to animals with NSF and SIVnoE (one-way Kruskal-Wallis ANOVA, $p<0.05$, with Dunn's multiple comparisons) **(Table 2.2).** There were similar numbers of cardiac CD163+, CD206+, CD68+, and MAC387+ macrophages in animals with CVD and SIVE compared to animals with CVD or SIVE alone, and similar numbers of cardiac CD3+ T lymphocytes **(Table 2.2)**.

2.4.3 Animals with CVD pathology and SIVE had greater cardiac collagen deposition than animals with NSF and SIVnoE.

Animals with both CVD and SIVE (2.5-fold; $20 \pm 1.5\%$), and CVD or SIVE alone (1.9-fold; $15.4 \pm 2.1\%$) had similar areas of collagen deposition, but greater percent of collagen deposition than animals with NSF and SIVnoE ($7.9 \pm 0.5\%$) (one-way Kruskal-Wallis ANOVA, $p<0.05$, with Dunn's multiple comparisons) **(Figure 2.1).** There were no correlations between the numbers of cardiac macrophages and percent area of cardiac collagen deposition in any of the groups.

2.4.4 Animals with SIVE alone had greater cardiac inflammation and collagen deposition than animals with SIVnoE.

Animals with SIVE alone had greater numbers of CD68+ (1.9-fold), CD163+ (2.1-fold), CD206+ (2.4-fold), and MAC387+ (1.9-fold) cardiac macrophages compared to animals with SIVnoE alone (Mann-Whitney t-test, p<0.05) **(Supplementary Table 2.2A).** SIVE alone animals had more cardiac collagen deposition (1.8-fold) than SIVnoE animals (Mann-Whitney t-test, p<0.01) **(Supplementary Table 2.2B).** There were no significant differences between the numbers of cardiac CD3+ T lymphocytes in these groups.

2.4.5 Animals with both CVD and SIVE had more SIV-RNA+ and SIV-gp41+ cells in the CNS and heart than animals with CVD or SIVE alone, and NSF and SIVnoE animals.

Overall, we found a greater number of SIV-RNA+ cells (3.8-fold) (Mann-Whitney t-test, p<0.05) and SIV-gp41+ cells (8.2-fold) in the CNS compared to the cardiac tissues in all animals. Animals with CVD pathology and SIVE had a greater number of SIV-RNA + (3.6-fold) and SIV-gp41+ cells (8.7-fold) in the CNS compared to the heart. Animals with CVD and SIVE had a trend of increased numbers of CNS SIV-RNA+ cells (3.8-fold), CNS SIV-gp41+ cells (1.7-fold), cardiac SIV-RNA+ (2.7-fold), cardiac SIV-gp41+ cells (3.6-fold) than animals with CVD or SIVE alone **(Table 2.3).** All cardiac SIV-RNA+ cells were CD68+ and CD206+ macrophages not CD3+ T lymphocytes **(Figure 2.2).**

2.4.6 Animals with SIVE alone had increased numbers of CNS SIV-RNA+ macrophages compared to SIVnoE animals.

Animals with SIVE alone had increased numbers of CNS SIV-RNA+ cells (18.4-fold), and but similar, low numbers of cardiac SIV-RNA+ cells and SIV-gp41+ cells, and CNS SIV-gp41+ cells compared to animals with SIVnoE alone (Mann-Whitney t-test p<0.01) **(Supplementary Table 2.3).** Animals with CVD-pathology alone had similar numbers of CNS SIV-RNA+ cells, cardiac SIV-RNA+ cells, and CNS SIV-gp41+ cells compared to NSF animals **(Supplementary Table 2.3).**

2.4.7 Animals with CVD-pathology and SIVE have greater numbers of CD14+ CD16+ monocytes compared to NSF and SIVnoE animals.

Animals with CVD and SIVE had increased numbers of CD14+ CD16+ monocytes early [8 dpi (81.3 ± 13.4 CD14+ CD16+ monocytes; 2.8-fold) and 19 dpi (104.8 ± 23.6 CD14+ CD16+ monocytes; 3.1-fold)] and terminally (223.6 ± 63.1 CD14+ CD16+ monocytes; 5.9-fold) compared to animals with NSF and SIVnoE (29.5 ± 5.1, 34 ± 11.7, and 37.8 ± 3.1 CD14+ CD16+ monocytes, respectively) (one-way Kruskal-Wallis ANOVA, *p<0.05, with Dunn's multiple comparisons) **(Figure 2.3A).** Animals with CVD and SIVE had similar numbers of CD14+ CD16+ monocytes early (8 dpi; 1.3-fold) and a trend of increased CD14+ CD16+ monocytes terminally (2.9-fold) compared to CVD-pathology or SIVE alone animals (62.5 ± 15.9 and 78.1 ± 18.6 respectively) **(Figure 2.3A).** There was a correlation between the numbers of CD14+ CD16+ monocytes early (8 dpi; r= 0.70, p<0.01 and 19 dpi; r= 0.57, p<0.05) and terminally (r= 0.61, p<0.05) with cardiac collagen deposition (Spearman's correlation, p<0.05) **(Figure 2.3B-D).**

2.4.8 Animals with CVD and SIVE had increased plasma biomarkers associated with monocyte and macrophage activation.

Animals with CVD and SIVE had increased plasma sCD163 (2.9-fold) and IL-18 (2.4-fold), compared to animals with CVD or SIVE alone, and NSF and SIVnoE animals (one-way Kruskal-Wallis ANOVA, *p<0.05, with Dunn's multiple comparisons) (Table 2.4), and similar levels of galectin-3 (1.2-fold) and galectin-9 (1.5-fold) compared to animals with CVD or SIVE alone, and NSF and SIVnoE animals **(Table 2.4)**. Plasma sCD163 positively correlated with galectin-3 (r= 0.74, p<0.05) and IL-18 (r= 0.93, p<0.001), and trended to correlate with galectin-9 (r= 0.67, p= 0.06). Consistent with previous studies in HIV infected individuals [82, 83], there was a positive correlation between plasma galectin-9 and plasma viral load (r= 0.76, p<0.01) (Spearman's correlation, p<0.05) **(Figure 2.4)** but there were no significant correlations between plasma virus and galectin-3, IL-18, and sCD163. Animals with CVD-pathology alone had a trend of increased plasma sCD163 (2.2-fold) and similar levels of IL-18, galectin-3, and galectin-9 compared to NSF animals (Mann-Whitney t-test p<0.05) **(Table 2.5).** SIVE alone animals had greater plasma IL-18 (4.4-fold), galectin-3 (2-fold), and galectin-9 (2.1-fold) levels, and a trend of increased sCD163 (2.1-fold) compared to animals SIVnoE animals **(Table 2.5).**

2.4.9 HIV-infected individuals with HIVE have greater cardiac inflammation and fibrosis than HIVnoE individuals.

We next sought to determine whether HIV-infected individuals with HIVE (n =11) had increased cardiac inflammation and fibrosis over that seen in HIV infected individuals without encephalitis (HIVnoE) (n =11) **(Table 2.6).** In age-, race- and sex-matched

individuals, we found that the HIVE group had greater numbers of CD68+ (1.7-fold, 200.62 ± 12.41 cells), CD163+ (1.5-fold, 254.29 ± 8.05 cells), and MAC387+ (1.7-fold, 78.52 ± 4.94 cells) cardiac macrophages compared to individuals with HIVnoE (120.49 ± 8.44 CD68+ macrophage, 173.42 ± 7.55 CD163+ macrophage, and 46.58 ± 4.29 MAC387+ macrophage) (Mann-Whitney t test, p<0.05) **(Figure 2.5A-C).** There were similar numbers of cardiac CD3+ T lymphocytes in individuals with HIVE (28.15 ± 6.97 cells) compared to individuals with HIVnoE (22.11 ± 5.39 cells) **(Figure 2.5D).** Additionally, there was a higher percentage of cardiac collagen deposition (1.8-fold, 29.87 ± 1.63%) in the HIVE group compared to the HIVnoE group (17.06 ± 1.26%) (Mann-Whitney t test, p<0.05) **(Figure 2.5E).** These data are similar to the results we find in SIV infected monkeys, supporting the translational nature of the monkey data.

Table 1. CVD-pathology and SIVE co-develops more frequently with AIDS than CVD-pathology or SIVE alone.					
Group	Animal ID	Cardiac inflammation	Cardiac fibrosis	Cardiomyocyte degeneration	CNS pathology
NSF and SIVnoE	186-05	NSF	NSF	NSF	SIVnoE
NSF and SIVnoE	168-05	NSF	NSF	NSF	SIVnoE
NSF and SIVnoE	288-07	NSF	NSF	NSF	SIVnoE
NSF and SIVnoE	FT73	NSF	NSF	NSF	SIVnoE
NSF and SIVnoE	FG73	NSF	NSF	NSF	SIVnoE
NSF and SIVnoE	JR51	NSF	NSF	NSF	SIVnoE
NSF and SIVnoE	JR93	NSF	NSF	NSF	SIVnoE
CVD or SIVE alone	FD37	Mild	Mild	NSF	SIVnoE
CVD or SIVE alone	FC42	Mild	Mild	Moderate	SIVnoE
CVD or SIVE alone	FB92	Mild	Severe	NSF	SIVnoE
CVD or SIVE alone	FD80	NSF	NSF	NSF	SIVE
CVD or SIVE alone	IK28	NSF	NSF	NSF	SIVE
CVD or SIVE alone	KN69	NSF	NSF	NSF	SIVE
CVD and SIVE	JD29	NSF	NSF	Mild	SIVE
CVD and SIVE	JE87	Mild	NSF	NSF	SIVE
CVD and SIVE	DB79	Mild	Mild	NSF	SIVE
CVD and SIVE	FR56	Mild	Mild	Mild	SIVE
CVD and SIVE	LB12	Mild	NSF	Mild	SIVE
CVD and SIVE	KT79	Mild	NSF	NSF	SIVE
CVD and SIVE	CM07	Mild	Moderate	NSF	SIVE
CVD and SIVE	244-96	Moderate	Mild	NSF	SIVE
CVD and SIVE	55-05	Moderate	Severe	Mild	SIVE
CVD and SIVE	FD05	Severe	Severe	Moderate	SIVE

Table 2.1. CVD pathology and SIVE develop together more frequently than does CVD pathology or SIVE alone. Twenty-three SIV-infected, CD8+ T-lymphocyte depleted rhesus macaques were used in this study, all of which were sacrificed with AIDS. Sections of left ventricular tissue (cardiac tissue) were examined blindly by a veterinary pathologist and the presence and severity of cardiac inflammation, cardiac fibrosis and cardiomyocyte degeneration was determined. Animals were scored with no significant findings (NSF), mild, moderate, or severe CVD pathology. Ten animals were found to have NSF, and 13 animals were found to have CVD pathology. SIVE was diagnosed postmortem and based

on the presence of SIV virus in the CNS and MNGC. Thirteen animals had SIVE and ten

animals had SIVnoE. Animals were grouped by the presence of CVD and SIVE together

(CVD and SIVE, n = 10), one of either CVD or SIVE alone (n = 6), or NSF and SIVnoE

(n =7).

Pathology	CD68+ Macrophage (cells/ mm²)	CD163+ Macrophage (cells/ mm²)	CD206+ Macrophage (cells/ mm²)	MAC387+ Macrophages (cells/ mm²)	CD3+ T lymphocytes (cells/ mm²)
CVD and SIVE	143.1 ± 19.6	325.3 ± 36.8	202 ± 19	31.4 ± 8.8	23.1 ± 4.7
CVD or SIVE alone	107.6 ± 14.6 **	229 ± 34.4 **	116 ± 26.5 **	22.3 ± 5.4 *	22.1 ± 8.3
NSF and SIVnoE	56.6 ± 8.2	122.1 ± 22.9	82.5 ± 16.6	17.4 ± 5.1	10.9 ± 4.2
ANOVA	p< 0.01	p< 0.001	p< 0.01	p< 0.05	p= 0.11

Table 2. Animals with CVD-pathology and SIVE had more cardiac macrophages than animals with CVD-pathology or SIVE alone, and NSF and SIVnoE animals.

Table 2.2. Animals with CVD pathology and SIVE had increased numbers of cardiac macrophages compared to animals with CVD pathology or SIVE alone, and NSF and SIVnoE animals. Animals were grouped based on the development of both CVD and SIVE (n=8), CVD or SIVE alone (n=5), or NSF and SIVnoE (n=7). Sections of cardiac tissue were stained immunohistochemically with antibodies recognizing CD163+, CD68+, MAC387+, or CD206+ macrophages (A-D) and CD3+ T-lymphocytes (E). Twenty random, non-overlapping images were sampled at 200x fields of view and the average number of cells/mm^2 were expressed as plus or minus the SEM. P-values were calculated using a one-way Kruskal-Wallis ANOVA, *p< 0.05, with Dunn's multiple comparisons (*p<0.05, **p<0.01, ***p<0.001).

Pathology	Cardiac SIV-DNA+ (cells/mm^2)	CNS SIV-RNA+ (cells/mm^2)	Cardiac SIV-RNA+ (cells/mm^2)	CNS SIV-gp41+ (cells/mm^2)	Cardiac SIV-gp41+ (cells/mm^2)
Table 3. Animals with CVD-pathology and SIVE had more SIV-RNA+ and SIV-gp41+ cells in the CNS than animals with CVD-pathology or SIVE alone.					
CVD and SIVE	0.4 ± 0.2	19.3 ± 2.3 ⎤ *	5.40 ± 2.4	31.5 ± 11.2	3.6 ± 1.9
CVD or SIVE alone	0.7 ± 0.4	5.1 ± 3.1 ⎦	0.45 ± 0.4	18.5 ± 8.8	0
NSF and SIVnoE	1.7 ± 0.3	0.7 ± 0.2	2.7 ± 1.9	8.1 ± 2.3	4.1 ± 1.3
ANOVA	p= 0.24	p< 0.05	p= 0.20	p= 0.67	p= 0.15

Table 2.3. Animals with CVD pathology and SIVE had more productively infected cells in the CNS compared to animals with CVD-pathology or SIVE alone, and NSF and SIVnoE animals. Animals were grouped based on the development of both CVD and SIVE, CVD or SIVE alone, and NSF and SIVnoE. The average number of SIV-DNA+ cells in the heart and, SIV-RNA+ and SIV-gp41+ cells in CNS cortical and cardiac tissues were reported. One section of left ventricle and three sections of CNS cortical from SIV-infected macaques (n=10) were assessed for SIV-RNA+ cells/mm2. Measurements of CNS SIV-RNA+ cells/mm2 were determined by averaging counts from three CNS cortical sections. One section of CNS cortical and cardiac tissues (n=13) were assessed for SIV-gp41+ cells/mm2 plus or minus SEM. Twenty, random, non-overlapping 400x fields of view were sampled for each section per animal and the average number of SIV-gp41+ cells/mm2 were determined. P-values were calculated using a one-way Kruskal-Wallis ANOVA, *p< 0.05, with Dunn's multiple comparisons. NS, no statistical significance (*p<0.05, **p<0.01, ***p<0.001, ****p<0.0001).

Pathology	Plasma sCD163 (ng/mL)	Plasma IL-18 (pg/mL)	Plasma galectin-3 (ng/mL)	Plasma galectin-9 (ng/mL)
CVD and SIVE	956 ± 248.6	2431 ± 474.7	60.2 ± 11.4	76.5 ± 14.7
CVD or SIVE alone	333.8 ± 76.7	1017 ± 250	50.3 ± 8.6	52.5 ± 16.1
NSF and SIVnoE	501.8	298.9	20.5	62.6
ANOVA	p< 0.05	p< 0.05	p= 0.6	p= 0.24

Table 4. Plasma sCD163, IL-18, galectin -3 and -9 are higher in animals with CVD-pathology and SIVE than animals with CVD–pathology or SIVE alone.

Table 2.4. Plasma biomarkers associated with myeloid cell activation are increased in SIV infected animals with CVD-pathology and SIVE. Terminal plasma sCD163, IL-18, galectin-3 and galectin-9 were measured in animals with NSF and SIVnoE, CVD or SIVE alone, and CVD and SIVE. ELISAs were performed according to the manufacturer's protocol. P-values were calculated using a one-way Kruskal-Wallis ANOVA, *p< 0.05, with Dunn's multiple comparisons. (*p<0.05, **p<0.01, ***p<0.001, ****p<0.0001).

Table 5. Animals with SIVE alone had more plasma sCD163, IL-18, and galectin-3 and -9 than animals with SIVnoE alone.				
SIVE Pathology	**Plasma sCD163 (ng/mL)**	**Plasma IL-18 (pg/mL)**	**Plasma galectin-3 (ng/mL)**	**Plasma galectin-9 (ng/mL)**
SIVE	793.3 ± 197.7	2081 ± 338 ⎤**	62.3 ± 7.7 ⎤*	78.9 ± 12 ⎤*
SIVnoE	379.2 ± 122.6	476.9 ± 147.7 ⎦	30.7 ± 5.9 ⎦	37.8 ± 9.17 ⎦
Cardiac Pathology	**Plasma sCD163 (ng/mL)**	**Plasma IL-18 (pg/mL)**	**Plasma galectin-3 (ng/mL)**	**Plasma galectin-9 (ng/mL)**
CVD	878.3 ± 232.6	1720 ± 452.3	51.5 ± 8.7	62.5 ± 12.5
NSF	395.1 ± 80.6	1198.9 ± 334.7	55 ± 12.7	78.9 ± 15.5

Table 2.5. Animals with SIVE alone had more plasma sCD163, IL-18, and galectin-3 and -9 than animals with SIVnoE. Terminal plasma sCD163, IL-18, galectin-3 and galectin-9 were measured in animals with SIVnoE or SIVE alone., and NSF or CVD alone. P-values were calculated using non-parametric Mann-Whitney T-tests with significance accepted at $p < 0.05$. NSF, no significant findings. CVD-pathology, cardiovascular pathology. SIVnoE, SIV with no encephalitis. SIVE, SIVE encephalitis (*$p<0.05$, **$p<0.01$, ***$p<0.001$, ****$p<0.0001$).

Table 6. Patients used in study.					
MHBB ID	**AGE**	**SEX**	**RACE**	**CD4+ T lymphocytes (< 200 cells/mL)**	**HIVE**
MHBB552	47	m	w	YES	HIVnoE
MHBB558	51	m	h	YES	HIVnoE
MHBB625	48	m	b	YES	HIVnoE
010003	45	m	w	NO	HIVnoE
010011	42	m	h	YES	HIVnoE
MHBB532	47	m	h	YES	HIVnoE
010171	45	m	b	YES	HIVnoE
MHBB533	41	m	h	NO	HIVnoE
030025	46	m	b	YES	HIVnoE
020025	37	m	h	YES	HIVnoE
030024	43	m	b	YES	HIVnoE
MHBB509	46	m	w	NO	HIVE
MHBB519	50	m	h	YES	HIVE
MHBB540	47	m	b	YES	HIVE
010017	43	m	w	YES	HIVE
010026	37	m	h	YES	HIVE
010065	46	m	h	YES	HIVE
010070	37	m	b	YES	HIVE
010103	40	m	h	YES	HIVE
010129	43	m	b	YES	HIVE
010231	47	m	h	YES	HIVE
030015	43	m	b	YES	HIVE

Table 2.6. Patients from the Manhattan HIV Brain Bank (MHBB) were examined for the prevalence of HIVE. Twenty-two HIV infected males from the MHBB were assessed. Eleven individuals had HIV with no encephalitis (HIVnoE) and an average age of 44.7± 1.15 years. Nine HIVnoE individuals had a CD4+ T lymphocyte count <200 cells. Eleven individuals have HIV encephalitis (HIVE) and an average age of 43.5± 1.27 years. Ten HIVE individuals had a CD4+ T lymphocyte count <200 cells. Each individual with HIVE was matched in sex, race, and age to an individual with HIVnoE.
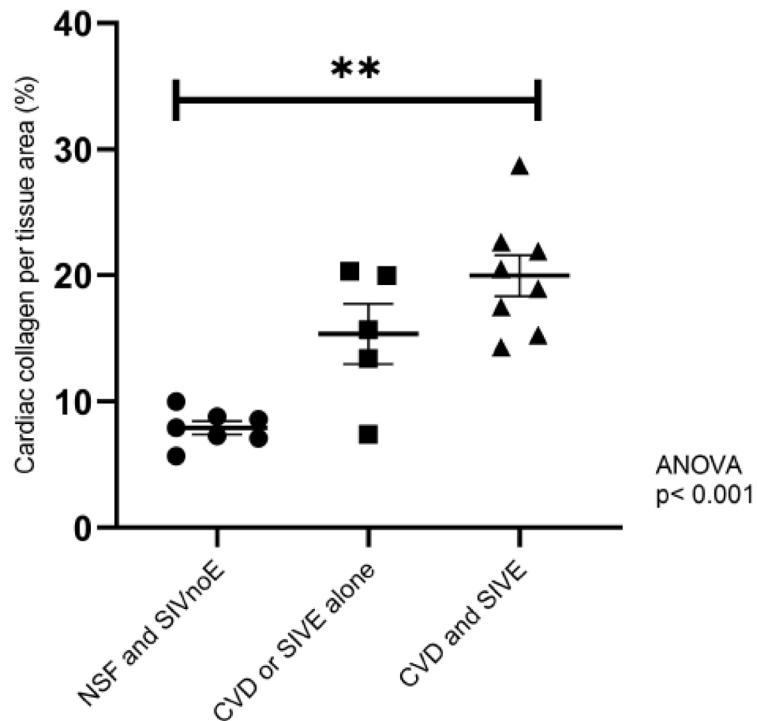
Figure 2.1. Animals with CVD-pathology and SIVE had a greater percentage of area of cardiac collagen deposition than animals with CVD-pathology or SIVE alone, and NSF and SIVnoE animals. Left ventricle sections from animals grouped as having NSF and SIVnoE (n=7, circles), CVD or SIVE alone (n= 5, squares) and CVD and SIVE (n=8, triangles) were assessed for cardiac collagen deposition using a Massons trichrome stain. Fibrosis was determined as the percentage of collagen per total tissue area and was quantified for each animal using ImageJ Analysis software (non-parametric, one-way ANOVA, Dunn's multiple comparisons (*p<0.05, **p<0.01, ***p<0.001, ****p<0.0001).
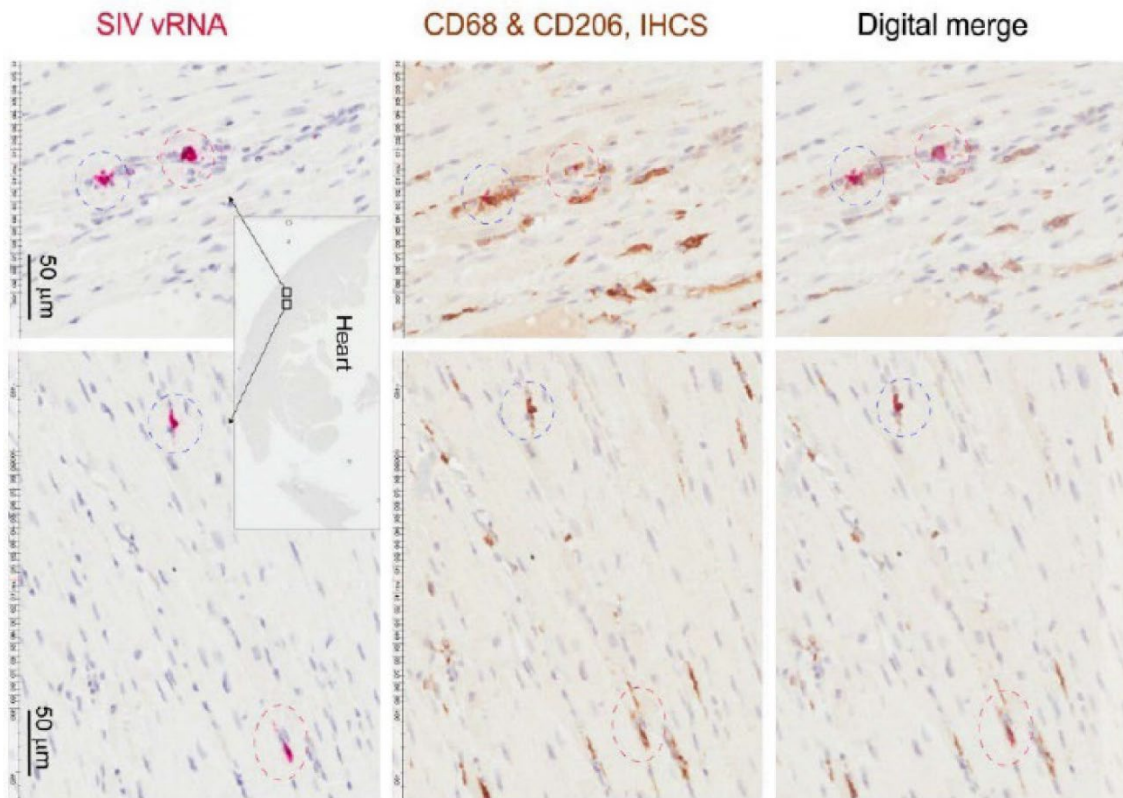
Figure 2.2. CD68+ and CD206+ cardiac macrophages are SIV-RNA+ in SIV infected monkeys. Sections of left ventricle were stained immunohistochemically for CD68+ and CD206+ macrophages. Cardiac SIV-RNA was detected using RNAscope *in situ* hybridization. Images were digitally merged using Aperio's Specturm Plus analysis program.
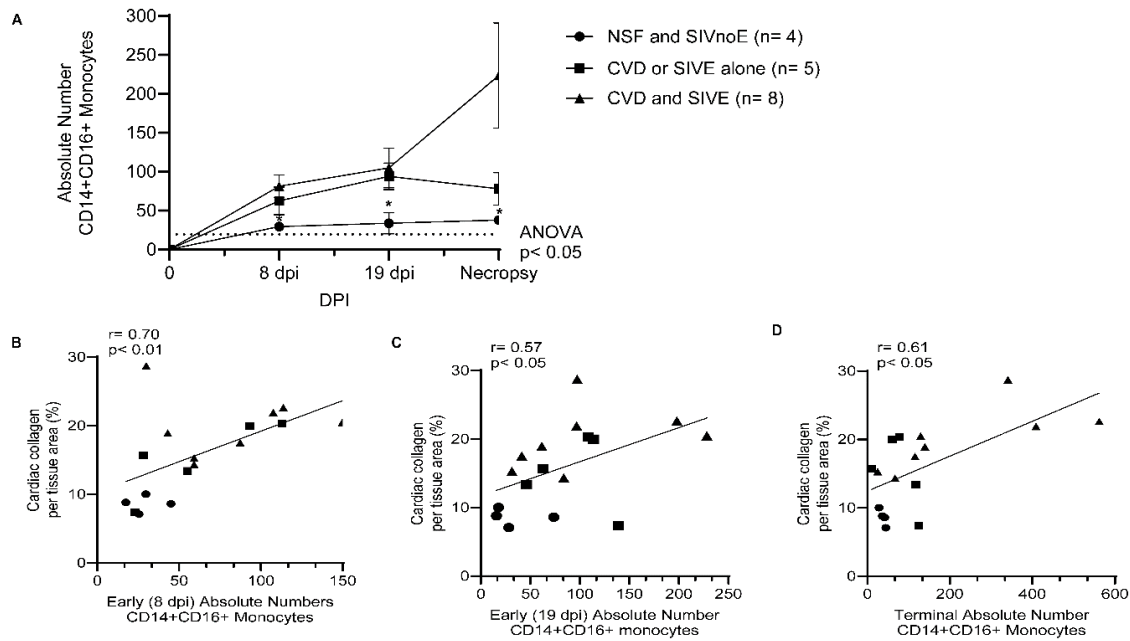
Figure 2.3. Animals with CVD and SIVE had increased numbers of CD14+ CD16+ monocytes early and terminally compared to animals with CVD or SIVE alone, and NSF and SIVnoE animals. (A). Absolute numbers of CD14+ CD16+ monocytes, as determined by flow cytometry and CBC, were assessed early (8 dpi and 19 dpi) and terminally in animals with NSF and SIVnoE (n=4, circle), CVD or SIVE alone (n= 5, square and CVD and SIVE (n=8, triangle). The pre-infection baseline was 19.38 CD14+ CD16+ monocytes (one-way ANOVA, post-hoc, non-parametric, Mann-Whitney t-test, * $p<0.05$ **(B-D).** The absolute numbers of CD14+ CD16+ monocytes at early infection (8 dpi and 19 dpi) and terminally from animals with NSF and SIVnoE (n=4, circle), CVD or SIVE alone (n= 5, square), and CVD and SIVE (n= 8, triangle) positively correlated with the percent cardiac collagen per tissue area (non-parametric, Spearman's correlation, $p< 0.05$) (*$p<0.05$, **$p<0.01$, ***$p<0.001$, ****$p<0.0001$).
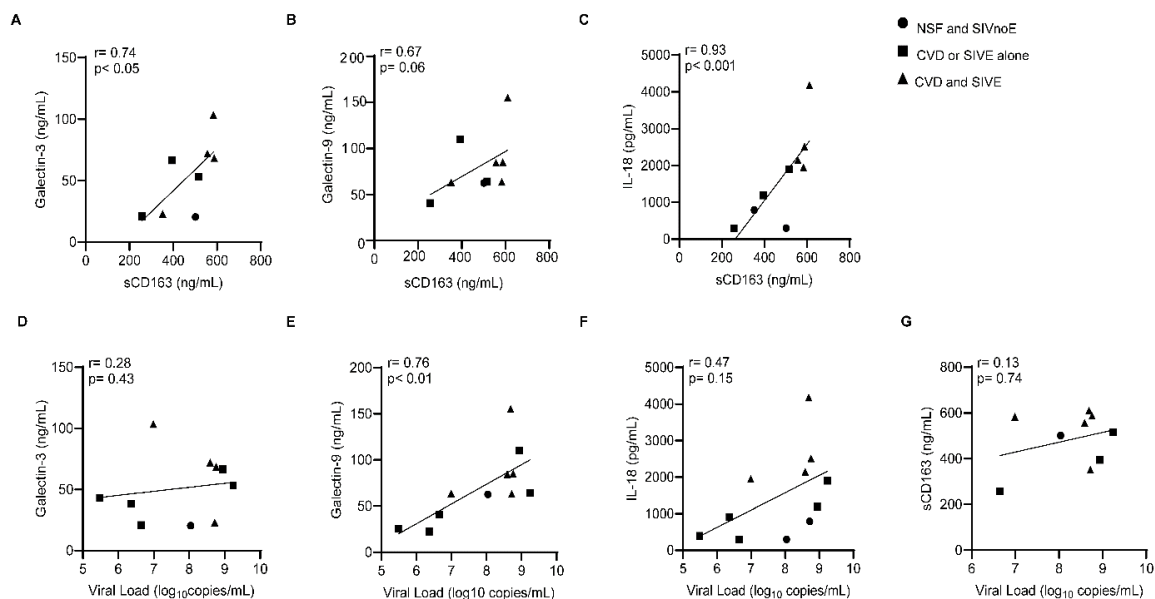
Figure 2.4. Plasma sCD163 correlates with galectins- 3 and -9, and IL-18 in SIV-infected monkeys. (A-C). Spearman's correlation was used to assess the relationship between terminal levels of plasma galectins -3 and -9, and IL-18, and terminal plasma sCD163. **(D-G).** Spearman's correlation was used to assess the relationship between terminal levels of plasma galectins-3 and -9, IL-18, and sCD163, and plasma viral load. Data generated here, were from n=23 animals. P-values accepted at Spearman's p< 0.05. (*p<0.05, **p<0.01, ***p<0.001, ****p<0.0001).
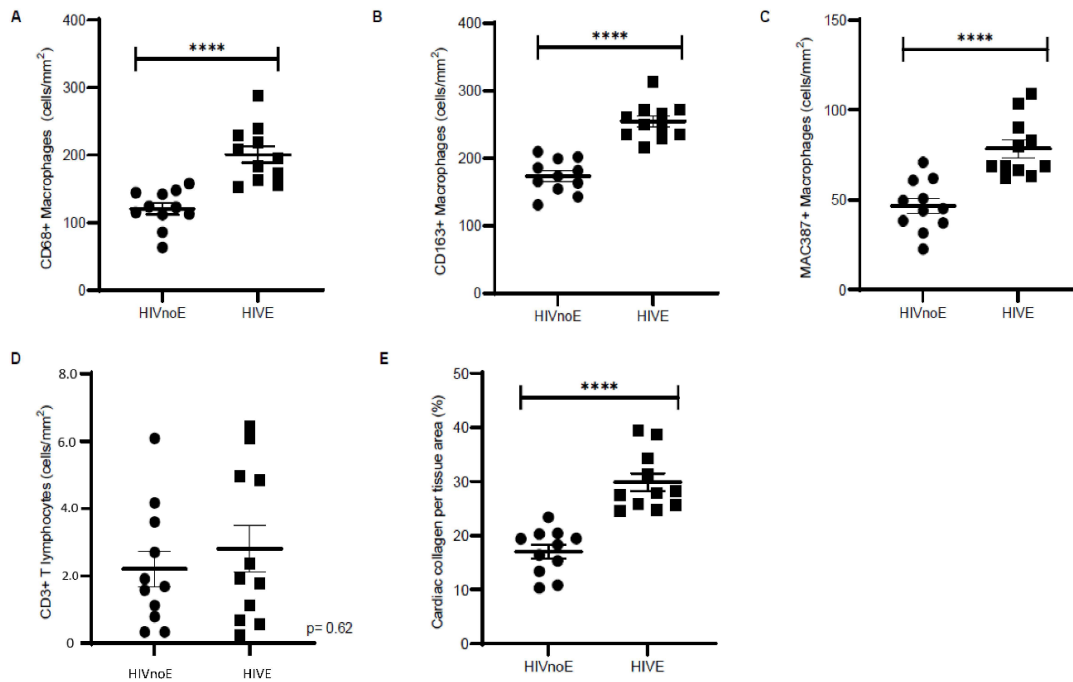
Figure 2.5. Individuals with HIVE had greater numbers of cardiac macrophages and collagen deposition than HIVnoE individuals. (A-D). Increased CD68+, CD163+, and MAC387+ cardiac macrophages in individuals with HIVE. Trend of increased numbers of cardiac CD3+ T lymphocytes regardless of HIVE. Sections of cardiac tissue were stained immunohistochemically with antibodies recognizing CD68+, CD163+, or MAC387+ macrophages, and CD3+ T-lymphocytes. Twenty random, non-overlapping images were sampled at 200x fields of view, and the data was expressed as the average number of cells/mm^2 plus or minus the SEM. Increased cardiac collagen deposition in individuals with HIVE. Cardiac collagen deposition was assessed using a Masson's trichrome stain.

Fibrosis was determined as the percentage of cardiac collagen per total tissue area and was quantified by using ImageJ Analysis software with twenty random, non-overlapping images sampled at 200x fields of view. Cardiac tissues were supplied by the Manhattan HIV Brain Bank. Data was presented as the average percentage of collagen plus or minus the SEM. P-values were calculated using a nonparametric, Mann-Whitney t test, HIVnoE (circles); HIV with no encephalitis. HIVE (squares); HIV encephalitis (*$p < 0.05$, **$p < 0.01$, ***$p < 0.001$, ****$p < 0.0001$).

2.6 Supplementary Tables

Supplementary Table 1. Characteristics of the rhesus macaques examined.				
Group	**Animal ID**	**Sex**	**Age (years)**	**Weight (kg)**
NSF and SIVnoE	168-05	M	3.6	4.6
NSF and SIVnoE	288-07	M	1.3	4.9
NSF and SIVnoE	FT73	M	5.1	6.1
NSF and SIVnoE	FG73	M	12.3	8.8
NSF and SIVnoE	JR51	M	5.6	7.3
NSF and SIVnoE	JR93	M	6.3	12.3
CVD or SIVE alone	FD37	M	6.4	10.3
CVD or SIVE alone	FC42	M	6.5	9.0
CVD or SIVE alone	FB92	M	5.5	1.3
CVD or SIVE alone	FD80	M	6.2	8.9
CVD or SIVE alone	IK28	M	10.3	12.3
CVD or SIVE alone	KN69	M	6.3	9.9
CVD and SIVE	JD29	M	9.4	10.9
CVD and SIVE	JE87	M	9.4	12.2
CVD and SIVE	DB79	M	10.3	10.5
CVD and SIVE	FR56	M	5.4	9.0
CVD and SIVE	LB12	M	5.5	11.2
CVD and SIVE	KT79	M	6.2	12.5
CVD and SIVE	CM07	M	9.4	11.9
CVD and SIVE	244-96	M	12.6	9.1
CVD and SIVE	55-05	M	3.7	4.0
CVD and SIVE	FD05	M	5.4	8.4

Supplementary Table 2.1. Characteristics of the rhesus macaques examined in this study. Twenty-three SIV-infected, CD8+ T-lymphocyte depleted rhesus macaques were used in this study, all of which were sacrificed with AIDS. Sections of left ventricular tissue (cardiac tissue) were examined blindly by a veterinary pathologist and the presence and severity of cardiac histopathology was scored as no significant cardiac pathology (findings) (NSF) or cardiac pathology was present (CVD). SIV encephalitis (SIVE) was diagnosed postmortem and based on the presence of SIV virus in the CNS and MNGC. All animals were males and were euthanized following the development of simian AIDS.

A.

Cardiac Macrophage Subsets (cells/mm^2)	SIVnoE	SIVE	p-value
CD163+ macrophages	148.18 ± 22.84	312 ± 33.13	< 0.01
CD206+ macrophages	81.96 ± 13.16	195.35 ± 17.14	< 0.05
CD68+ macrophages	69.47 ± 12.09	132.15 ± 15.72	< 0.01
MAC387+ macrophages	16.97 ± 3.59	31.45 ± 7.31	NS
CD3+ T-lymphocytes	14.83 ± 5.14	22.21 ± 4.10	NS

B.

Percent Cardiac Collagen per Tissue Area (%)	SIVnoE	SIVE	p-value
	10.45 ± 1.36	18.75 ± 1.71	< 0.01

Supplementary Table 2.2. Animals with SIVE alone had greater numbers of cardiac macrophages and cardiac collagen deposition compared to animals with SIVnoE. (A). Animals were grouped based on SIVnoE alone (n=10) and SIVE alone (n=10). Sections of cardiac tissue from all animals were stained immunohistochemically with antibodies recognizing CD163+, CD68+, MAC387+, or CD206+ macrophages and CD3+ T-lymphocytes. Twenty random, non-overlapping images were sampled at 200x fields and the average number of cells/mm^2 were calculated and expressed as plus or minus the SEM. **(B).** Left ventricle sections were assessed for cardiac collagen deposition using a Massons trichrome stain. The percentage of collagen per total tissue area was averaged from 20 non-overlapping 200x fields of view and expressed as the average plus or minus the standard error of the mean. Fibrosis, determined as the percentage of collagen per total tissue area, was quantified for each animal using ImageJ Analysis software. P-values were calculated using a non-parametric, Mann-Whitney t-tests with significance accepted at p<0.05.

Cardiac Pathology	Cardiac SIV-DNA+ (cells/mm^2)	CNS SIV-RNA+ (cells/mm^2)	Cardiac SIV-RNA+ (cells/mm^2)	CNS SIV-gp41+ (cells/mm^2)	Cardiac SIV-gp41+ (cells/mm^2)
CVD	0.53 ± 0.21	14.9 ± 3.2	3.60 ± 1.9	26.3 ± 9.3	2.70 ± 1.5
NSF	1.69 ± 0.32	4.62 ± 3.2	2.25 ± 1.3	15.9 ± 6.9	3.04 ± 1.3
SIVE Pathology	Cardiac SIV-DNA+ (cells/mm^2)	CNS SIV-RNA+ (cells/mm^2)	Cardiac SIV-RNA+ (cells/mm^2)	CNS SIV-gp41+ (cells/mm^2)	Cardiac SIV-gp41+ (cells/mm^2)
SIVE	0.36 ± 0.16	18.4 ± 2.1 ⎤ **	4.59 ± 1.4	32.4 ± 9.8	3.09 ± 1.7
SIVnoE	1.29 ± 0.32	1.01 ± 0.5 ⎦	1.35 ± 1.2	8.11 ± 2.1	2.43 ± 1.2

Supplementary Table 2.3. Animals with SIVE alone had greater numbers of SIV-RNA+ and SIV-gp41+ cells in the CNS. Animals were grouped based on the development of CVD and no significant findings (NSF) in cardiac tissues, or SIVE alone and SIVnoE. The average number of cardiac SIV-DNA+ cells, SIV-RNA+ and SIV-gp41+ cells in CNS cortical and cardiac tissues were reported plus or minus the SEM. One section of left ventricle was assessed for cardiac SIV-DNA+ cells in animals with CVD (n=4) compared to NSF (n=3), and in animals with SIVE (n=5) compared to SIVnoE (n=2). One section of left ventricle was assessed for cardiac SIV-RNA+ cells in animals with CVD (n=6) compared to NSF (n=3), and in animals with SIVE (n=5) compared to SIVnoE (n= 4). Three sections of CNS cortical tissues were assessed for CNS SIV-RNA+ cells in animals with SIVE (n=7) compared to SIVnoE (n=4), and in animals with CVD (n=8) compared to NSF animals (n=3). One section of left ventricle was assessed for cardiac SIV-gp41+ cells and were compared between animals with CVD (n=8) and animals with NSF (n=4), and between animals with SIVE (n=7) and animals with SIVnoE (n=5). One section of CNS cortical tissue was assessed for CNS SIV-gp41+ cells and were compared in animals with SIVE (n= 8) versus SIVnoE (n =5), and in animals with CVD (n=9) versus NSF (n=4). P-

values were calculated using a nonparametric, Mann-Whitney t-test, p< 0.05, (*p<0.05, **p<0.01, ***p<0.001, ****p<0.0001).

2.7 Conclusion- Discussion

Monocyte and macrophage activation and accumulation in the heart or the CNS are consistently correlated with the development of CVD and CVD pathology, HAND and HIVE, and SIVE [45, 61, 73, 114, 200]. Less is known or reported about the frequency that CVD, CVD pathology, HIVE and HAND with AIDS in humans and animal models, and in PLWH [177-179], or whether co-development is associated with increased monocyte activation, macrophage accumulation, or HIV and SIV infection. Here, we find that animals with AIDS co-developed CVD pathology and SIVE more frequently than CVD pathology or SIVE alone, and individuals with HIVE have increased numbers of cardiac macrophages and fibrosis compared to age- and sex-matched non-HIVE controls. We report that animals that co-developed CVD-pathology and SIVE have higher numbers of CD14+ CD16+ monocytes, and plasma sCD163, IL-18, and galectin-3 and -9, and cardiac macrophage accumulation/collagen deposition than animals with CVD or SIVE alone, and NSF and SIVnoE animals. These observations support the notion of increased monocyte activation and cardiac macrophage accumulation with the co-development of cardiac inflammation and fibrosis and SIVE, and underscore the translational findings in the monkey studies with those in HIV infected individuals.

Macrophages are key regulators of fibrogenesis through their interactions with myofibroblasts, wound healing responses, and production of profibrotic factors like galectin-3, osteopontin, and transforming growth factor- beta (TGF-β) [53, 119, 201, 202]. We and others have previously shown that CD163+ and CD206+ cardiac macrophage accumulation and monocyte activation correlates with cardiac inflammation and fibrosis

62

with HIV and SIV infection [46, 121, 122, 124]. Similarly, CD163+ and CD206+ perivascular macrophages and 5-bromo-2'-deoxyuridine-labeled (BrdU+) MAC387+ macrophage accumulation in the CNS are major components of HIVE and SIVE lesions [6, 87, 95, 97]. These observations are consistent with the notion that macrophage accumulation in the heart and CNS correlate with cardiac and SIVE pathogenesis. Our findings extend those observations to suggest that higher levels of monocyte activation, biomarkers of myeloid cell activation in plasma, and macrophage accumulation in the heart correlate with the co-development of cardiac inflammation and fibrosis and SIVE. We have previously shown, by blocking macrophage accumulation with the anti-alpha-4 integrin antibody [132, 149], the polyamine biosynthesis inhibitor methylglyoxal-bis-guanylhydrazone (MGBG) [2] or minocycline [148] correlates with decreased cardiac and CNS inflammation, cardiac fibrosis and tissue histopathology further supporting the role that macrophage accumulation has in the development of CVD alone and SIVE alone [2]. Here, we report that animals with CVD and SIVE had more CD68+, CD163+, CD206+, and MAC387+ cardiac macrophages, and cardiac collagen deposition than animals with CVD or SIVE alone, demonstrating that concomitant CVD-pathology and SIVE correlates with higher levels of cardiac macrophage activation, plasma markers of myeloid activation and cardiac fibrosis than CVD-pathology or SIVE alone. We report that animals with CVD alone had more cardiac macrophages and collagen deposition than animals with NSF alone, consistent with previous reports [46, 53, 203]. We demonstrate parallel observations in an HIVE cohort compared to age- and sex-matched controls with HIV infection without HIVE, that have increased cardiac macrophages and collagen. Increased cardiac collagen deposition is linked to cardiac macrophage accumulation, although we did not find a statistically

significant correlation between macrophage accumulation and percent collagen in the CVD-pathology and SIVE groups. It is possible that we did not find a correlation between the numbers of cardiac macrophages and cardiac collagen in this study due in part to the CD8+ T lymphocyte-depletion model of rapid AIDS. SIV infected macaques with CD8+ T lymphocyte-depletion are more likely to develop AIDS and SIVE and CVD-pathology within 3-4 months, as opposed to 1-3 years, but do not develop chronic cardiovascular diseases [42, 51]. Indeed, Shannon *et al.* (2000) found that acutely infected rhesus macaques did not develop contractile dysfunction and cardiac pathology when compared to chronically infected macaques [204], suggesting that rapid AIDS pathogenesis in macaques does not consistently result in severe cardiomyopathy. We found that animals with SIVE alone had a greater number of cardiac macrophages and collagen deposition than animals with SIVnoE alone, and we found higher numbers of cardiac macrophages and fibrosis in individuals with HIVE, than age and sex matched HIV infected controls without HIVE. Overall, these findings suggest that increased cardiac macrophage accumulation and fibrosis correlate with HIVE in HIV infected individuals and SIVE in SIV infected macaques. Kuroda et al. (2019), demonstrated that CD163+ and CD206+ cardiac macrophages are the most abundant cardiac macrophage subsets in uninfected rhesus macaques with severe cardiac inflammation [205]. We report that CD163+ and CD206+ cardiac macrophage subsets are the most abundant cardiac in SIV infected macaques with AIDS. We found that animals with CVD-pathology and SIVE have higher numbers of CD163+ and CD206+ cardiac macrophages than animals with NSF and SIVnoE, indicating that CD163+ and CD206+ cardiac macrophage subsets are correlated with the severity of CVD and SIVE pathologies. Similarly, we find that CD163+ cardiac macrophages are the

most abundant cardiac macrophage subset in HIV infected individuals with HIVE, suggesting that CD163+ cardiac macrophage accumulation is associated with HIVE pathogenesis.

We found that higher numbers of activated CD14+ CD16+ monocytes occur with the co-development of CVD pathology and SIVE. The CD14+ CD16+ monocyte subset normally comprises 5-10% of the total monocyte population, but their expansion with SIV infection and AIDS correlates with the development of CVD-pathology alone, or SIVE alone [45, 54, 58, 60, 206]. Moreover, animals with CVD and SIVE had greater numbers and percentages of CD14+ CD16+ monocytes early in infection and terminally compared to CVD or SIVE alone animals, and animals with NSF and SIVnoE, suggesting that CD14+ CD16+ monocyte activation is a biomarker of AIDS pathogenesis and concomitant CVD pathology and SIVE similar to CVD with HIV and HAND in humans [61, 143, 207, 208]. Prior reports have shown that CD14+ CD16+ monocytes are increased/associated with HAND alone [59], and CVD-pathology alone [182, 209]. These blood monocytes are thought to be a mature subset of activated monocytes [60, 210] that are persistently activated and are more susceptible to HIV and SIV infection [63, 211]. Indeed, early infection and trafficking of C-C chemokine receptor 2 (CCR2)-positive CD14+ CD16+ monocytes into the CNS correlates with the development of HIVE and SIVE [47, 211, 212]. Further, increased CD14+ CD16+ monocyte activation correlates with cardiovascular and cerebrovascular inflammation in HIV infected individuals on ART, suggesting that monocyte activation persists despite ART and is linked to the development of CVD and vasculopathy with infection [129, 209, 213]. Here, we show that numbers of CD14+ CD16+ monocytes early and

terminally also correlate with the percentage of cardiac collagen deposition in all animals with AIDS, indicating that increased CD14+ CD16+ monocytes correlate with cardiac fibrogenesis. Together our findings suggest that the development of concomitant CVD-pathology and SIVE with AIDS is correlated with increased levels of CD14+ CD16+ monocyte activation, and plasma biomarkers of monocyte activation.

We find that animals with concomitant CVD pathology and SIVE had more SIV-RNA+ and SIV-gp41+ cells in the CNS and heart than animals with CVD-pathology or SIVE alone, and NSF and SIVnoE animals. We note that in all SIV infected monkeys with AIDS, there are far fewer SIV-RNA+ and SIV-gp41+ cells in the heart than the CNS suggesting that macrophage accumulation more so than SIV-RNA+ and SIV-gp41+ cells, are linked to the co-development of CVD pathology and SIVE. This remains the case when plasma virus is undetectable with ART because both CVD-pathology, and HAND persists in the post-ART era, and correlates with markers of monocyte/macrophage activation like plasma sCD163 and sCD14, IL-18, galectin -3 and -9 [74, 153, 184, 214]. This is consistent with previous studies showing few SIV-RNA+ cells in the heart regardless of the severity of cardiac inflammation [46, 123].   Conversely, other studies have shown that myocardial SIV-RNA correlates with diastolic dysfunction [215, 216]. We found that cardiac SIV-RNA+ cells are CD68+CD206+ macrophages and not CD3+ T lymphocytes in all animals, suggesting that a small population of macrophage are productively infected in the heart. We found little to no SIV-DNA+ latently infected cells in the heart. We postulate that the difference of magnitudes in SIV-DNA+, SIV-RNA+, and SIV-gp41+ cells is likely due to the sensitivity of the assays used. We and others have previously shown that productively

infected, CD14+CD163+ perivascular macrophages and multinucleated giant cells (MNGCs) comprise the main population of infected macrophages in the brain and correlate with the development of SIVE lesions [6, 45, 92, 95, 206, 217]. Overall, our findings support the notion that animals with concomitant CVD-pathology and SIVE have more SIV-RNA+ macrophages and SIV-gp41+ productively infected cells in the heart and CNS than animals with CVD-pathology or SIVE alone.

We found higher levels of biomarkers of plasma sCD163 and IL-18 in animals with CVD and SIVE compared to animals with CVD or SIVE alone, and animals with NSF and SIVnoE consistent with the notion that concomitant CVD and SIVE is correlated with higher monocyte/macrophage activation, and numbers of CD14+ CD16+ monocytes. We and others have previously reported that increased plasma sCD163 correlates with non-calcified coronary plaque [153], HAND [74], and all-cause mortality [70] in HIV infected individuals on ART, and in SIV infected rhesus macaques [7, 74]. Similarly, plasma IL-18 is produced by macrophages and is also increased with atherosclerosis and CVD in HIV infected individuals [146, 147, 218], and SIV infected macaques [145]. Increased NLR Family Pyrin Domain-Containing 3 (NLRP3) inflammasome activation occurs in macrophages with HIV-infection and drives IL-18 and IL-1β production. NLRP3 inflammasome activation is correlated with macrophage activation and pyroptosis [219, 220], disease progression in gut-associated lymphoid tissues [191], neuroinflammation [221, 222] and atherosclerosis in HIV infected individuals [223]. This data, and that of others show higher levels of plasma IL-18 in animals that co-developed CVD-pathology and SIVE, suggesting that NLRP3 inflammasome activation may drive both cardiac inflammation and SIVE

pathogenesis. We also found similar levels of plasma galectin-3 and -9 in all animals regardless of pathology. Other studies have shown that plasma galectin-3 is increased with HIV-infection [187] and correlates with non-calcified coronary plaque in HIV infected individuals [140]; and increased plasma galectin-9 correlates with acute HIV-infection [82, 83, 85], neurocognitive dysfunction [86], and all-cause mortality [81]. We found increased galectin-3 and -9 in animals with SIVE alone animals compared to SIVnoE animals. Studies in mice show that increased galectin-3 expression in the brain correlates with microglia activation and neuroinflammation post-CNS injury [224-227], suggesting that there may be a connection between increased galectin-3 and SIVE pathogenesis. We did not find increased plasma galectin-3 in animals with CVD alone likely because of the acute nature of our rapid AIDS model. Previous studies have shown that increased plasma galectin-3 correlates with cardiac inflammation and fibrosis in the uninfected population [134, 138, 228-231] and may correlate with cardiac pathogenesis in HIV infected individuals [114, 140, 187]. Our findings indicate that plasma galectin-3 and -9, biomarkers of myeloid cell activation, are higher in animals with SIVE and may correlate with the severity of AIDS pathologies. We also find that plasma sCD163 correlates with plasma galectin-3 and -9, and IL-18 in all animals, and plasma galectin-9, but not sCD163, galectin-3, and IL-18, correlates with plasma viral load. This is consistent with recent reports showing that plasma galectin-9 correlates with plasma viral load in HIV infected individuals [82]. Together, these data demonstrate that plasma IL-18 and galectin-3 and -9, are better correlated with monocyte/macrophage activation than plasma viral load. Our findings are consistent with previous data from the Multicenter AIDS Cohort Study (MACS) showing that subclinical

atherosclerosis and cognitive dysfunction are correlated with increased biomarkers of monocyte/macrophage activation despite plasma HIV suppression with ART [142, 143, 232].

The concept of the "heart-brain axis," in which pathogenesis in the heart and CNS are linked, has been discussed in the uninfected population [169, 172, 233], but has not been thoroughly studied with HIV- or SIV- infection. In this study, we report that animals with AIDS co-developed CVD and SIVE and had higher levels of CD14+ CD16+ monocyte activation, plasma biomarkers of myeloid cell activation, cardiac inflammation and fibrosis, and SIV-RNA+ and SIV-gp41+ cells in the CNS and heart than animals with CVD or SIVE alone, and animals with NSF and SIVnoE. We also show that cardiac SIV-RNA+ cells are CD68+ CD206+ cardiac macrophage. Importantly, we show that HIV infected individuals with HAND also have more cardiac inflammation and fibrosis than individuals with no HAND. This study sheds further light on the importance of monocyte and macrophage activation in AIDS pathogenesis, and suggests that the development of future therapies in HIV infected individuals should target and inhibit myeloid cell activation in the heart and CNS together.

3.0 Decreased monocyte activation, cardiac inflammation, and collagen deposition in SIV-infected rhesus macaques on ART alone, and ART with adjunct methylglyoxal-bis-guanylhydrazone (MGBG)

Authors: Kevin White[1], Soon-ok Kim[1], Katherine Murphy[1], Natalie Tessier[1], Maia Jakubowski[1], Andrew Miller[2], Patrick Autissier[1], Tricia Burdo[3], and Kenneth Williams[1*]

[1]Boston College, Department of Biology, Chestnut Hill, MA, USA

[2]Cornell University, College of Veterinary Medicine, Ithaca, NY, USA

[3]Temple University, Lewis Katz School of Medicine, Philadelphia, PA, USA

[*]Corresponding author can be contacted at:

Department of Biology- Boston College

120 Commonwealth, Massachusetts, 02467 USA

Telephone Number: (617) 552-1168

E-mail: Kenneth.williams.3@bc.edu

3.1 Abstract

The persistence of cardiovascular diseases (CVD) in the post-ART era suggests that while ART successfully blocks viral replication and AIDS pathogenesis, ART fails to target monocyte/macrophages activation correlated with CVD. Methylglyoxal-bis-guanylhydrazone (MGBG) is a polyamine biosynthesis inhibitor that is selectively taken up by monocytes/macrophages, blocks monocyte activation *in vitro*, and decreases macrophages accumulation in SIV-infected macaques. This suggests that a potential strategy for decreasing the prevalence of CVD in PLWH includes blocking viral replication with ART, and targeting monocyte/ macrophages activation with adjunctive MGBG treatment. We asked whether animals on ART and adjunctive MGBG (ART+MGBG) had an additive decrease in biomarkers of monocyte activation and turnover, cardiac macrophages inflammation, and cardiac collagen deposition compared to animals on ART. Using twenty-six CD8+ T lymphocyte-depleted, SIV-infected macaques on ART (n= 9), ART+MGBG (n= 10), and untreated controls (n= 7), we assessed the severities of left ventricle histopathology (inflammation, fibrosis, and cardiomyocyte degeneration), cardiac macrophages inflammation and collagen, SIV-RNA+ cardiac macrophages, and biomarkers of monocyte activation and turnover. We found an additive decrease in the percentage of cardiac collagen deposition in animals on ART+MGBG compared to animals on ART. Animals on ART, and ART+MGBG did not develop AIDS, and had decreased cardiac inflammation and collagen, numbers of cardiac SIV-RNA+ cells, levels of plasma galectin-3, galectin-9, IL-18, and sCD163, CD14+ CD16+ monocyte activation, and BrdU+ monocyte turnover compared to untreated animals with AIDS. These findings demonstrate that decreased cardiac inflammation, collagen deposition, monocyte

activation, and BrdU+ monocyte turnover are correlated with the inhibition of AIDS in animals on ART, and ART+MGBG. This study emphasizes the importance of developing therapeutic approaches targeting myeloid cell activation and accumulation, that can be used in conjunction with ART to decrease the prevalence of CVD in PLWH.

3.2 Introduction

Cardiovascular diseases (CVD) persist in people living with HIV (PLWH) despite plasma HIV suppression with durable antiretroviral therapy (ART) [34, 107, 108]. Traditional risk factors for assessing CVD development in the uninfected population including the Framingham risk score [5, 234, 235], and plasma levels of D-dimer and high-sensitivity C-reactive protein [106, 236], are insufficient for predicting the risk of developing CVD in PLWH. Monocyte and macrophages activation correlates with the development of HIV-associated comorbidities. Indeed, monocyte activation and macrophage accumulation in the heart and vasculature consistently correlate with CVD in PLWH [130, 142, 237], and cardiac pathogenesis in SIV- infected rhesus macaques [46, 124]. Increased percentages of 5-bromo-2'-deoxyuridine positive (BrdU+) monocytes (> 10-15%) from the bone marrow early in SIV- infection and terminally correlates with the severity of AIDS and SIVE pathogenesis in rhesus macaques [7, 71]. Activated CD14+ CD16+ monocytes correlate with acute coronary disease [238] and atherosclerosis [129, 130] in PLWH. Together, these findings suggest that the rates of monocyte activation and extravasation from the bone marrow are key factors contributing to morbidity in PLWH in the post-ART era.

Plasma biomarkers of monocyte and macrophages activation including, sCD163 [114, 153], sCD14 MCP-1/CCL2 [142], IL-18 [145, 239], and tissue factor [237, 240], correlates with AIDS and CVD pathogenesis in PLWH and SIV- infected macaques. Plasma sCD163 is decreased in PLWH on ART, but remains elevated compared to the HIV-uninfected population [1], indicating that ART alone does not block monocyte and macrophages activation. For this reason, identifying plasma biomarkers that reliably correlate with

specific non-AIDS comorbidities (i.e. CVD or HAND), may lead to the discovery of therapeutic targets specific to myeloid cell activation in PLWH. Recent studies in PLWH have focused on the roles of galectins, a family of β-galactoside binding lectins, in the development of CVD and HIV-associated neurological disorder (HAND) [81, 86, 140, 241, 242]. Plasma galectin-3 and galectin-9 are secreted by activated macrophages [86, 137, 228, 243], and are increased with HIV- infection in PLWH [82, 83, 85, 141, 242]. Plasma galectin-3 correlates with non-calcified coronary plaque [140], and galectin-9 correlates with plasma HIV RNA [82, 83, 85], neuroinflammation [86], and all-cause mortality [81] in PLWH on ART, suggesting that plasma galectins are macrophages-related biomarkers linked to CVD and HAND.

Cardiac macrophages activation is increased with CVD in PLWH [121, 122], and cardiac pathogenesis in SIV-infected rhesus macaques [46, 124]. In the heart, activated galectin-3 positive (Gal-3+) macrophages correlate with cardiac hypertrophy in HIV-uninfected individuals [137]. Galectin-3 deletion in mice correlates with fewer F4/80+ cardiac macrophages, cardiac collagen synthesis, increased M2-cardiac macrophage polarization, cardiovascular inflammation, and hypertrophy [137, 228, 244], showing that Gal-3+ macrophages are mediators of CVD development. It is not known if cardiac Gal-3+ macrophages accumulation correlates with AIDS and cardiac pathogenesis. Macrophage expression of the M2-polarized receptors CD163, hemoglobin-haptoglobin scavenger receptor, and CD206, macrophage mannose receptor in gastrointestinal, lung, and central nervous system (CNS) tissues occurs with SIV- infection and correlates with AIDS pathogenesis [70, 87, 245-248]. In the heart and aorta, single-positive CD163+ and CD206+ macrophages accumulation correlates with cardiovascular inflammation and fibrosis [46, 121,

[122]. The persistence of CVD in PLWH on ART suggests that despite ART-mediated inhibition of viral replication and AIDS, high levels of monocyte and macrophage activation persist and correlate with cardiac pathogenesis.

The connection between myeloid cell activation, AIDS, and CVD indicates that a potential strategy for blocking AIDS and CVD includes targeting monocyte and macrophages activation in conjunction with ART-mediated HIV suppression. PLWH treated with ART and adjunctive methotrexate had improved survivability compared to PLWH that developed AIDS-related primary CNS lymphoma [249], and decreased CD4+ and CD8+ T lymphocyte activation and arterial inflammation compared to PLWH on placebo [250-252]. Treatment of macrophages with the antioxidant, dimethyl fumarate (DMF), decreases HIV-replication, oxidative stress, and CCL2-mediated monocyte trafficking *in vitro* [253, 254]. Studies in SIV-infected rhesus macaques reveal that treatments with the CCR5 antagonist, maraviroc [255], the tetracycline antibiotic, minocycline [148, 256], and anti-alpha-4 integrin antibody [132, 257] correlates with decreased SIV- replication in blood, lymph node, and CNS tissues, macrophages inflammation in cardiac, CNS, and lymph node tissues, monocyte activation, and CNS injury. These findings demonstrate the advantages that blocking monocyte and macrophages activation and accumulation have in decreasing the prevalences and severities of SIV-associated comorbidities.

Recently, we have tested methylglyoxal-bis-guanylhydrazone (MGBG), a polyamine biosynthesis inhibitor that is selectively taken up by monocytes and macrophages, but not T lymphocytes [150]. We and others have found that MGBG treatment

downregulates monocyte CD16 expression *in vitro* and in SIV-infected macaques, and blocks HIV-DNA integration *in vitro* [150, 151]. SIV-infected macaques treated with an oral formulation of MGBG have decreased macrophages inflammation in cardiac and CNS tissues, and do not develop AIDS[2, 152]. These findings suggest that ART with adjunctive MGBG may decrease the prevalence of CVD in PLWH by blocking viral replication and myeloid cell activation.

In this study, we used twenty-six SIV infected, CD8+ T lymphocyte-depleted rhesus macaques that were either untreated (n= 7), or treated with ART (n= 9) or ART+MGBG (n= 10). We asked whether there was an additive decrease in monocyte activation and turnover, cardiac inflammation, and cardiac collagen deposition with ART+MGBG animals compared to ART animals. We measured plasma biomarkers of monocyte activation, numbers of CD14+ CD16+ monocytes, BrdU+ monocyte turnover, numbers of cardiac macrophages, and the percentage of cardiac collagen.

3.3 Materials and Methods

3.3.1 Ethical statement

All animals assessed in this study were handled in accordance with the American Association for Accreditation of Laboratory Animal Care, and with the approval from the Institutional Animal Care and Use Committee of Harvard University. All animals were housed at the Tulane National Primate Research Center (Covington, Louisiana). The development of simian AIDS was determined postmortem by the presence of opportunistic infections and tumors, the development of SIV giant cell pneumonia, cytomegalovirus pneumonia, SIVE with giant cells, pneumocystis carinii, or lymphoma. All rhesus macaques examined were anesthetized with ketamine-HCl and euthanized intravenously (i.v.) by pentobarbital overdose and exsanguinated.

3.3.2 Study design

Twenty-six rhesus macaques were inoculated i.v. with 1 mL of SIVmac251 viral swarm (1.1 ng/mL) provided by Dr. Ron Desroisiers, and prepared by Dr. Xavier Alvarez (Tulane National Primate Research Center (TNPRC), Covington, Louisiana, U.S.). CD8+ T lymphocytes were depleted with the CD8-depleting antibody, cM-T807, subcutaneously (subQ) at 6 days' post infection (dpi) (10 mg/kg), and i.v. at 8 dpi and 12 dpi (5 mg/kg). Seven rhesus macaques were inoculated with SIVmac251, CD8+ T lymphocyte-depleted, and remained untreated until euthanasia with the development of simian AIDS. Animals on ART were euthanized at 106 dpi (n= 3) and 125 dpi (n= 6). Starting at 21 dpi, nine SIV-infected, CD8+ T lymphocyte-depleted macaques were placed on an ART regimen

consisting of the HIV nucleoside analog reverse transcriptase inhibitors, tenofovir (30 mg/kg, administered subQ once daily) and emtricitabine (10 mg/kg, administered subQ once daily), and the integrase inhibitor, raltegravir (22 mg/kg, administered orally twice daily). Prior pharmokinetic analysis determined the daily dosing of oral MGBG (30 mg/kg) to be a non-toxic, effective biological concentration of 70 ng/mL of drug in plasma, brain, liver and kidney [152]. At 21 dpi, ten animals received the same ART regimen plus, an oral formulation of methylglyoxal-bis guanylhydrazone (MGBG, 30 mg/kg; formulated as a syrup by Wedgewood Pharmacy, Swedesboro, NJ) until euthanasia at 106 dpi (n= 5), 120 dpi (n= 3), and 125 dpi (n= 2).

3.3.3 Cardiac histopathology

Following euthanasia, animals underwent exsanguination; followed by a full SIV-necropsy during which, all major organs were collected and fixed in a 10% neutral-buffered formalin, embedded in paraffin, and sectioned at 5 μm. Sections of cardiac left ventricle tissue were stained with hematoxylin and eosin (H&E) and graded blindly by a veterinary pathologist. Left ventricle tissues were subjectively assessed for the presence and severity of cardiac inflammation, cardiac fibrosis, and cardiomyocyte degeneration and were graded as having no significant cardiac findings (NSF), minimal, mild, moderate, or severe.

3.3.4 Immunohistochemistry of cardiac tissues

Single-label immunohistochemistry was performed on 5 μm thick sections of formalin-fixed, paraffin embedded cardiac left ventricle. Cardiac macrophages were identified with

monoclonal antibodies against CD68 (clone KP1, Dako; Glostrup, Denmark), CD163 (clone EdHu-1, Serotec; Oxford, UK), CD206 (clone 685645, R&D Systems; Minneapolis, MN), and Myeloid/Histiocyte Antigen (clone MAC387, Dako). T-lymphocytes were identified using a polyclonal antibody against CD3 (Dako). The secondary antibodies used were horseradish peroxidase-conjugated anti-mouse or anti-rabbit (Dako). Chromogenic detection of positive cells was achieved with 3,3'-diaminobenzidine tetrahydrochloride (DAB) (Dako). The average number of positive cells were determined from a randomly selected, 100 tile field of view (area= 3.0 mm^2) using a Zeiss Plan-APOCHROMAT 40x/0.95 Korr on a Zeiss Axio Imager.M1 microscope, and Zen Blue software (Version 3.2, Zeiss; Oberkochen, Germany). Data are presented as the average number of positive cells per mm^2 plus or minus the standard error of the mean (SEM).

Double-label immunohistochemistry was performed on 5 μm thick sections of formalin-fixed, paraffin embedded cardiac left ventricle using the ImmPRESS Duet Double Staining Polymer Kit (VECTOR Laboratories; San Francisco, California, U.S.) according to the manufacturer's protocol. Cardiac macrophages were characterized for galectin-3 (polyclonal, abcam; Waltham, MA, U.S.) and CD163 (clone 10D6, Leica Biosystems; Deer Park, Illinois, U.S.) expression. The average number of positive cells were determined from a randomly selected, 100 tile field of view (area= 3.0 mm^2) using a Zeiss Plan-APOCHROMAT 40x/0.95 Korr on a Zeiss Axio Imager.M1 microscope, and Zen Blue (Version 3.2, Zeiss). Data are presented as the average number of positive cells per mm^2 plus or minus the SEM.

3.3.5 Cardiac collagen

The percentage of cardiac collagen was determined with the Masson's Trichrome, Aniline Blue stain (NewcomerSupply; Middleton, WI, U.S.) according to the manufacturer's protocol. Collagen and mucin are blue; muscle fibers, cytoplasm, and keratin are red; and nuclei are black. Data was acquired from 20 non-overlapping images using a Zeiss Plan-Apochromat 20x/ 0.8 M27 objective (field area= 0.148 mm^2) on a Zeiss Axio Imager.M1 microscope, and Zen Blue (Version 3.2, Zeiss). The percentage of cardiac collagen deposition was analyzed using ImageJ Analysis Software. The amount of cardiac collagen was expressed as the average percent of cardiac collagen per tissue area plus or minus the SEM.

3.3.6 In situ hybridization for SIV-RNA

Cardiac SIV-RNA was detected *in situ* using the RNAscope ® 2.5 HD Assay-Red kit (Advanced Cell Diagnostics [ACD]; Newark, CA, U.S.) on 5 μm thick sections of formalin-fixed, paraffin-embedded cardiac left ventricle tissues according to the manufacturer's protocol. Sections were deparaffinized in graded ethanols and xylenes, pre-treated, then incubated with RNAscope specific probes targeting SIVmac239 (SIVmac239-RNA no Env; ACD), Mmu-PPIB (positive control; ACD), or DapB (negative control; ACD). The number of cardiac SIV-RNA+ cells were determined from a randomly selected, 100 tile field of view (area= 3.0 mm^2) using a Zeiss Plan-APOCHROMAT 40x/0.95 Korr on a Zeiss Axio Imager.M1 microscope, and Zen Blue (Version 3.2, Zeiss). Data are presented as the average number of positive cells per mm^2 plus or minus the SEM.

3.3.7 BrdU administration

To assess the rate of monocyte turnover from the bone marrow, a stock solution (30 mg/mL) of the thymidine analog 5-bromo-2′-deoxyuridine (BrdU) (Millipore Sigma; Burlington, MA, U.S.) was prepared with 1X Dulbecco's PBS (without Ca^{+2} and Mg^{+2}), U.S.P. grade (Aestus Pharmaceuticals; Durham, NC, U.S.), and heated to 60°C in a water bath, as previously described[71, 258]. BrdU was administered via slow bolus i.v. injection (60 mg/kg per body weight) throughout the study at 6, 19, 41, and 76 dpi, and terminally.

3.3.8 Flow cytometry

Flow cytometric analyses were performed with 100 µl aliquots of EDTA whole blood. Erythrocytes were lysed using ImmunoPrep Reagent System (Beckman Coulter; Indianapolis, IN, U.S.), washed twice with 2% FBS-PBS, then incubated for 15 minutes at room temperature with fluorochrome-conjugated surface antibodies including anti-HLA-DR-ECD (clone Immu-357; Beckman Coulter), anti-CD16-PE-Cy7 (clone 3G8; BD Biosciences; San Diego, CA, U.S.), anti-CD3-APC-Cy7 (clone SP34-2; BD Biosciences), anti-CD20-APC-Cy7 (clone 2H7; BioLegend; San Diego, CA, U.S.), and anti-CD14-Pacific blue (clone M5E2) (BD Biosciences). For intracellular staining, cells were fixed and permeabilized with BD Cytofix/Cytoperm™ buffer (BD Biosciences) for 20 mins at room temperature. Cells were washed and incubated with BD Cytoperm Plus™ buffer for 10 mins on ice, then washed and incubated with DNase (30mg) for 1hr at 37°C, washed, and stained for intracellular antigen with anti-BrdU-FITC (clone 3D4; BD Biosciences)

and anti-Ki-67-PE (clone B56; BD Biosciences) for 20 mins at room temperature. For controls, BrdU naïve animals and isotype controls were used. Dead monocytes were gated out using LIVE/DEAD Fixable Yellow Dead Cell Stain-AmCyan (ThermoFisher Scientific). Samples were acquired on a BD FACS Aria (BD Biosciences) and analyzed with Tree Star Flow Jo version 8.7. Monocytes were first selected based on size and granularity (FSC vs. SSC), followed by exclusion of doublets (FSC-A vs. FSC-H), then selection of CD3- CD20- HLA-DR+ cells. From this acquisition gate, the percentage of monocyte subsets expressing CD14 and/or CD16 could be determined. The absolute number of peripheral blood monocytes was calculated by multiplying the total white blood cell count by the percentage of monocytes determined by flow.

3.3.9 Plasma biomarkers

Levels of plasma galectin-3 (R & D Systems; Minneapolis, MN, U.S.), galectin-9 (R & D Systems), IL-18 (R & D Systems) and soluble CD163 (sCD163) (IQ Products; Groningen, Netherlands) were measured at pre-infection, 7, 20 and 63 dpi, and terminally, by ELISAs according to the manufacturer's protocol. ELISAs were measured using the BioTek Powerwave 340 (BioTek; Winooski, VT, U.S.) at a wavelength of 450 nm and a correction wavelength of 540 nm. Concentrations of plasma galectin-3, galectin-9 and sCD163 were presented as ng/mL. Concentrations of plasma IL-18 were presented as pg/mL.

3.3.10 Statistical analyses

Statistical analyses were performed using Prism v.9.4.1 software (Graphpad Software Inc.; San Diego, CA). Average numbers of immune-positive cardiac macrophages, CD3+ T lymphocytes, cardiac SIV-RNA+ macrophages, percentages of cardiac collagen and BrdU+ monocytes, longitudinal concentrations of plasma biomarkers, and numbers of CD14+ CD16+ monocytes, were tested for statistical significance using a one-way analysis of variance (ANOVA) with significance accepted at $p < 0.05$, and post-hoc nonparametric Mann-Whiney t tests with significance accepted at $p < 0.05$. Non-parametric spearman's rank correlation was performed between the numbers of cardiac macrophages and the percentages of cardiac collagen with significance accepted at $p < 0.05$.

3.4 Results

3.4.1 AIDS was blocked, but cardiac pathology was detected in animals on ART, and ART+MGBG.

We first examined the prevalence and severity of cardiac histopathology in animals on ART (n= 8, no cardiac tissue was available for JH68), ART+MGBG (n= 10), and untreated animals (n= 7). All untreated animals had AIDS, and six animals developed SIVE (85.7%). No animals on ART, and ART+MGBG developed AIDS. In total, five untreated (71.4%), two ART (25%), and seven ART+MGBG (70%) animals had fibrosis, inflammation, or cardiomyocyte degeneration in left ventricle tissues. Two animals on ART [two mild (25%)], and seven animals on ART+MGBG [four minimal (40%); three mild (30%)] had cardiac inflammation compared to four untreated animals [four mild (57.1%)]. One animal on ART+MGBG [one mild (10%)] developed cardiac fibrosis. One animal on ART [one mild (12.5%)], three animals on ART+MGBG [two mild (20%); one moderate (10%)], and three untreated animals [three mild (42.9%)] had cardiomyocyte degeneration (**Table 3.1**). There were no significant differences in the ages and weights of animals on ART (7.3±0.6 years; 10.8±0.6 kg), ART+MGBG (7.4±0.5 years; 9.4±0.5 kg), and untreated animals (7.0±0.6 years; 9.3±0.9 kg) at necropsy (**Supplementary Table 3.1**).

3.4.2 The number of cardiac macrophages are decreased in animals on ART, and ART+MGBG.

Animals on ART, and ART+MGBG had fewer CD68+ (4.1-fold and 5.2-fold), CD163+ (2.76-fold and 2.43-fold), CD206+ (3.04-fold and 3.49-fold), and MAC387+ (9.15-fold

and 4.51-fold) cardiac macrophages than untreated animals (**Table 3.2**) (nonparametric ANOVA, p< 0.05; post-hoc Mann-Whitney t test, p< 0.05). We found trends of additive decreases in the numbers of CD68+ (1.27-fold) and CD206+ (1.15-fold) cardiac macrophages, and no differences in MAC387+ and CD163+ cardiac macrophages in animals on ART+MGBG compared to animals on ART. There was a trend of decreased numbers of cardiac CD3+ T lymphocytes in animals on ART (1.58-fold), and ART+MGBG (2.04-fold) compared to untreated animals (**Table 3.1**). There were fewer SIV-RNA+ cardiac macrophages in animals on ART (16.3-fold; 0.16 ± 0.09 cells/mm^2), and ART+MGBG (5.78-fold; 0.45 ± 0.3 cells/mm^2) compared to untreated animals (2.60 ± 0.51 cells/mm^2) (**Figure 3.1**) (non-parametric ANOVA, p< 0.05; non-parametric Mann Whitney t test, p< 0.05).

3.4.3 ART+MGBG animals had less cardiac collagen deposition than animals on ART.

We found significantly less cardiac collagen in animals on ART (1.55-fold, $11 \pm 1.24\%$), and ART+MGBG (3.56-fold, $4.8 \pm 0.52\%$) compared to untreated animals ($17.1 \pm 2\%$). There was more of a decrease in cardiac collagen in animals on ART+MGBG (2.29-fold) compared to animals on ART (**Figure 3.2**) (non-parametric ANOVA, p< 0.05; post-hoc Mann-Whitney t test, p< 0.05). There was a positive correlation between cardiac collagen deposition and CD68+ (r= 0.65, p< 0.001) and CD206+ (r= 0.61, p< 0.01) cardiac macrophages, and a trend of correlation with CD163+ (r= 0.37, p= 0.07) and MAC387+ (r= 0.33, p= 0.11) macrophages (**Figure 3.3A-D**) (Spearman's correlation, p< 0.05). When animals were grouped by treatment, there was a positive correlation between cardiac

collagen and the number of CD68+ macrophages (r= 0.86, p< 0.05), and a trend of correlation with CD163+ (r= 0.59, p= 0.17) and CD206+ (r= 0.58, p= 0.19) macrophages in untreated animals (**Figure 3.3E-G**) (Spearman's correlation, p< 0.05). There were no significant correlations between the numbers of CD68+, CD163+, and CD206+ macrophages, and cardiac collagen in animals on ART, and ART+MGBG. There was no significant correlation between the number of MAC387+ cardiac macrophage and cardiac collagen deposition in animals on ART, ART+MGBG, and untreated animals (**Figure 3.3H**).

3.4.4 CD163+ Gal-3+ cardiac macrophages were decreased in animals on ART, and ART+MGBG.

We found two subsets of Gal-3+ positive cells in the heart: CD163+ Gal-3+ and CD163- Gal-3+ cells. Numbers of CD163+ Gal-3+ cardiac macrophages were decreased in animals on ART (5.6-fold, 1.3 ± 0.2 cells/mm^2) and ART+MGBG (2.6-fold, 2.8 ± 1 cells/mm^2) compared to untreated animals (7.3 ± 1.6 cells/mm^2) (**Figure 3.4A**) (nonparametric ANOVA, p< 0.05; post-hoc Mann-Whitney t test, p< 0.05). There were decreased numbers of CD163+ Gal-3- cardiac macrophages in animals on ART (5.4-fold, 50.8 ± 18.3 cells/mm^2), and ART+MGBG (4.6-fold, 60.3 ± 12.2 cells/mm^2) compared to untreated animals (275 ± 32.6 cells/mm^2) (**Figure 3.4B**) (nonparametric ANOVA, p< 0.05; post-hoc Mann-Whitney t test, p< 0.05). There were similar numbers of CD163- Gal-3+ cardiac cells in all animals regardless of treatment (untreated, 5.7 ± 1.4 cells/mm^2; ART, 6.1 ± 2.2 cells/mm^2; and ART+MGBG, 4.8 ± 1.4 cells/mm^2) (**Figure 3.4C**). There were no additive

decreases in the numbers of CD163+ Gal-3+ and CD163+ Gal-3- cardiac macrophages in animals on ART+MGBG.

3.4.5 Biomarkers of monocyte and macrophages activation and turnover in the blood were decreased in animals on ART, and ART+MGBG.

Biomarkers associated with monocyte and macrophage activation were decreased in animals on ART+MGBG at 63 dpi and terminally [galectin-3 (3.14-fold and 5.98-fold); galectin-9 (2.63-fold and 6.76-fold); IL-18 (3-fold and 18.5-fold); sCD163(1.9-fold and 1.7-fold)] compared to untreated animals (**Figure 3.5A-D** and **Supplementary Table 3.2**) (nonparametric ANOVA, p< 0.05; post-hoc Mann-Whitney t test, p< 0.05). We also found decreased levels of the same plasma biomarkers in animals on ART at 63 dpi [galectin-3 (2.7 fold); galectin-9(6.78- fold); IL-18 (3.4- fold); and sCD163(2.1- fold)] and terminally [galectin-3 (2.67-fold); galectin-9 (11.1-fold); IL-18 (20.8-fold); and sCD163 (2.6-fold)] compared to untreated animals (**Table 3.5A-D** and **Supplementary Table 3.2**). There was a trend of decreased plasma galectin-3 in animals on ART+MGBG at 63 dpi (1.17-fold) and terminally (2.24-fold) compared to animals on ART. There were no significant differences in any of the plasma biomarkers at 7 dpi and 20 dpi in all animals. There were no additive decreases in galectin-9, IL-18 and sCD163 in ART+MGBG animals compared to ART. Numbers of CD14+CD16+ monocytes were decreased at 63 dpi and terminally in animals on ART (3.27-fold, 45.8 ± 12 cells and 7.9-fold, 17.9 ± 5.1 cells), and ART+MGBG (2.27-fold, 66.1 ± 19.7 cells and 5.42-fold, 26.1 ± 8 cells) compared to untreated animals (149.9 ± 79.8 cells and 141.4 ± 72 cells) (**Figure 3.5E**) (nonparametric ANOVA, p< 0.05; post-hoc Mann-Whitney t test, p< 0.05). There were no statistically

significant differences in the number of CD14+ CD16- monocytes in all animals (data not shown). As early as 7 dpi, all of the animals studied had greater than 10% BrdU+ monocytes (*red line*) (17.1 ± 2.5% untreated, 13.3 ± 3.8% ART, and 19.6 ± 5.3% ART+MGBG animals). The percentage of BrdU+ monocytes was decreased at 42 dpi and terminally in animals on ART (4.1-fold, 6.2 ± 1.9% and 5.15-fold, 6.5 ± 2.3%), and ART+MGBG (2-fold, 13.1 ± 6.8% and 5-fold, 9.6 ± 4.6%) compared to untreated animals (25.5 ± 2.9% and 33.5 ± 4%) (**Figure 3.5F**) (nonparametric ANOVA, $p < 0.05$; nonparametric Mann-Whitney t test, $p < 0.05$). There was no additive decrease in the percentage of BrdU+ monocytes in ART+MGBG animals compared to animals on ART.

3.5 Figures and Tables

Table 1. ART, and ART+MGBG blocks AIDS, but not the prevalence of cardiac histopathology					
Treatment Cohort	**N**	**AIDS Defining Criteria**	**Cardiac Histopathology**		
			Inflammation	**Fibrosis**	**Cardiomyocyte Degeneration**
Untreated	7	0 No AIDS (0%) 7 AIDS (100%) 6 SIVE (85.7%)	3 NSF (42.9%) 4 Mild (57.1%)	7 NSF (64.3%)	4 NSF (57.1%) 3 Mild (42.9%)
ART	8	8 No AIDS (100%) 0 AIDS (0%) 0 SIVE (0%)	6 NSF (75%) 2 Mild (25%)	8 NSF (100%)	7 NSF (87.5%) 1 Mild (12.5%)
ART+MGBG	10	10 No AIDS (100%) 0 AIDS (0%) 0 SIVE (0%)	4 NSF (40%) 4 Minimal (40%) 2 Mild (20%)	9 NSF (90%) 1 Mild (10%)	7 NSF (70%) 2 Mild (20%) 1 Moderate (10%)

Table 3.1. ART, and ART+MGBG blocks AIDS, but not the prevalence of cardiac histopathology. In total, five untreated (5/7, 71.4%), two ART treated (2/8, 25%), and seven ART+MGBG treated (7/10, 70%) animals had some degree of cardiac histopathology. All untreated animals had AIDS and six developed SIVE, while no animals on ART, and ART+MGBG developed AIDS/SIVE. Six animals on ART+MGBG, two animals on ART, and four untreated animals had severe cardiac inflammation. Three animals on ART+MGBG, one animal on ART, and three untreated animals had cardiomyocyte degeneration. One ART+MGBG animal developed mild cardiac fibrosis. Sections of left ventricle from untreated (n= 7), ART treated (n= 8), and ART+MGBG treated (n= 10) animals were examined blindly by a veterinary pathologist. Observations from one ART cohort animal (JH68) is omitted due to a lack of available cardiac tissue for examination. The severity of cardiac inflammation, cardiac fibrosis and cardiomyocyte

degeneration were determined, and animals were subjectively scored as having no significant cardiac pathology (NSF), mild, moderate, or severe cardiac pathology.

Table 2. Decreased numbers of cardiac macrophages in animals on ART, and ART+MGBG.					
Cohorts	CD68+ macrophage (cells/mm²)	CD163+ macrophage (cells/mm²)	CD206+ macrophage (cells/mm²)	MAC387+ macrophage (cells/mm²)	CD3+ T lymphocytes (cells/mm²)
Untreated (n= 7)	134.8 ± 15.6	210.6 ± 50.8	209.7 ± 46.8	66.8 ± 22.7	19.8 ± 4.4
ART (n= 8)	32.9 ± 4.7	76.2 ± 13	68.9 ± 12.5	7.3 ± 2	12.5 ± 9.5
ART+MGBG (n= 10)	25.9 ± 8.3	86.7 ± 16.6	60.1 ± 10.3	14.8 ± 6.6	9.7 ± 3.5
ANOVA	< 0.001	< 0.01	< 0.01	< 0.01	0.23

Table 3.2. Decreased numbers of cardiac macrophages in animals on ART, and ART+MGBG. Numbers of CD68+, CD163+, CD206+, and MAC387+ cardiac macrophages are decreased in animals on ART, and ART+MGBG compared to untreated animals. There are similar numbers of cardiac CD3+ T lymphocytes in all animals. Sections of left ventricle were stained immunohistochemically for CD68+, CD163+, CD206+, and MAC387+ cardiac macrophages, and CD3+ T lymphocytes. The average number of cells were determined from a randomly selected 100 tile area of tissue (mm^2) at 40x objective. The number of cells per mm^2 are expressed as the mean plus or minus the SEM. P-values were determined with the nonparametric, one-way ANOVA, p< 0.05, and post-hoc nonparametric Mann- Whitney t test, p< 0.05.

Figure 3.1. Decreased numbers of SIV-RNA+ cardiac macrophages in animals on ART, and ART+MGBG. Numbers of cardiac SIV-RNA+ macrophages are similar in animals on ART, and ART+MGBG. Sections of left ventricle were examined for SIV-RNA+ cardiac macrophages using RNAscope *in situ* hybridization. Numbers of cardiac SIV-RNA+ macrophages were determined from a randomly selected 100 tile area of cardiac tissue (mm^2) taken at 40x objective. Significance was determined with the nonparametric, one-way ANOVA, $p < 0.05$, and post-hoc nonparametric Mann- Whitney t test, $p < 0.05$.
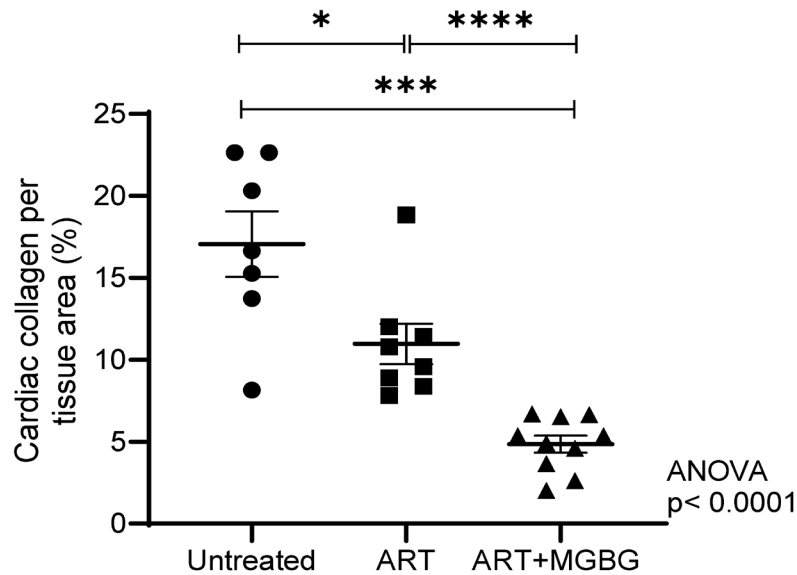
Figure 3.2. ART+MGBG animals have an additive decrease in cardiac collagen deposition. Cardiac collagen is decreased in animals on ART, and ART+MGBG compared to untreated animals. Cardiac collagen deposition was determined by staining sections of left ventricle with the Masson's Trichrome, Aniline blue kit. The percentage of cardiac collagen deposition was measured from twenty random, non-overlapping images taken at 20x objective, and analyzed using ImageJ Analysis software. Significance was determined using a non-parametric ANOVA, $p < 0.05$ and post-hoc nonparametric Mann- Whitney t test, $p < 0.05$.
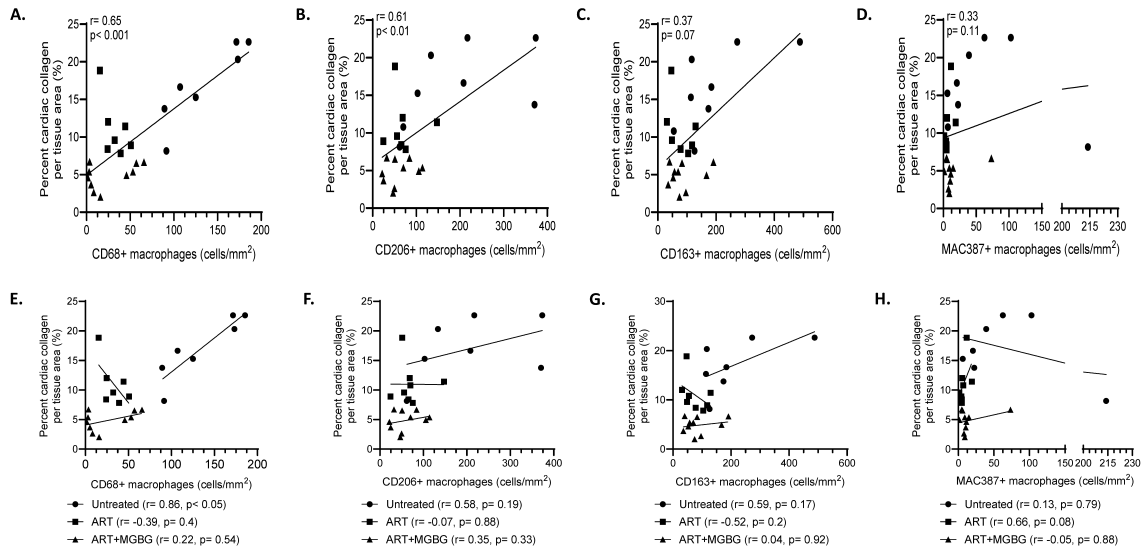
Figure 3.3. Cardiac macrophages numbers are not correlated with cardiac collagen deposition in animals on ART, and ART+MGBG. (A-C). There is a positive correlation between the percentages of cardiac collagen deposition and numbers of CD68+ and CD206+ cardiac macrophages, and a trend of correlation with CD163+ macrophages in all animals. **(E-G).** The percentage of cardiac collagen deposition is positively correlated with numbers of CD68+ macrophages, and trends of correlation with CD163+ and CD206+ macrophages in untreated animals, but is not correlated with cardiac macrophages in animals on ART, and ART+MGBG. **(D,H).** There is no correlation between cardiac collagen deposition and cardiac MAC387+ macrophages. Nonparametric Spearman's rank correlation was used to determine correlations between the cardiac macrophages and cardiac collagen deposition in untreated (n= 7), ART treated (n= 8), and ART+MGBG (n= 10) animals. Statistical significance was accepted at p< 0.05.
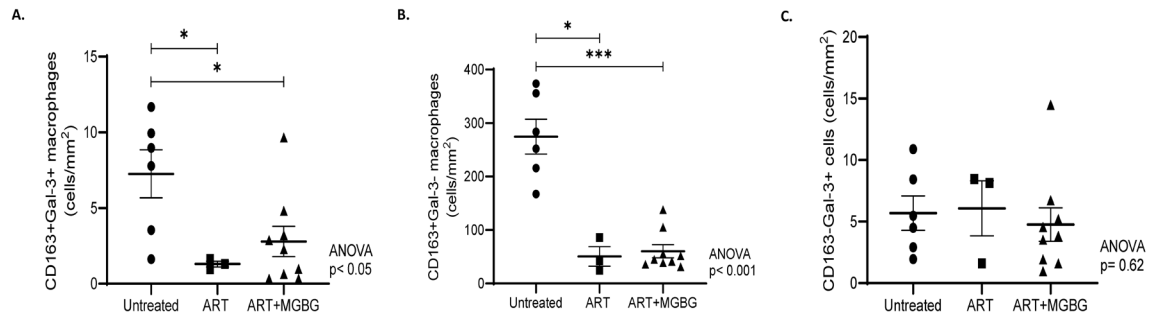
Figure 3.4. Decreased numbers of CD163+ Gal-3+ and CD163+ Gal-3- cardiac macrophages in animals on ART, and ART+MGBG. (A-B). Numbers of CD163+ Gal-3+ and CD163+ Gal-3- cardiac macrophages are decreased in animals on ART, and ART+MGBG compared to untreated animals.**(C).**There are similar numbers of CD163-Gal-3+ cells in all animals. Sections of left ventricle were stained immunohistochemically with antibodies specific for CD163 and Gal-3. Numbers of cells were determined from a randomly selected 100 tile area of tissue (mm^2) at 40x objective. The number of cells per mm^2 are expressed as the mean plus or minus the SEM. P-values were determined with the nonparametric, one-way ANOVA, p< 0.05, and post-hoc nonparametric Mann- Whitney t test, p< 0.05.
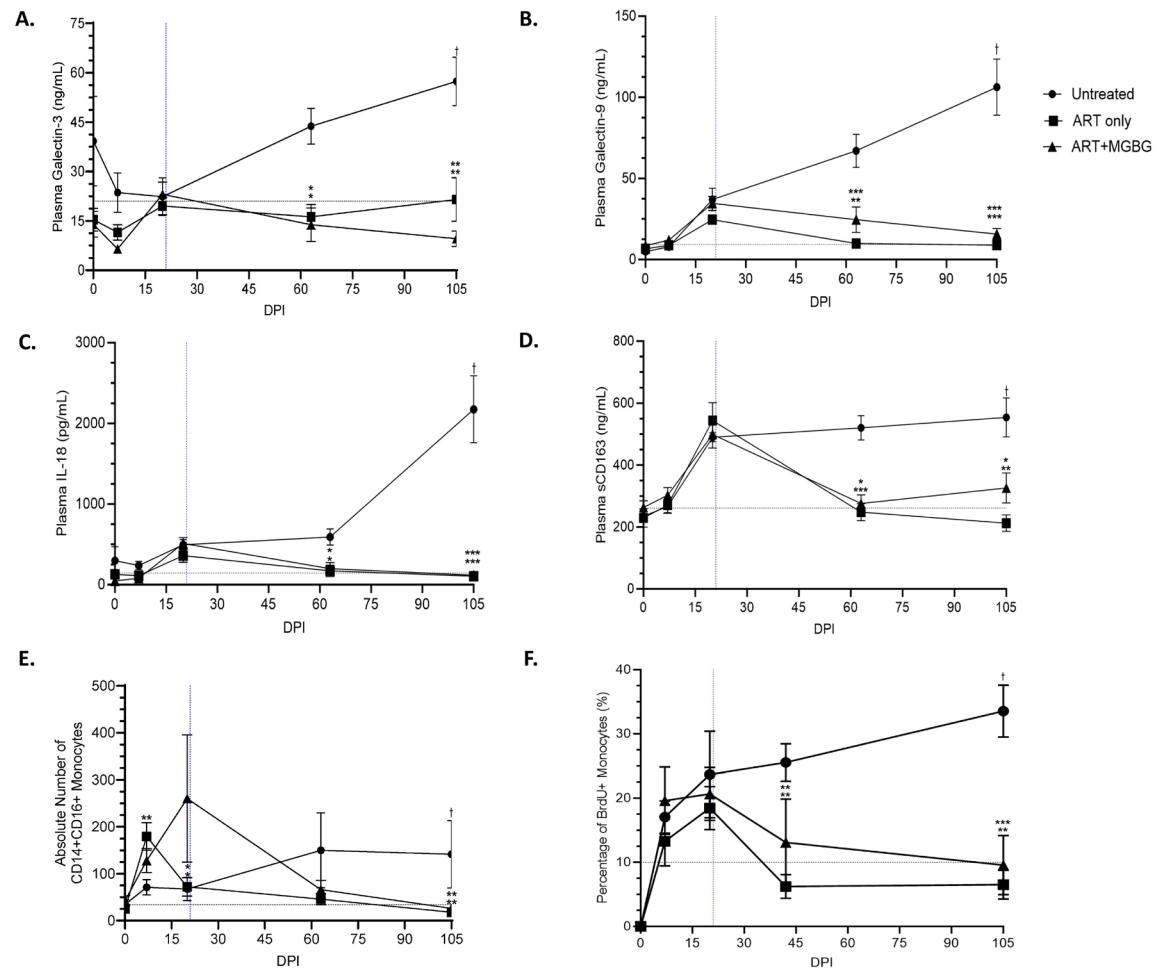
Figure 3.5. Decreased biomarkers of monocyte/macrophage activation and monocyte turnover in animals on ART, and ART+MGBG. (A-D). Levels of plasma galectin-3, galectin-9, IL-18, and sCD163 increased in all animals prior to treatment (7 and 20 dpi) and decreased at 63 dpi and necropsy in animals on ART, and ART+MGBG compared to untreated animals. There are no additive decreases in plasma biomarkers in animals on ART+MGBG compared to animals on ART. The pre-infection baselines (*black dashed*

line) are as follows: galectin-3 (21 ng/mL); galectin-9 (9.34 ng/mL); IL-18 (143.8 pg/mL); and sCD163 (261.5 ng/mL). **(E).** Numbers of CD14+ CD16+ monocytes increased in all animals prior to treatment (7 and 20 dpi) and decreased at 63 dpi and necropsy in animals on ART, and ART+MGBG compared to untreated animals. The pre-infection baseline (black *dashed line*) of CD14+ CD16+ monocytes is 33.9 cells. **(F).** Before treatment, the percentage of BrdU+ monocytes in all animals increased above the previously reported percentage of BrdU+ monocyte baseline (>10%) associated with predicting rapid AIDS development (*black dashed line*) (Burdo *et al.,* 2010). Percentages of BrdU+ monocytes decreased at 42 dpi and necropsy in animals on ART, and ART+MGBG compared to untreated animals. There is no additive decrease in the percentage of BrdU+ monocytes in animals on ART+MGBG compared to animals on ART. P-values were determined with the nonparametric, one-way ANOVA, p< 0.05, and post-hoc nonparametric Mann-Whitney t test, p< 0.05. The administration of ART and ART+MGBG treatments began at 21 dpi (*blue dashed line*).

3.6 Supplementary Tables

Supplementary Table 1. Characteristics of rhesus macaque AIDS-defining criteria and cardiac histopathology.								
Treatment	Animal ID	Sex	Age (yr)	Weight (kg)	AIDS-defining criteria	Left ventricle fibrosis	Left ventricle inflammation	Cardiomyocyte degeneration
No treatment	IP79	M	7.6	11	AIDS no E	NSF	Mild	NSF
No treatment	KN69	M	6.3	9.9	SIVE	NSF	NSF	NSF
No treatment	LB12	M	5.5	11.2	SIVE	NSF	Mild	Mild
No treatment	KT79	M	6.2	12.5	SIVE	NSF	Mild	NSF
No treatment	JE87	M	9.4	12.2	SIVE	NSF	Mild	Mild
No treatment	JD29	M	9.4	10.9	SIVE	NSF	NSF	Mild
No treatment	IK28	M	10.3	12.3	SIVE	NSF	NSF	NSF
ART	JI15	M	6.1	8.4	No AIDS	NSF	Mild	Mild
ART	GI68	M	10.3	9.8	No AIDS	NSF	NSF	NSF
ART	JB07	M	6.4	10.4	No AIDS	NSF	NSF	NSF
ART	GH18	M	10.4	8.1	No AIDS	NSF	NSF	NSF
ART	JF58	M	6.2	11.1	No AIDS	NSF	NSF	NSF
ART	JJ86	M	7.9	12.4	No AIDS	NSF	Mild	NSF
ART	KD67	M	6.8	13.2	No AIDS	NSF	NSF	NSF
ART	KM38	M	5.7	13.3	No AIDS	NSF	NSF	NSF
ART	JH68	M	6.2	10.5	No AIDS	NA	NA	NA
ART+MGBG	JL41	M	6.0	8.2	No AIDS	NSF	Mild	Mild
ART+MGBG	HI45	M	9.8	8.4	No AIDS	NSF	NSF	NSF
ART+MGBG	JF50	M	7.0	9.2	No AIDS	NSF	NSF	NSF
ART+MGBG	JL63	M	6.0	8.7	No AIDS	NSF	Mild	NSF
ART+MGBG	IH02	M	8.1	8.3	No AIDS	NSF	NSF	NSF
ART+MGBG	LI74	M	5.3	9.1	No AIDS	NSF	Minimal	NSF
ART+MGBG	KJ07	M	7.7	12.6	No AIDS	NSF	Minimal	NSF
ART+MGBG	LA93	M	6.5	8.4	No AIDS	NSF	Mild	Moderate
ART+MGBG	JF44	M	10.4	10.2	No AIDS	NSF	Minimal	Mild
ART+MGBG	KT52	M	7.4	10.9	No AIDS	Mild	Minimal	NSF

Supplementary Table 3.1. Characteristics of AIDS-defining criteria and cardiac histopathology in SIV-infected animals. Twenty-six rhesus macaques were inoculated with SIVmac251 viral swarm and treated with CD8-depleting antibody at 6, 8 and 12 dpi. The administration of ART or ART+MGBG began at 21 dpi. Animal age and weight were recorded post-mortem. The development of AIDS was determined post-mortem by the presence of opportunistic infections, tumors, or SIVE. Sections of left ventricle were graded blindly by a veterinary pathologist. The severity of cardiac inflammation, cardiac fibrosis and cardiomyocyte degeneration were determined, and animals were scored as having no significant cardiac pathology (NSF), mild, moderate, or severe cardiac

pathology. Observations from one ART cohort animal (JH68) is omitted due to a lack of

available cardiac tissue for examination.

Supplementary Table 2. Plasma biomarker concentrations in all cohorts.								
Plasma Galectin-3 (ng/mL)					**Plasma Galectin-9 (ng/mL)**			
DPI	Untreated	ART	ART+MGBG	ANOVA p	DPI	Untreated	ART	ART+MGBG	ANOVA p
0	39.3 ± 13.6	15.4 ± 3.4	14 ± 3.9	0.21	0	4.9 ± 1.2	6.7 ± 1.1	8.7 ± 2.5	0.44
7	23.6 ± 6	11.5 ± 2.4	6.5 ± 0.8	0.12	7	7.9 ± 1.4	8.8 ± 0.9	12 ± 2.3	0.36
20	22.4 ± 5.7	19.5 ± 2.7	23.1 ± 3.7	0.76	20	37 ± 7	24.6 ± 2.2	34.7 ± 4.3	0.17
63	43.7 ± 5.4	16.2 ± 3.8	13.9 ± 5.1	< 0.01	63	67.1 ± 10.2	9.9 ± 1.5	24.5 ± 7.9	< 0.01
Necropsy	57.4 ± 7.4	21.5 ± 6.6	9.6 ± 2.4	< 0.01	Necropsy	106.2 ± 17.3	9 ± 1.9	15.7 ± 3.5	< 0.001
Plasma IL-18 (pg/mL)					**Plasma sCD163 (ng/mL)**			
DPI	Untreated	ART	ART+MGBG	ANOVA p	DPI	Untreated	ART	ART+MGBG	ANOVA p
0	298.6 ± 172.9	128.7 ± 44.3	47.5 ± 16.2	< 0.05	0	235.1 ± 13.5	229.5 ± 29.8	263.3 ± 21.4	0.73
7	238.2 ± 52.2	111 ± 37.4	80.2 ± 11.5	< 0.05	7	266.4 ± 19.9	270.7 ± 26.1	302.8 ± 25.1	0.45
20	496.2 ± 64.5	383.2 ± 82	511.5 ± 74.5	0.44	20	490.2 ± 14.6	543.9 ± 58	499 ± 44.4	0.61
63	591.3 ± 100.4	198.5 ± 69.5	199.2 ± 75.2	< 0.05	63	520.5 ± 39.5	248 ± 27.7	276.5 ± 28	< 0.01
Necropsy	21756 ± 414.3	126.8 ± 31.3	104.4 ± 28.5	< 0.001	Necropsy	554.2 ± 63	212.4 ± 26.7	326.5 ± 48.9	< 0.001
Absolute number of CD14+CD16+ monocytes					**Percentage of BrdU+ monocytes**			
DPI	Untreated	ART	ART+MGBG	ANOVA p	DPI	Untreated	ART	ART+MGBG	ANOVA p
0	34.5 ± 9.9	25.3 ± 4.2	42.6 ± 10.6	0.46	0	0	0	0	N/A
7	71.1 ± 16.2	179.4 ± 29.4	128.1 ± 25.8	< 0.05	7	17.1 ± 2.5	13.4 ± 4.4	13.2 ± 3.2	0.26
20	67.3 ± 24.6	71.9 ± 19.6	260.4 ± 135.5	< 0.05	20	23.7 ± 6.7	17.4 ± 3.7	18 ± 5.1	0.76
63	149.9 ± 79.8	45.8 ± 12	66.1 ± 19.7	0.31	63	25.6 ± 2.9	6 ± 2.1	5.5 ± 1.5	< 0.001
Necropsy	141.4 ± 72	17.9 ± 5.1	26.1 ± 8	< 0.01	Necropsy	33.6 ± 4	4.5 ± 1.2	2.6 ± 0.9	< 0.0001

Supplementary Table 3.2. Plasma biomarkers of monocyte/macrophage activation and BrdU+ monocyte turnover are decreased in animals on ART, and ART+MGBG. Levels of plasma galectin-3, galectin-9, IL-18, and sCD163, numbers of CD14+ CD16+ monocytes, and percentages of BrdU+ monocytes were increased in all animals at 7 and 20 dpi. All biomarkers were decreased at 63 dpi and necropsy in animals on ART, and ART+MGBG compared to untreated animals. There are no additive decreases in the levels of biomarkers tested in animals on ART+MGBG compared to animals on ART. Biomarker concentrations are expressed as the mean plus or minus the SEM. P-values were determined with the nonparametric, one-way ANOVA, p< 0.05.

3.7 Conclusion-Discussion

CVD persists in PLWH and correlates with increased monocyte activation and cardiac macrophages accumulation [103, 107, 109, 126]. Previously, we showed that blocking monocyte and macrophages activation with the polyamine biosynthesis inhibitor, MGBG, correlated with decreased cardiac inflammation and fibrosis in a rapid AIDS model of SIV-infection [2]. In this study, we find that animals on ART, and ART+MGBG do not develop AIDS, have lower levels of biomarkers associated with CD14+ CD16+ monocyte activation, BrdU+ monocyte turnover, and decreased cardiac inflammation and collagen compared to untreated animals. We also find that animals on ART+MGBG have more of a decrease in cardiac collagen compared to animals on ART. Consistent with previous findings[2, 46], we find that cardiac collagen correlates with the numbers of cardiac CD68+ and CD206+ macrophages. However, we do not find a correlation between cardiac macrophages and collagen, based on treatments. We report similar levels of gross cardiac histopathology, cardiac SIV-RNA+ macrophages, CD3+ T lymphocytes, and CD163- Gal-3+ cells across all animals examined, regardless of treatment. Our findings indicate that decreased monocyte activation, BrdU+ monocyte turnover, and cardiac macrophages inflammation correlates with the inhibition of AIDS pathogenesis in animals on ART, and ART+MGBG.

Histopathological analysis of left ventricle tissues reveals that despite the inhibition of AIDS pathogenesis, animals on ART, and ART+MGBG have similar prevalences and severities of cardiac inflammation, fibrosis, and cardiomyocyte degermation compared to untreated animals. This finding is consistent with a report that ART treatment has little

effect on the development of myocardial lesions in SIV-infected macaques [131]. Similar to previous observations, all of the untreated animals we assessed developed AIDS, and a majority of those animals developed concomitant SIVE and cardiac pathology[133]. With CD8+ T lymphocyte-depletion, SIV- infected macaques rapidly develop AIDS/ SIVE within 3-4 months compared to 1-3 years in non-depleted animals [51, 259], and do not develop chronic cardiomyopathies [204, 260]. Thus, CD8+ T lymphocyte-depletion promotes a more acute form of cardiac pathogenesis in SIV- infected rhesus macaques compared to studies involving non-depleted, SIV-infected macaques fed with a high-fat diet[145]. This is further supported by studies showing that CD8+ T lymphocyte-depleted macaques with AIDS have more lymphocytic and immune cell infiltrates and cardiomyocyte degeneration in the heart, but do not develop chronic fibrosis and atherosclerosis [46, 124, 260]. Thus, the similar levels of decreased cardiac histopathology in animals on ART, and ART+MGBG likely stem from the acute nature of cardiac pathogenesis that occurs with T lymphocyte-depletion, and suggests that adjunctive MGBG therapy has little effect on the prevalence of cardiac histopathology.

We and others have shown that increased cardiac macrophages infiltration correlates with the development of AIDS and CVD in PLWH and SIV-infected macaques[46, 122-124, 133, 242], suggesting that inhibiting cardiac macrophages activation is a potential therapeutic strategy for HIV-associated CVD. Targeting and inhibiting myeloid cell activation and accumulation in SIV-infected macaques correlates with decreased viral infection and inflammation in cardiac, CNS and gut tissues [2, 132, 149, 152]. Here, we find decreased cardiac macrophages inflammation in animals on ART, and ART+MGBG

compared to untreated animals. This is consistent with reports in SIV- infected rhesus macaques on ART having decreased hepatic macrophages activation and infiltration compared to untreated controls [261]. Consistent with a previous report, we find that CD163+ and CD206+ cardiac macrophages are the most abundant cardiac macrophages subsets in all animals examined [205]. The accumulation of CD163+ and CD206+ cardiac macrophages correlates with arterial inflammation in PLWH [121, 122], and cardiac inflammation and fibrosis [46], pulmonary arterial hypertension and right ventricle systolic pressure [262] in SIV-infected macaques. Similar to previous reports, we find low numbers of scattered CD3+ T lymphocytes in all of the animals examined [2, 46, 132]. The lack of significant change in the numbers of cardiac CD3+ T lymphocytes in ART+MGBG animals suggests that MGBG adjunct therapy specifically targets macrophages, and does not affect cardiac lymphocyte accumulation. Cardiac galectin-3 expression is co-localized to CD68+ macrophages and Tcf21+ fibroblasts in mice [263], and activated major histocompatibility complex II (MHC-II) positive macrophages in rats [137]. Increased myocardial galectin-3 mRNA expression correlates with heart failure and cardiomyopathy in HIV-uninfected individuals [138, 231], indicating that Gal-3+ cardiac macrophages are key actors during CVD development. We next sought to determine whether treatment with ART, and ART+MGBG decreased Gal-3+ cardiac macrophages infiltration compared to untreated animals. We identified two Gal-3+ populations of cells in the heart, CD163+ Gal-3+ macrophages and CD163- Gal-3+ cells. We find that increased CD163+ Gal-3+ cardiac macrophages correlate with AIDS pathogenesis in untreated animals. We find fewer CD163+ Gal-3+ and CD163+ Gal-3- macrophages in animals on ART, and ART+MGBG compared to untreated animals, and find similar numbers of CD163- Gal-3+ cells in all

animals regardless of treatment. Others report that CD163- Gal-3+ cells in the heart include endothelial cells and fibroblasts [264, 265], suggesting that CD163- Gal-3+ cells are not macrophages. Further investigation is needed to characterize the identity and functions of cardiac CD163- Gal-3+ cells in SIV-infected macaques. These findings suggest that the inhibition of AIDS pathogenesis in animals on ART, and ART+MGBG correlates with decreased CD163+ Gal-3+ cardiac macrophages accumulation, but does not affect the quantity of CD163- Gal-3+ cells in the heart. Our findings show that blocking cardiac macrophages accumulation with ART and ART+MGBG correlates with decreased cardiac inflammation.

Cardiac magnetic resonance imaging data shows that HIV- infection and AIDS pathogenesis are correlated with cardiac fibrosis, myocardial dysfunction, and pericardial effusion in PLWH [109, 111, 112]. As mediators of cardiac fibrogenesis, activated cardiac macrophages facilitate wound healing and cardiac remodeling following myocardial ischemic injury [53, 115, 119, 266]. We find less cardiac collagen in animals on ART, and ART+MGBG compared to untreated animals suggesting that decreased cardiac collagen deposition correlates with AIDS inhibition. We also find that animals on ART+MGBG have less cardiac collagen than animals on ART suggesting that MGBG adjunct therapy has an additive effect on collagen formation in the heart.

The presence of different levels of cardiac collagen in animals on ART, ART+MGBG, and untreated animals is inconsistent with our observations that the prevalence of cardiac fibrosis is similar across all of the animals examined, regardless of

treatment. A possible explanation for this discrepancy is the presence of variation in the color thresholding analyses performed (per image) to highlight and measure the percent area of cardiac collagen deposition. Indeed, we and others have previously shown that blocking cardiac macrophages activation and accumulation with MGBG alone, and the anti-alpha 4 integrin antibody correlates with decreased cardiac fibrosis in SIV-infected macaques [2, 132], emphasizing the importance of macrophages accumulation in driving cardiac fibrogenesis. Consistent with previous studies[46, 266], we find a positive correlation between the numbers of cardiac macrophages and the percentage of cardiac collagen in all animals regardless of treatment. When animals are grouped by treatment, cardiac collagen correlates with cardiac macrophages in untreated animals but does not correlate in animals on ART, and ART+MGBG, suggesting that cardiac macrophages inflammation and collagen are not correlated with treatment. Despite the lack of correlation, we observe that decreases in cardiac collagen track with cardiac macrophages in animals on ART, and ART+MGBG.

The accumulation of productively infected macrophages in lung and CNS tissues correlates with chronic SIV-infection, HIVE, and SIVE [6, 45, 92, 267, 268], indicating that the accumulation of productively infected macrophages drives AIDS pathogenesis. When detected, cardiac SIV-RNA+ cells are co-localized to CD68+ CD206+ cardiac macrophages[133], and myocardial viral load correlates with diastolic dysfunction in SIV-infected macaques [215]. Overall, there are few SIV-RNA+ macrophages in the cardiac tissues of all animals examined, irrespective of the severity of cardiac pathology and treatment [46, 124]. We find fewer SIV-RNA+ productively infected cardiac macrophages in

animals on ART, and ART+MGBG compared to untreated animals. This is consistent with Annamalai *et al.*'s (2010) data showing a low viral burden in the cardiac tissues of SIV-infected animals regardless of ART administration [131]. Treatment with MGBG alone inhibits HIV- infection and HIV-DNA integration in monocytes *in vitro* [150], and blocks the development of AIDS and SIVE in SIV-infected macaques[152]. We did not find any additive decrease of cardiac SIV-RNA+ macrophages in animals on ART+MGBG compared to animals on ART, suggesting that treatment with ART alone is sufficient to decrease numbers of productively infected cardiac macrophages.

Recent studies show that levels of myeloid cell activation biomarkers in the blood including, galectin-9 and sCD163, correlate with CVD, AIDS pathogenesis, and all-cause mortality in PLWH [70, 81, 82, 86, 114, 153]. We report that levels of plasma galectin-3, galectin-9, IL-18, and sCD163 are increased longitudinally in untreated animals that develop AIDS. We find that galectin-3, galectin-9, IL-18, and sCD163 are decreased in animals on ART, and ART+MGBG compared to untreated animals, suggesting that blocking monocyte activation correlates with the inhibition of AIDS. Our data is consistent with studies showing that treatment with ART decreases levels of galectin-9 and sCD163 in PLWH [1, 85]. Increased plasma galectin-3 correlates with cardiac inflammation and fibrosis in the uninfected population [137, 138], and in encephalomyocarditis virus- (ECMV-) infected mice [188]. Previous studies show that MGBG downregulates the secretion of the extracellular matrix remodeling protein, osteopontin (OPN), in monocytes *in vitro* [151]. Increased plasma OPN and galectin-3 are associated with maladaptive ventricular remodeling [201, 202], and dilated cardiomyopathy [269] in the uninfected population. Recent studies suggest

that increased plasma galectin-3 in PLWH is correlated with cardiovascular inflammation[114, 140, 187]. Our findings suggest that ART-/ ART+MGBG- mediated decreases in galectin-3 correlates with the inhibition of AIDS. Levels of plasma IL-18 rapidly increase during the acute phase of SIV- infection and correlates with plasma viral load in PLWH and SIV- infected macaques [68, 146, 147]. The NLR Family Pyrin Domain Containing 3 (NLRP3) inflammasome is a potent innate immune response that results in the caspase-1 dependent cleavage and secretion of the proinflammatory cytokines IL-1β and IL-18 [270]. NLRP3 inflammasome activation correlates with atherosclerosis [223], HAND [222, 271], and acute inflammation and pyroptosis in PLWH regardless of adherence to ART [191, 220, 272]. Our findings suggest that decreased IL-18 in animals on ART, and ART+MGBG correlates with lower levels of NLRP3 inflammasome activation.

Signaling pathways associated with monocyte chemotaxis, wound healing, inflammation, the innate immune response, and cellular death are enriched in SIV-infected rhesus macaques [66, 273] , and in PLWH with CVD and HAND[274, 275]. Activated CD14+ CD16+ monocyte expression of inflammatory markers including tissue factor and CCR2 contribute to the development of atherosclerosis, CVD, and AIDS in PLWH [129, 142, 237, 276]. We also find that CD14+ CD16+ monocyte activation increases as untreated animals develop AIDS. Previous studies show that CD14+ CD16+ monocytes continue to show signs of immune dysregulation of blips of activation despite ART treatment in PLWH[277-279]. We find decreased numbers of CD14+ CD16+ monocytes in animals on ART, and ART+MGBG compared to untreated animals. MGBG treatment decreased CD16 expression in monocytes *in vitro* suggesting that MGBG has the capacity to independently

decrease CD16 expression and monocyte activation [151]. We did not find an additive decrease in activated CD14+ CD16+ monocytes in animals on ART+MGBG.

Increased BrdU+ monocyte turnover (> 10% BrdU+ monocytes) early with infection (7 and 19 days' post infection) and terminally are correlated with the rate and severity of SIVE pathogenesis, plasma sCD163, and lung interstitial macrophage apoptosis in SIV-infected macaques [7, 91, 246]. Consistent with this, we find that early in infection (7 dpi), all animals had percentages of BrdU+ monocytes greater than 10%, indicating that all animals were likely to rapidly progress to AIDS without antiretroviral intervention. Following ART, and ART+MGBG initiation, BrdU+ monocyte turnover decreased until necropsy compared to untreated animals. MGBG treatment decreases BrdU incorporation in monocytes *in vitro,* suggesting that MGBG can decrease the rate of monocyte activation and extravasation from the bone marrow [151]. We did not find an additive decrease in BrdU+ monocyte turnover in animals on ART+MGBG. Our findings suggest that decreased BrdU+ monocyte turnover is a result of plasma viral suppression and AIDS inhibition in animals on ART, and ART+MGBG.

In this study, we show that animals on ART, and ART+MGBG had decreased cardiac inflammation and fibrosis, monocyte activation, and BrdU+ monocyte turnover compared to untreated animals with AIDS. We show that the targeted inhibition of myeloid cell activation and accumulation correlates with AIDS inhibition and decreased cardiac pathology. We also identified a population of Gal-3+ CD163+ cardiac macrophages that were decreased with ART, and ART+MGBG treatments. We also show that there are little

to no SIV-RNA+ cardiac macrophages in all animals regardless of treatment. Together, our data emphasizes the importance of utilizing therapies that block myeloid cell activation and accumulation, and can be used in conjunction with ART to decrease the prevalence of CVD in PLWH.

4.0 Conclusion

Adherence to ART suppresses plasma virus replication, inhibits AIDS pathogenesis, and has ultimately transformed HIV-infection from an acute disease to a chronic, manageable condition[27, 28]. Despite adherence to ART, persistent monocyte activation and macrophages accumulation drives the development of HIV-associated comorbidities such as CVD and HAND in PLWH[30, 73, 129, 242, 280]. These findings indicate that ART administration does not block monocyte and macrophages activation sufficiently to prevent the development of comorbidities. Multiple studies show that targeting monocyte and macrophages activation correlates with decreased inflammation in the heart and CNS, prevents viral infection of macrophages, and blocks AIDS pathogenesis[2, 132, 148, 149, 152]. For these reasons, it is likely that the optimal therapeutic approach for HIV-infection includes the targeted inhibition of monocyte and macrophages activation and accumulation, suppression of viral replication and AIDS pathogenesis.

In chapter two, we explored the roles that CD14+ CD16+ monocyte activation and cardiac macrophages inflammation have in influencing the severity of concomitant cardiac and SIVE pathologies in CD8+ T lymphocyte-depleted, SIV-infected rhesus macaques. We asked whether animals with AIDS co-developed CVD and SIVE more so than animals developed CVD or SIVE alone, and NSF and SIVnoE. We also asked whether animals with concomitant CVD and SIVE had more monocyte activation, cardiac inflammation and fibrosis, and productively infected cells in the heart and CNS compared to animals with CVD or SIVE alone, and NSF and SIVnoE animals. We found that animals with AIDS co-developed CVD and SIVE more frequently than CVD or SIVE alone, and NSF and

SIVnoE. Animals with concomitant CVD and SIVE had increased CD14+ CD16+ monocyte activation early and terminally with infection, cardiac macrophages inflammation, and cardiac fibrosis. We found a more SIV-RNA+ and SIV-gp41+ cells in the CNS compared to the hearts of all animals, suggesting that the heart is not a major site of productive SIV- infection. When detected, cardiac SIV-RNA+ cells were CD68+ and CD206+ cardiac macrophages. We next sought to determine whether concomitant CVD and HIVE were correlated with cardiac macrophages inflammation in PLWH with HIVE and HIVnoE. We found that PLWH with HIVE had more cardiac macrophages and fibrosis than PLWH with HIVnoE, suggesting that the severity of HAND pathogenesis correlates with increased cardiac inflammation. Our findings highlight the importance of monocyte and macrophages activation in driving cardiac and CNS pathogenesis, and emphasizes the need for therapies targeting myeloid cell activation, which can be used in conjunction with ART.

In chapter three, we sought to determine whether CD8+ T lymphocyte- depleted, SIV- infected macaques treated with ART and adjunctive MGBG had an additive decrease in cardiac pathology compared to animals on ART alone. We found that animals on ART+MGBG had an additive decrease in cardiac collagen deposition compared to animals on ART, suggesting that MGBG adjunctive therapy decreases cardiac fibrogenesis. Animals on ART, and ART+MGBG did not develop AIDS, and had decreased monocyte activation and turnover, cardiac macrophages inflammation, SIV-RNA+ cardiac macrophages, and collagen deposition compared to untreated animals with AIDS. We also identified two subsets of Gal-3+ cells in the heart: CD163+ Gal-3+ macrophages, and

CD163- Gal-3+ cells. We found that animals on ART, and ART+MGBG had fewer CD163+ Gal-3+ cardiac macrophages than untreated animals, and similar numbers of CD163- Gal-3+ cells. Together, these findings suggest that the inhibition of AIDS pathogenesis in animals on ART, and ART+MGBG correlates with decreased myeloid cell activation, turnover and accumulation. This study highlights the need for future therapeutic approaches to HIV- infection that block the development of AIDS and non-AIDS comorbidities via the inhibition of viral replication, and monocyte and macrophages activation.

The studies presented in this thesis highlight the importance of monocyte and macrophages activation and accumulation in influencing the development of CVD and HIVE/SIVE. Using a rapid AIDS model of SIV-infection, we show that CD14+ CD16+ monocyte activation and turnover, and cardiac macrophages accumulation are better correlates of AIDS and cardiac pathogenesis than the infiltration of productively infected SIV-RNA+ and SIV-gp41+ cells in the heart and CNS. We demonstrate that plasma galectin-3 and galectin-9 are promising biomarkers of cardiac and CNS inflammation, and AIDS pathogenesis. Levels of galectin-3 and galectin-9 are increased in animals that develop AIDS, and are decreased with ART, and ART+MGBG treatments. We show that targeting myeloid cell activation and accumulation correlates with decreased cardiac inflammation, and AIDS inhibition. We also show that the heart is not a major site of productive or latent SIV infection, further highlighting the significance of targeting and blocking cardiac macrophages accumulation. Finally, we demonstrate that MGBG is a

promising adjunctive therapy with ART and is a potent and specific inhibitor of myeloid cell activation.

5.0 References

1. Burdo TH, Lentz MR, Autissier P, Krishnan A, Halpern E, Letendre S, et al. **Soluble CD163 made by monocyte/macrophages is a novel marker of HIV activity in early and chronic infection prior to and after anti-retroviral therapy**. *The Journal of infectious diseases* 2011; 204(1):154-163.

2. Walker JA, Miller AD, Burdo TH, McGrath MS, Williams KC. **Direct Targeting of Macrophages With Methylglyoxal-Bis-Guanylhydrazone Decreases SIV-Associated Cardiovascular Inflammation and Pathology**. *Journal of acquired immune deficiency syndromes (1999)* 2017; 74(5):583-592.

3. Hsue PY, Waters DD. **HIV infection and coronary heart disease: mechanisms and management**. *Nature reviews Cardiology* 2019; 16(12):745-759.

4. Abreu CM, Veenhuis RT, Avalos CR, Graham S, Parrilla DR, Ferreira EA, et al. **Myeloid and CD4 T Cells Comprise the Latent Reservoir in Antiretroviral Therapy-Suppressed SIVmac251-Infected Macaques**. *mBio* 2019; 10(4).

5. Achhra AC, Lyass A, Borowsky L, Bogorodskaya M, Plutzky J, Massaro JM, et al. **Assessing Cardiovascular Risk in People Living with HIV: Current Tools and Limitations**. *Current HIV/AIDS reports* 2021; 18(4):271-279.

6. Nowlin BT, Burdo TH, Midkiff CC, Salemi M, Alvarez X, Williams KC. **SIV encephalitis lesions are composed of CD163(+) macrophages present in the central nervous system during early SIV infection and SIV-positive macrophages recruited terminally with AIDS**. *The American journal of pathology* 2015; 185(6):1649-1665.

7. Burdo TH, Soulas C, Orzechowski K, Button J, Krishnan A, Sugimoto C, et al. **Increased monocyte turnover from bone marrow correlates with severity of SIV encephalitis and CD163 levels in plasma**. *PLoS pathogens* 2010; 6(4):e1000842.

8. Maartens G, Celum C, Lewin SR. **HIV infection: epidemiology, pathogenesis, treatment, and prevention**. *Lancet (London, England)* 2014; 384(9939):258-271.

9. Hendricks CM, Cordeiro T, Gomes AP, Stevenson M. **The Interplay of HIV-1 and Macrophages in Viral Persistence**. *Frontiers in microbiology* 2021; 12:646447.

10. Williams KC, Hickey WF. **Central nervous system damage, monocytes and macrophages, and neurological disorders in AIDS**. *Annual review of neuroscience* 2002; 25:537-562.

11. Simon V, Ho DD, Abdool Karim Q. **HIV/AIDS epidemiology, pathogenesis, prevention, and treatment**. *Lancet (London, England)* 2006; 368(9534):489-504.

12. Vangipuram R, Tyring SK. **AIDS-Associated Malignancies**. *Cancer Treat Res* 2019; 177:1-21.

13. Ouyang J, Yan J, Zhou X, Isnard S, Harypursat V, Cui H, et al. **Relevance of biomarkers indicating gut damage and microbial translocation in people living with HIV**. *Front Immunol* 2023; 14:1173956.

14. Epple HJ, Allers K, Tröger H, Kühl A, Erben U, Fromm M, et al. **Acute HIV infection induces mucosal infiltration with CD4+ and CD8+ T cells, epithelial apoptosis, and a mucosal barrier defect**. *Gastroenterology* 2010; 139(4):1289-1300.

15. Ancuta P, Kamat A, Kunstman KJ, Kim EY, Autissier P, Wurcel A, et al. **Microbial translocation is associated with increased monocyte activation and dementia in AIDS patients**. *PloS one* 2008; 3(6):e2516.

16. Brenchley JM, Price DA, Schacker TW, Asher TE, Silvestri G, Rao S, et al. **Microbial translocation is a cause of systemic immune activation in chronic HIV infection**. *Nature medicine* 2006; 12(12):1365-1371.

17. Anderson AM, Harezlak J, Bharti A, Mi D, Taylor MJ, Daar ES, et al. **Plasma and Cerebrospinal Fluid Biomarkers Predict Cerebral Injury in HIV-Infected Individuals on Stable Combination Antiretroviral Therapy**. *Journal of acquired immune deficiency syndromes (1999)* 2015; 69(1):29-35.

18. Hagberg L, Cinque P, Gisslen M, Brew BJ, Spudich S, Bestetti A, et al. **Cerebrospinal fluid neopterin: an informative biomarker of central nervous system immune activation in HIV-1 infection**. *AIDS research and therapy* 2010; 7:15.

19. Ramdas P, Sahu AK, Mishra T, Bhardwaj V, Chande A. **From Entry to Egress: Strategic Exploitation of the Cellular Processes by HIV-1**. *Frontiers in microbiology* 2020; 11:559792.

20. Chen B. **Molecular Mechanism of HIV-1 Entry**. *Trends in microbiology* 2019; 27(10):878-891.

21. Fassati A, Goff SP. **Characterization of intracellular reverse transcription complexes of human immunodeficiency virus type 1**. *Journal of virology* 2001; 75(8):3626-3635.

22. Selyutina A, Persaud M, Lee K, KewalRamani V, Diaz-Griffero F. **Nuclear Import of the HIV-1 Core Precedes Reverse Transcription and Uncoating**. *Cell reports* 2020; 32(13):108201.

23. Burdick RC, Li C, Munshi M, Rawson JMO, Nagashima K, Hu WS, et al. **HIV-1 uncoats in the nucleus near sites of integration**. *Proceedings of the National Academy of Sciences of the United States of America* 2020; 117(10):5486-5493.

24. Ciuffi A. **The benefits of integration**. *Clinical microbiology and infection : the official publication of the European Society of Clinical Microbiology and Infectious Diseases* 2016; 22(4):324-332.

25. Henderson BR, Percipalle P. **Interactions between HIV Rev and nuclear import and export factors: the Rev nuclear localisation signal mediates specific binding to human importin-beta**. *Journal of molecular biology* 1997; 274(5):693-707.

26. Phanuphak N, Gulick RM. **HIV treatment and prevention 2019: current standards of care**. *Current opinion in HIV and AIDS* 2020; 15(1):4-12.

27. Al-Harthi L, Voris J, Patterson BK, Becker S, Eron J, Smith KY, et al. **Evaluation of the impact of highly active antiretroviral therapy on immune recovery in antiretroviral naive patients**. *HIV medicine* 2004; 5(1):55-65.

28. Sabin CA. **Do people with HIV infection have a normal life expectancy in the era of combination antiretroviral therapy?** *BMC medicine* 2013; 11:251.

29. Nakagawa F, May M, Phillips A. **Life expectancy living with HIV: recent estimates and future implications**. *Current opinion in infectious diseases* 2013; 26(1):17-25.

30. Heaton RK, Franklin DR, Ellis RJ, McCutchan JA, Letendre SL, Leblanc S, et al. **HIV-associated neurocognitive disorders before and during the era of combination antiretroviral therapy: differences in rates, nature, and predictors**. *Journal of neurovirology* 2011; 17(1):3-16.

31. Lichtfuss GF, Hoy J, Rajasuriar R, Kramski M, Crowe SM, Lewin SR. **Biomarkers of immune dysfunction following combination antiretroviral therapy for HIV infection**. *Biomarkers in medicine* 2011; 5(2):171-186.

32. Belmonte L, Baré P, Picchio GR, Perez Bianco R, de Tezanos Pinto M, Corti M, et al. **Decreased recovery of replication-competent HIV-1 from peripheral blood mononuclear cell-derived monocyte/macrophages of HIV-positive patients after 3 years on highly active antiretroviral therapy**. *AIDS (London, England)* 2002; 16(9):1289-1292.

33. Ahlenstiel CL, Symonds G, Kent SJ, Kelleher AD. **Block and Lock HIV Cure Strategies to Control the Latent Reservoir**. *Front Cell Infect Microbiol* 2020; 10:424.

34. Barnes RP, Lacson JC, Bahrami H. **HIV Infection and Risk of Cardiovascular Diseases Beyond Coronary Artery Disease**. *Current atherosclerosis reports* 2017; 19(5):20.

35. Rabezanahary H, Clain J, Racine G, Andreani G, Benmadid-Laktout G, Borde C, et al. **Early Antiretroviral Therapy Prevents Viral Infection of Monocytes and Inflammation in Simian Immunodeficiency Virus-Infected Rhesus Macaques**. *Journal of virology* 2020; 94(22).

36. Abreu C, Shirk EN, Queen SE, Mankowski JL, Gama L, Clements JE. **A Quantitative Approach to SIV Functional Latency in Brain Macrophages**. *Journal of neuroimmune pharmacology : the official journal of the Society on NeuroImmune Pharmacology* 2019; 14(1):23-32.

37. Shahid A, Jones BR, Yang JSW, Dong W, Shaipanich T, Donohoe K, et al. **HIV proviral genetic diversity, compartmentalization and inferred dynamics in lung and blood during long-term suppressive antiretroviral therapy**. *PLoS pathogens* 2022; 18(11):e1010613.

38. Andrade VM, Mavian C, Babic D, Cordeiro T, Sharkey M, Barrios L, et al. **A minor population of macrophage-tropic HIV-1 variants is identified in recrudescing viremia following analytic treatment interruption**. *Proceedings of the National Academy of Sciences of the United States of America* 2020; 117(18):9981-9990.

39. Abreu C, Shirk EN, Queen SE, Beck SE, Mangus LM, Pate KAM, et al. **Brain macrophages harbor latent, infectious simian immunodeficiency virus**. *AIDS (London, England)* 2019; 33 Suppl 2(Suppl 2):S181-s188.

40. Oliveira MF, Chaillon A, Nakazawa M, Vargas M, Letendre SL, Strain MC, et al. **Early Antiretroviral Therapy Is Associated with Lower HIV DNA Molecular Diversity and Lower Inflammation in Cerebrospinal Fluid but Does Not Prevent the Establishment of Compartmentalized HIV DNA Populations**. *PLoS pathogens* 2017; 13(1):e1006112.

41. Hansen SG, Piatak M, Jr., Ventura AB, Hughes CM, Gilbride RM, Ford JC, et al. **Immune clearance of highly pathogenic SIV infection**. *Nature* 2013; 502(7469):100-104.

42. Mallard J, Williams KC. **Animal models of HIV-associated disease of the central nervous system**. *Handbook of clinical neurology* 2018; 152:41-53.

43. Williams K, Westmoreland S, Greco J, Ratai E, Lentz M, Kim WK, et al. **Magnetic resonance spectroscopy reveals that activated monocytes contribute to neuronal injury in SIV neuroAIDS**. *The Journal of clinical investigation* 2005; 115(9):2534-2545.

44. Micci L, Alvarez X, Iriele RI, Ortiz AM, Ryan ES, McGary CS, et al. **CD4 depletion in SIV-infected macaques results in macrophage and microglia infection with rapid turnover of infected cells**. *PLoS pathogens* 2014; 10(10):e1004467.

45. Kim WK, Corey S, Alvarez X, Williams K. **Monocyte/macrophage traffic in HIV and SIV encephalitis**. *Journal of leukocyte biology* 2003; 74(5):650-656.

46. Walker JA, Sulciner ML, Nowicki KD, Miller AD, Burdo TH, Williams KC. **Elevated numbers of CD163+ macrophages in hearts of simian immunodeficiency virus-infected monkeys correlate with cardiac pathology and fibrosis**. *AIDS research and human retroviruses* 2014; 30(7):685-694.

47. Williams K, Lackner A, Mallard J. **Non-human primate models of SIV infection and CNS neuropathology**. *Current opinion in virology* 2016; 19:92-98.

48. Hunt RD, Blake BJ, Chalifoux LV, Sehgal PK, King NW, Letvin NL. **Transmission of naturally occurring lymphoma in macaque monkeys**. *Proceedings of the National Academy of Sciences of the United States of America* 1983; 80(16):5085-5089.

49. Strickland SL, Gray RR, Lamers SL, Burdo TH, Huenink E, Nolan DJ, et al. **Significant genetic heterogeneity of the SIVmac251 viral swarm derived from different sources**. *AIDS research and human retroviruses* 2011; 27(12):1327-1332.

50. Gumber S, Amancha PK, Yen PJ, Villinger F, Gabuzda D, Byrareddy SN. **In vivo characterization of macrophage-tropic simian immunodeficiency virus molecular clones in rhesus macaques**. *Journal of neurovirology* 2018; 24(4):411-419.

51. Strickland SL, Gray RR, Lamers SL, Burdo TH, Huenink E, Nolan DJ, et al. **Efficient transmission and persistence of low-frequency SIVmac251 variants in CD8-depleted rhesus macaques with different neuropathology**. *The Journal of general virology* 2012; 93(Pt 5):925-938.

52. Revelo XS, Parthiban P, Chen C, Barrow F, Fredrickson G, Wang H, et al. **Cardiac Resident Macrophages Prevent Fibrosis and Stimulate Angiogenesis**. *Circulation research* 2021; 129(12):1086-1101.

53. Wynn TA, Barron L. **Macrophages: master regulators of inflammation and fibrosis**. *Seminars in liver disease* 2010; 30(3):245-257.

54. Ziegler-Heitbrock L. **Blood Monocytes and Their Subsets: Established Features and Open Questions**. *Front Immunol* 2015; 6:423.

55. Ziegler-Heitbrock L, Ancuta P, Crowe S, Dalod M, Grau V, Hart DN, et al. **Nomenclature of monocytes and dendritic cells in blood**. *Blood* 2010; 116(16):e74-80.

56. Wong KL, Tai JJ, Wong WC, Han H, Sem X, Yeap WH, et al. **Gene expression profiling reveals the defining features of the classical, intermediate, and nonclassical human monocyte subsets**. *Blood* 2011; 118(5):e16-31.

57. Sodora DL, Silvestri G. **Immune activation and AIDS pathogenesis**. *AIDS (London, England)* 2008; 22(4):439-446.

58. Kim WK, Sun Y, Do H, Autissier P, Halpern EF, Piatak M, Jr., et al. **Monocyte heterogeneity underlying phenotypic changes in monocytes according to SIV disease stage**. *Journal of leukocyte biology* 2010; 87(4):557-567.

59. Williams DW, Veenstra M, Gaskill PJ, Morgello S, Calderon TM, Berman JW. **Monocytes mediate HIV neuropathogenesis: mechanisms that contribute to HIV associated neurocognitive disorders**. *Current HIV research* 2014; 12(2):85-96.

60. Ziegler-Heitbrock L. **The CD14+ CD16+ blood monocytes: their role in infection and inflammation**. *Journal of leukocyte biology* 2007; 81(3):584-592.

61. Anzinger JJ, Butterfield TR, Angelovich TA, Crowe SM, Palmer CS. **Monocytes as regulators of inflammation and HIV-related comorbidities during cART**. *Journal of immunology research* 2014; 2014:569819.

62. Kim WK, McGary CM, Holder GE, Filipowicz AR, Kim MM, Beydoun HA, et al. **Increased Expression of CD169 on Blood Monocytes and Its Regulation by Virus and CD8 T Cells in Macaque Models of HIV Infection and AIDS**. *AIDS research and human retroviruses* 2015; 31(7):696-706.

63. Veenstra M, Byrd DA, Inglese M, Buyukturkoglu K, Williams DW, Fleysher L, et al. **CCR2 on Peripheral Blood CD14(+)CD16(+) Monocytes Correlates with Neuronal Damage, HIV-Associated Neurocognitive Disorders, and Peripheral HIV DNA: reseeding of CNS**

reservoirs? *Journal of neuroimmune pharmacology : the official journal of the Society on NeuroImmune Pharmacology* 2019; 14(1):120-133.

64. Veenstra M, León-Rivera R, Li M, Gama L, Clements JE, Berman JW. **Mechanisms of CNS Viral Seeding by HIV(+) CD14(+) CD16(+) Monocytes: Establishment and Reseeding of Viral Reservoirs Contributing to HIV-Associated Neurocognitive Disorders**. *mBio* 2017; 8(5).

65. Muema DM, Akilimali NA, Ndumnego OC, Rasehlo SS, Durgiah R, Ojwach DBA, et al. **Association between the cytokine storm, immune cell dynamics, and viral replicative capacity in hyperacute HIV infection**. *BMC medicine* 2020; 18(1):81.

66. Nowlin BT, Wang J, Schafer JL, Autissier P, Burdo TH, Williams KC. **Monocyte subsets exhibit transcriptional plasticity and a shared response to interferon in SIV-infected rhesus macaques**. *Journal of leukocyte biology* 2018; 103(1):141-155.

67. Pulliam L, Gascon R, Stubblebine M, McGuire D, McGrath MS. **Unique monocyte subset in patients with AIDS dementia**. *Lancet (London, England)* 1997; 349(9053):692-695.

68. Keating SM, Heitman JW, Wu S, Deng X, Stacey AR, Zahn RC, et al. **Magnitude and Quality of Cytokine and Chemokine Storm during Acute Infection Distinguish Nonprogressive and Progressive Simian Immunodeficiency Virus Infections of Nonhuman Primates**. *Journal of virology* 2016; 90(22):10339-10350.

69. Miedema F, Hazenberg MD, Tesselaar K, van Baarle D, de Boer RJ, Borghans JA. **Immune activation and collateral damage in AIDS pathogenesis**. *Front Immunol* 2013; 4:298.

70. Knudsen TB, Ertner G, Petersen J, Møller HJ, Moestrup SK, Eugen-Olsen J, et al. **Plasma Soluble CD163 Level Independently Predicts All-Cause Mortality in HIV-1-Infected Individuals**. *The Journal of infectious diseases* 2016; 214(8):1198-1204.

71. Hasegawa A, Liu H, Ling B, Borda JT, Alvarez X, Sugimoto C, et al. **The level of monocyte turnover predicts disease progression in the macaque model of AIDS**. *Blood* 2009; 114(14):2917-2925.

72. Robertson KR, Smurzynski M, Parsons TD, Wu K, Bosch RJ, Wu J, et al. **The prevalence and incidence of neurocognitive impairment in the HAART era**. *AIDS (London, England)* 2007; 21(14):1915-1921.

73. Burdo TH, Lackner A, Williams KC. **Monocyte/macrophages and their role in HIV neuropathogenesis**. *Immunological reviews* 2013; 254(1):102-113.

74. Burdo TH, Weiffenbach A, Woods SP, Letendre S, Ellis RJ, Williams KC. **Elevated sCD163 in plasma but not cerebrospinal fluid is a marker of neurocognitive impairment in HIV infection**. *AIDS (London, England)* 2013; 27(9):1387-1395.

75. Kamat A, Lyons JL, Misra V, Uno H, Morgello S, Singer EJ, et al. **Monocyte activation markers in cerebrospinal fluid associated with impaired neurocognitive testing in advanced HIV infection**. *Journal of acquired immune deficiency syndromes (1999)* 2012; 60(3):234-243.

76. Williams ME, Stein DJ, Joska JA, Naudé PJW. **Cerebrospinal fluid immune markers and HIV-associated neurocognitive impairments: A systematic review**. *Journal of neuroimmunology* 2021; 358:577649.

77. Guha D, Mukerji SS, Chettimada S, Misra V, Lorenz DR, Morgello S, et al. **Cerebrospinal fluid extracellular vesicles and neurofilament light protein as biomarkers of central nervous system injury in HIV-infected patients on antiretroviral therapy**. *AIDS (London, England)* 2019; 33(4):615-625.

78. Meeker RB, Poulton W, Markovic-Plese S, Hall C, Robertson K. **Protein changes in CSF of HIV-infected patients: evidence for loss of neuroprotection**. *Journal of neurovirology* 2011; 17(3):258-273.

79. González RG, Fell R, He J, Campbell J, Burdo TH, Autissier P, et al. **Temporal/compartmental changes in viral RNA and neuronal injury in a primate model of NeuroAIDS**. *PloS one* 2018; 13(5):e0196949.

80. Abdel-Mohsen M, Chavez L, Tandon R, Chew GM, Deng X, Danesh A, et al. **Human Galectin-9 Is a Potent Mediator of HIV Transcription and Reactivation**. *PLoS pathogens* 2016; 12(6):e1005677.

81. Premeaux TA, Moser CB, McKhann A, Hoenigl M, Laws EI, Aquino DL, et al. **Plasma galectin-9 as a predictor of adverse non-AIDS events in persons with chronic HIV during suppressive antiretroviral therapy**. *AIDS (London, England)* 2021; 35(15):2489-2495.

82. Shete A, Dhayarkar S, Dhamanage A, Kulkarni S, Ghate M, Sangle S, et al. **Possible role of plasma Galectin-9 levels as a surrogate marker of viremia in HIV infected patients on antiretroviral therapy in resource-limited settings**. *AIDS research and therapy* 2020; 17(1):43.

83. Tandon R, Chew GM, Byron MM, Borrow P, Niki T, Hirashima M, et al. **Galectin-9 is rapidly released during acute HIV-1 infection and remains sustained at high levels despite viral suppression even in elite controllers**. *AIDS research and human retroviruses* 2014; 30(7):654-664.

84. Elahi S, Niki T, Hirashima M, Horton H. **Galectin-9 binding to Tim-3 renders activated human CD4+ T cells less susceptible to HIV-1 infection**. *Blood* 2012; 119(18):4192-4204.

85. Saitoh H, Ashino Y, Chagan-Yasutan H, Niki T, Hirashima M, Hattori T. **Rapid decrease of plasma galectin-9 levels in patients with acute HIV infection after therapy**. *The Tohoku journal of experimental medicine* 2012; 228(2):157-161.

86. Premeaux TA, D'Antoni ML, Abdel-Mohsen M, Pillai SK, Kallianpur KJ, Nakamoto BK, et al. **Elevated cerebrospinal fluid Galectin-9 is associated with central nervous system immune activation and poor cognitive performance in older HIV-infected individuals**. *Journal of neurovirology* 2019; 25(2):150-161.

87. Holder GE, McGary CM, Johnson EM, Zheng R, John VT, Sugimoto C, et al. **Expression of the mannose receptor CD206 in HIV and SIV encephalitis: a phenotypic switch of brain perivascular macrophages with virus infection**. *Journal of neuroimmune pharmacology : the official journal of the Society on NeuroImmune Pharmacology* 2014; 9(5):716-726.

88. Williams KC, Corey S, Westmoreland SV, Pauley D, Knight H, deBakker C, et al. **Perivascular macrophages are the primary cell type productively infected by simian immunodeficiency virus in the brains of macaques: implications for the neuropathogenesis of AIDS**. *The Journal of experimental medicine* 2001; 193(8):905-915.

89. Witwer KW, Gama L, Li M, Bartizal CM, Queen SE, Varrone JJ, et al. **Coordinated regulation of SIV replication and immune responses in the CNS**. *PloS one* 2009; 4(12):e8129.

90. Clay CC, Rodrigues DS, Ho YS, Fallert BA, Janatpour K, Reinhart TA, et al. **Neuroinvasion of fluorescein-positive monocytes in acute simian immunodeficiency virus infection**. *Journal of virology* 2007; 81(21):12040-12048.

91. Williams K, Schwartz A, Corey S, Orandle M, Kennedy W, Thompson B, et al. **Proliferating cellular nuclear antigen expression as a marker of perivascular macrophages in simian immunodeficiency virus encephalitis**. *The American journal of pathology* 2002; 161(2):575-585.

92. Kim WK, Alvarez X, Fisher J, Bronfin B, Westmoreland S, McLaurin J, et al. **CD163 identifies perivascular macrophages in normal and viral encephalitic brains and potential precursors to perivascular macrophages in blood**. *The American journal of pathology* 2006; 168(3):822-834.

93. Pulliam L, Clarke JA, McGrath MS, Moore D, McGuire D. **Monokine products as predictors of AIDS dementia**. *AIDS (London, England)* 1996; 10(13):1495-1500.

94. Ratto-Kim S, Chuenchitra T, Pulliam L, Paris R, Sukwit S, Gongwon S, et al. **Expression of monocyte markers in HIV-1 infected individuals with or without HIV associated dementia and normal controls in Bangkok Thailand**. *Journal of neuroimmunology* 2008; 195(1-2):100-107.

95. Filipowicz AR, McGary CM, Holder GE, Lindgren AA, Johnson EM, Sugimoto C, et al. **Proliferation of Perivascular Macrophages Contributes to the Development of Encephalitic Lesions in HIV-Infected Humans and in SIV-Infected Macaques**. *Scientific reports* 2016; 6:32900.

96. Burudi EM, Marcondes MC, Watry DD, Zandonatti M, Taffe MA, Fox HS. **Regulation of indoleamine 2,3-dioxygenase expression in simian immunodeficiency virus-infected monkey brains**. *Journal of virology* 2002; 76(23):12233-12241.

97. Soulas C, Conerly C, Kim WK, Burdo TH, Alvarez X, Lackner AA, et al. **Recently infiltrating MAC387(+) monocytes/macrophages a third macrophage population involved in SIV and HIV encephalitic lesion formation**. *The American journal of pathology* 2011; 178(5):2121-2135.

98. Barbaro G. **Cardiovascular manifestations of HIV infection**. *Circulation* 2002; 106(11):1420-1425.

99. Heidenreich PA, Eisenberg MJ, Kee LL, Somelofski CA, Hollander H, Schiller NB, et al. **Pericardial effusion in AIDS. Incidence and survival**. *Circulation* 1995; 92(11):3229-3234.

100. Barbaro G, Di Lorenzo G, Grisorio B, Barbarini G. **Cardiac involvement in the acquired immunodeficiency syndrome: a multicenter clinical-pathological study. Gruppo Italiano per lo Studio Cardiologico dei pazienti affetti da AIDS Investigators**. *AIDS research and human retroviruses* 1998; 14(12):1071-1077.

101. Cerrato E, D'Ascenzo F, Biondi-Zoccai G, Calcagno A, Frea S, Grosso Marra W, et al. **Cardiac dysfunction in pauci symptomatic human immunodeficiency virus patients: a meta-analysis in the highly active antiretroviral therapy era**. *European heart journal* 2013; 34(19):1432-1436.

102. Schuster C, Mayer FJ, Wohlfahrt C, Marculescu R, Skoll M, Strassl R, et al. **Acute HIV Infection Results in Subclinical Inflammatory Cardiomyopathy**. *The Journal of infectious diseases* 2018; 218(3):466-470.

103. Martin-Iguacel R, Llibre JM, Friis-Moller N. **Risk of Cardiovascular Disease in an Aging HIV Population: Where Are We Now?** *Current HIV/AIDS reports* 2015; 12(4):375-387.

104. Friis-Møller N, Ryom L, Smith C, Weber R, Reiss P, Dabis F, et al. **An updated prediction model of the global risk of cardiovascular disease in HIV-positive persons: The Data-**

collection on Adverse Effects of Anti-HIV Drugs (D:A:D) study. *European journal of preventive cardiology* 2016; 23(2):214-223.

105. Okello S, Asiimwe SB, Kanyesigye M, Muyindike WR, Boum Y, 2nd, Mwebesa BB, et al. **D-Dimer Levels and Traditional Risk Factors Are Associated With Incident Hypertension Among HIV-Infected Individuals Initiating Antiretroviral Therapy in Uganda**. *Journal of acquired immune deficiency syndromes (1999)* 2016; 73(4):396-402.

106. Ford ES, Greenwald JH, Richterman AG, Rupert A, Dutcher L, Badralmaa Y, et al. **Traditional risk factors and D-dimer predict incident cardiovascular disease events in chronic HIV infection**. *AIDS (London, England)* 2010; 24(10):1509-1517.

107. Crane HM, Paramsothy P, Drozd DR, Nance RM, Delaney JA, Heckbert SR, et al. **Types of Myocardial Infarction Among Human Immunodeficiency Virus-Infected Individuals in the United States**. *JAMA cardiology* 2017; 2(3):260-267.

108. Freiberg MS, Chang CC, Kuller LH, Skanderson M, Lowy E, Kraemer KL, et al. **HIV infection and the risk of acute myocardial infarction**. *JAMA internal medicine* 2013; 173(8):614-622.

109. Ntusi N, O'Dwyer E, Dorrell L, Wainwright E, Piechnik S, Clutton G, et al. **HIV-1-Related Cardiovascular Disease Is Associated With Chronic Inflammation, Frequent Pericardial Effusions, and Probable Myocardial Edema**. *Circulation Cardiovascular imaging* 2016; 9(3):e004430.

110. de Leuw P, Arendt CT, Haberl AE, Froadinadl D, Kann G, Wolf T, et al. **Myocardial Fibrosis and Inflammation by CMR Predict Cardiovascular Outcome in People Living With HIV**. *JACC Cardiovascular imaging* 2021; 14(8):1548-1557.

111. Luetkens JA, Doerner J, Schwarze-Zander C, Wasmuth JC, Boesecke C, Sprinkart AM, et al. **Cardiac Magnetic Resonance Reveals Signs of Subclinical Myocardial Inflammation in Asymptomatic HIV-Infected Patients**. *Circulation Cardiovascular imaging* 2016; 9(3):e004091.

112. Yan C, Li R, Guo X, Yu H, Li W, Li W, et al. **Cardiac Involvement in Human Immunodeficiency Virus Infected Patients: An Observational Cardiac Magnetic Resonance Study**. *Frontiers in cardiovascular medicine* 2021; 8:756162.

113. Chistiakov DA, Bobryshev YV, Orekhov AN. **Macrophage-mediated cholesterol handling in atherosclerosis**. *Journal of cellular and molecular medicine* 2016; 20(1):17-28.

114. Hanna DB, Lin J, Post WS, Hodis HN, Xue X, Anastos K, et al. **Association of Macrophage Inflammation Biomarkers With Progression of Subclinical Carotid Artery Atherosclerosis in HIV-Infected Women and Men**. *The Journal of infectious diseases* 2017; 215(9):1352-1361.

115. Kurose H. **Cardiac Fibrosis and Fibroblasts**. *Cells* 2021; 10(7).

116. Lafuse WP, Wozniak DJ, Rajaram MVS. **Role of Cardiac Macrophages on Cardiac Inflammation, Fibrosis and Tissue Repair**. *Cells* 2020; 10(1).

117. Barisione C, Garibaldi S, Ghigliotti G, Fabbi P, Altieri P, Casale MC, et al. **CD14CD16 monocyte subset levels in heart failure patients**. *Disease markers* 2010; 28(2):115-124.

118. Wrigley BJ, Shantsila E, Tapp LD, Lip GY. **CD14++CD16+ monocytes in patients with acute ischaemic heart failure**. *European journal of clinical investigation* 2013; 43(2):121-130.

119. Wynn TA, Ramalingam TR. **Mechanisms of fibrosis: therapeutic translation for fibrotic disease**. *Nature medicine* 2012; 18(7):1028-1040.

120. Stary HC, Chandler AB, Dinsmore RE, Fuster V, Glagov S, Insull W, Jr., et al. **A definition of advanced types of atherosclerotic lesions and a histological classification of atherosclerosis. A report from the Committee on Vascular Lesions of the Council on Arteriosclerosis, American Heart Association**. *Circulation* 1995; 92(5):1355-1374.

121. Zanni MV, Toribio M, Wilks MQ, Lu MT, Burdo TH, Walker J, et al. **Application of a Novel CD206+ Macrophage-Specific Arterial Imaging Strategy in HIV-Infected Individuals**. *The Journal of infectious diseases* 2017; 215(8):1264-1269.

122. Subramanian S, Tawakol A, Burdo TH, Abbara S, Wei J, Vijayakumar J, et al. **Arterial inflammation in patients with HIV**. *Jama* 2012; 308(4):379-386.

123. Yearley JH, Pearson C, Carville A, Shannon RP, Mansfield KG. **SIV-associated myocarditis: viral and cellular correlates of inflammation severity**. *AIDS research and human retroviruses* 2006; 22(6):529-540.

124. Yearley JH, Pearson C, Shannon RP, Mansfield KG. **Phenotypic variation in myocardial macrophage populations suggests a role for macrophage activation in SIV-associated cardiac disease**. *AIDS research and human retroviruses* 2007; 23(4):515-524.

125. Hsue PY, Scherzer R, Hunt PW, Schnell A, Bolger AF, Kalapus SC, et al. **Carotid Intima-Media Thickness Progression in HIV-Infected Adults Occurs Preferentially at the Carotid Bifurcation and Is Predicted by Inflammation**. *Journal of the American Heart Association* 2012; 1(2).

126. Hemkens LG, Bucher HC. **HIV infection and cardiovascular disease**. *European heart journal* 2014; 35(21):1373-1381.

127. Marincowitz C, Genis A, Goswami N, De Boever P, Nawrot TS, Strijdom H. **Vascular endothelial dysfunction in the wake of HIV and ART**. *The FEBS journal* 2018.

128. Rohde D, Nahrendorf M. **Bad company: monocytes in HIV and atherosclerosis**. *Cardiovascular research* 2021; 117(4):993-994.

129. Jaworowski A, Hearps AC, Angelovich TA, Hoy JF. **How Monocytes Contribute to Increased Risk of Atherosclerosis in Virologically-Suppressed HIV-Positive Individuals Receiving Combination Antiretroviral Therapy**. *Front Immunol* 2019; 10:1378.

130. Luo L, Han Y, Song X, Zhu T, Zeng Y, Li T. **CD16-expressing monocytes correlate with arterial stiffness in HIV-infected ART-naive men**. *HIV clinical trials* 2018; 19(2):39-45.

131. Annamalai L, Westmoreland SV, Domingues HG, Walsh DG, Gonzalez RG, O'Neil SP. **Myocarditis in CD8-depleted SIV-infected rhesus macaques after short-term dual therapy with nucleoside and nucleotide reverse transcriptase inhibitors**. *PloS one* 2010; 5(12):e14429.

132. Walker JA, Beck GA, Campbell JH, Miller AD, Burdo TH, Williams KC. **Anti-alpha4 Integrin Antibody Blocks Monocyte/Macrophage Traffic to the Heart and Decreases Cardiac**

Pathology in a SIV Infection Model of AIDS. *Journal of the American Heart Association* 2015; 4(7).

133. White KS, Walker JA, Wang J, Autissier P, Miller AD, Abuelezan NN, et al. **Simian immunodeficiency virus-infected rhesus macaques with AIDS co-develop cardiovascular pathology and encephalitis**. *Front Immunol* 2023; 14:1240946.

134. de Boer RA, Yu L, van Veldhuisen DJ. **Galectin-3 in cardiac remodeling and heart failure**. *Current heart failure reports* 2010; 7(1):1-8.

135. Rabkin SW, Tang JKK. **The utility of growth differentiation factor-15, galectin-3, and sST2 as biomarkers for the diagnosis of heart failure with preserved ejection fraction and compared to heart failure with reduced ejection fraction: a systematic review**. *Heart failure reviews* 2021; 26(4):799-812.

136. Sharma UC, Mosleh W, Chaudhari MR, Katkar R, Weil B, Evelo C, et al. **Myocardial and Serum Galectin-3 Expression Dynamics Marks Post-Myocardial Infarction Cardiac Remodelling**. *Heart, lung & circulation* 2017; 26(7):736-745.

137. Sharma UC, Pokharel S, van Brakel TJ, van Berlo JH, Cleutjens JP, Schroen B, et al. **Galectin-3 marks activated macrophages in failure-prone hypertrophied hearts and contributes to cardiac dysfunction**. *Circulation* 2004; 110(19):3121-3128.

138. Besler C, Lang D, Urban D, Rommel KP, von Roeder M, Fengler K, et al. **Plasma and Cardiac Galectin-3 in Patients With Heart Failure Reflects Both Inflammation and Fibrosis: Implications for Its Use as a Biomarker**. *Circulation Heart failure* 2017; 10(3).

139. Anyfanti P, Gkaliagkousi E, Gavriilaki E, Triantafyllou A, Dolgyras P, Galanopoulou V, et al. **Association of galectin-3 with markers of myocardial function, atherosclerosis, and vascular fibrosis in patients with rheumatoid arthritis**. *Clinical cardiology* 2019; 42(1):62-68.

140. Fitch KV, DeFilippi C, Christenson R, Srinivasa S, Lee H, Lo J, et al. **Subclinical myocyte injury, fibrosis and strain in relationship to coronary plaque in asymptomatic HIV-infected individuals**. *AIDS (London, England)* 2016; 30(14):2205-2214.

141. Gröschel B, Braner JJ, Funk M, Linde R, Doerr HW, Cinatl J, Jr., et al. **Elevated plasma levels of 90K (Mac-2 BP) immunostimulatory glycoprotein in HIV-1-infected children**. *Journal of clinical immunology* 2000; 20(2):117-122.

142. McKibben RA, Margolick JB, Grinspoon S, Li X, Palella FJ, Jr., Kingsley LA, et al. **Elevated levels of monocyte activation markers are associated with subclinical atherosclerosis in men with and those without HIV infection**. *The Journal of infectious diseases* 2015; 211(8):1219-1228.

143. Subramanya V, McKay HS, Brusca RM, Palella FJ, Kingsley LA, Witt MD, et al. **Inflammatory biomarkers and subclinical carotid atherosclerosis in HIV-infected and HIV-uninfected men in the Multicenter AIDS Cohort Study**. *PloS one* 2019; 14(4):e0214735.

144. Mansfield KG, Carville A, Wachtman L, Goldin BR, Yearley J, Li W, et al. **A diet high in saturated fat and cholesterol accelerates simian immunodeficiency virus disease progression**. *The Journal of infectious diseases* 2007; 196(8):1202-1210.

145. Yearley JH, Xia D, Pearson CB, Carville A, Shannon RP, Mansfield KG. **Interleukin-18 predicts atherosclerosis progression in SIV-infected and uninfected rhesus monkeys (Macaca mulatta) on a high-fat/high-cholesterol diet**. *Laboratory investigation; a journal of technical methods and pathology* 2009; 89(6):657-667.

146. Lindegaard B, Hansen AB, Gerstoft J, Pedersen BK. **High plasma level of interleukin-18 in HIV-infected subjects with lipodystrophy**. *Journal of acquired immune deficiency syndromes (1999)* 2004; 36(1):588-593.

147. Wiercinska-Drapalo A, Jaroszewicz J, Flisiak R, Prokopowicz D. **Plasma interleukin-18 is associated with viral load and disease progression in HIV-1-infected patients**. *Microbes and infection* 2004; 6(14):1273-1277.

148. Campbell JH, Burdo TH, Autissier P, Bombardier JP, Westmoreland SV, Soulas C, et al. **Minocycline inhibition of monocyte activation correlates with neuronal protection in SIV neuroAIDS**. *PloS one* 2011; 6(4):e18688.

149. Campbell JH, Ratai EM, Autissier P, Nolan DJ, Tse S, Miller AD, et al. **Anti-alpha4 antibody treatment blocks virus traffic to the brain and gut early, and stabilizes CNS injury late in infection**. *PLoS pathogens* 2014; 10(12):e1004533.

150. Jin X, McGrath MS, Xu H. **Inhibition of HIV Expression and Integration in Macrophages by Methylglyoxal-Bis-Guanylhydrazone**. *Journal of virology* 2015; 89(22):11176-11189.

151. Jin X, Xu H, McGrath MS. **Methylglyoxal-bis-guanylhydrazone inhibits osteopontin expression and differentiation in cultured human monocytes**. *PloS one* 2018; 13(3):e0192680.

152. Burdo THW, J.; Autissier, P.; Miller, A.D.; McGrath, M.S.; Williams, K.C. **An oral form of methylglyoxal-bis-guanylhydrazone stops SIVE**. 2022.

153. Burdo TH, Lo J, Abbara S, Wei J, DeLelys ME, Preffer F, et al. **Soluble CD163, a novel marker of activated macrophages, is elevated and associated with noncalcified coronary plaque in HIV-infected patients**. *The Journal of infectious diseases* 2011; 204(8):1227-1236.

154. Esser S, Gelbrich G, Brockmeyer N, Goehler A, Schadendorf D, Erbel R, et al. **Prevalence of cardiovascular diseases in HIV-infected outpatients: results from a prospective, multicenter cohort study**. *Clinical research in cardiology : official journal of the German Cardiac Society* 2013; 102(3):203-213.

155. Duprez DA, Neuhaus J, Kuller LH, Tracy R, Belloso W, De Wit S, et al. **Inflammation, coagulation and cardiovascular disease in HIV-infected individuals**. *PloS one* 2012; 7(9):e44454.

156. Mesquita EC, Coelho LE, Amancio RT, Veloso V, Grinsztejn B, Luz P, et al. **Severe infection increases cardiovascular risk among HIV-infected individuals**. *BMC infectious diseases* 2019; 19(1):319.

157. Hsue PY, Tawakol A. **Inflammation and Fibrosis in HIV: Getting to the Heart of the Matter**. *Circulation Cardiovascular imaging* 2016; 9(3):e004427.

158. Eggers C, Arendt G, Hahn K, Husstedt IW, Maschke M, Neuen-Jacob E, et al. **HIV-1-associated neurocognitive disorder: epidemiology, pathogenesis, diagnosis, and treatment**. *Journal of neurology* 2017; 264(8):1715-1727.

159. De Francesco D, Verboeket SO, Underwood J, Bagkeris E, Wit FW, Mallon PWG, et al. **Patterns of Co-occurring Comorbidities in People Living With HIV**. *Open Forum Infect Dis* 2018; 5(11):ofy272.

160. De Francesco D, Underwood J, Bagkeris E, Anderson J, Williams I, Vera JH, et al. **Risk factors and impact of patterns of co-occurring comorbidities in people living with HIV**. *AIDS (London, England)* 2019; 33(12):1871-1880.

161. Nanditha NGA, Paiero A, Tafessu HM, St-Jean M, McLinden T, Justice AC, et al. **Excess burden of age-associated comorbidities among people living with HIV in British Columbia, Canada: a population-based cohort study**. *BMJ Open* 2021; 11(1):e041734.

162. Yang X, Zhang J, Chen S, Weissman S, Olatosi B, Li X. **Comorbidity patterns among people living with HIV: a hierarchical clustering approach through integrated electronic health records data in South Carolina**. *AIDS Care* 2021; 33(5):594-606.

163. Jakabek D, Rae CD, Brew BJ, Cysique LA. **Brain aging and cardiovascular factors in HIV: a longitudinal volume and shape MRI study**. *AIDS (London, England)* 2022; 36(6):785-794.

164. Leon R, Reus S, Lopez N, Portilla I, Sanchez-Paya J, Giner L, et al. **Subclinical atherosclerosis in low Framingham risk HIV patients**. *European journal of clinical investigation* 2017; 47(8):591-599.

165. Cheruvu S, Holloway CJ. **Cardiovascular disease in human immunodeficiency virus**. *Internal medicine journal* 2014; 44(4):315-324.

166. Tahsili-Fahadan P, Geocadin RG. **Heart-Brain Axis: Effects of Neurologic Injury on Cardiovascular Function**. *Circulation research* 2017; 120(3):559-572.

167. Anstey KJ, Lipnicki DM, Low LF. **Cholesterol as a risk factor for dementia and cognitive decline: a systematic review of prospective studies with meta-analysis**. *The American journal*

of geriatric psychiatry : official journal of the American Association for Geriatric Psychiatry 2008; 16(5):343-354.

168. Silbert BS, Scott DA, Evered LA, Lewis MS, Maruff PT. **Preexisting cognitive impairment in patients scheduled for elective coronary artery bypass graft surgery**. *Anesthesia and analgesia* 2007; 104(5):1023-1028, tables of contents.

169. Friedman JI, Tang CY, de Haas HJ, Changchien L, Goliasch G, Dabas P, et al. **Brain imaging changes associated with risk factors for cardiovascular and cerebrovascular disease in asymptomatic patients**. *JACC Cardiovascular imaging* 2014; 7(10):1039-1053.

170. Hayden KM, Zandi PP, Lyketsos CG, Khachaturian AS, Bastian LA, Charoonruk G, et al. **Vascular risk factors for incident Alzheimer disease and vascular dementia: the Cache County study**. *Alzheimer disease and associated disorders* 2006; 20(2):93-100.

171. Russo C, Jin Z, Homma S, Elkind MS, Rundek T, Yoshita M, et al. **Subclinical left ventricular dysfunction and silent cerebrovascular disease: the Cardiovascular Abnormalities and Brain Lesions (CABL) study**. *Circulation* 2013; 128(10):1105-1111.

172. Dadu RT, Fornage M, Virani SS, Nambi V, Hoogeveen RC, Boerwinkle E, et al. **Cardiovascular biomarkers and subclinical brain disease in the atherosclerosis risk in communities study**. *Stroke* 2013; 44(7):1803-1808.

173. Newman AB, Fitzpatrick AL, Lopez O, Jackson S, Lyketsos C, Jagust W, et al. **Dementia and Alzheimer's disease incidence in relationship to cardiovascular disease in the Cardiovascular Health Study cohort**. *Journal of the American Geriatrics Society* 2005; 53(7):1101-1107.

174. Avalos CR, Abreu CM, Queen SE, Li M, Price S, Shirk EN, et al. **Brain Macrophages in Simian Immunodeficiency Virus-Infected, Antiretroviral-Suppressed Macaques: a Functional Latent Reservoir**. *mBio* 2017; 8(4).

175. Avalos CR, Price SL, Forsyth ER, Pin JN, Shirk EN, Bullock BT, et al. **Quantitation of Productively Infected Monocytes and Macrophages of Simian Immunodeficiency Virus-Infected Macaques**. *Journal of virology* 2016; 90(12):5643-5656.

176. Ko A, Kang G, Hattler JB, Galadima HI, Zhang J, Li Q, et al. **Macrophages but not Astrocytes Harbor HIV DNA in the Brains of HIV-1-Infected Aviremic Individuals on Suppressive Antiretroviral Therapy**. *Journal of neuroimmune pharmacology : the official journal of the Society on NeuroImmune Pharmacology* 2019; 14(1):110-119.

177. Wright EJ, Grund B, Robertson K, Brew BJ, Roediger M, Bain MP, et al. **Cardiovascular risk factors associated with lower baseline cognitive performance in HIV-positive persons**. *Neurology* 2010; 75(10):864-873.

178. Lipshultz SE, Easley KA, Orav EJ, Kaplan S, Starc TJ, Bricker JT, et al. **Left ventricular structure and function in children infected with human immunodeficiency virus: the prospective P2C2 HIV Multicenter Study. Pediatric Pulmonary and Cardiac Complications of Vertically Transmitted HIV Infection (P2C2 HIV) Study Group**. *Circulation* 1998; 97(13):1246-1256.

179. Antinori A, Giancola ML, Alba L, Soldani F, Grisetti S. **Cardiomyopathy and encephalopathy in AIDS**. *Annals of the New York Academy of Sciences* 2001; 946:121-129.

180. Liang H, Duan Z, Li D, Li D, Wang Z, Ren L, et al. **Higher levels of circulating monocyte-platelet aggregates are correlated with viremia and increased sCD163 levels in HIV-1 infection**. *Cellular & molecular immunology* 2015; 12(4):435-443.

181. Burdo TH, Walker J, Williams KC. **Macrophage Polarization in AIDS: Dynamic Interface between Anti-Viral and Anti-Inflammatory Macrophages during Acute and Chronic Infection**. *Journal of clinical & cellular immunology* 2015; 6(3).

182. Angelovich TA, Trevillyan JM, Hoy JF, Wong ME, Agius PA, Hearps AC, et al. **Monocytes from men living with HIV exhibit heightened atherogenic potential despite long term viral suppression with ART**. *AIDS (London, England)* 2019.

183. D'Antoni ML, Byron MM, Chan P, Sailasuta N, Sacdalan C, Sithinamsuwan P, et al. **Normalization of Soluble CD163 Levels After Institution of Antiretroviral Therapy During Acute HIV Infection Tracks with Fewer Neurological Abnormalities**. *The Journal of infectious diseases* 2018; 218(9):1453-1463.

184. Lyons JL, Uno H, Ancuta P, Kamat A, Moore DJ, Singer EJ, et al. **Plasma sCD14 is a biomarker associated with impaired neurocognitive test performance in attention and learning domains in HIV infection**. *Journal of acquired immune deficiency syndromes (1999)* 2011; 57(5):371-379.

185. Niki T, Fujita K, Rosen H, Hirashima M, Masaki T, Hattori T, et al. **Plasma Galectin-9 Concentrations in Normal and Diseased Condition**. *Cellular physiology and biochemistry : international journal of experimental cellular physiology, biochemistry, and pharmacology* 2018; 50(5):1856-1868.

186. Hirashima M, Kashio Y, Nishi N, Yamauchi A, Imaizumi TA, Kageshita T, et al. **Galectin-9 in physiological and pathological conditions**. *Glycoconjugate journal* 2002; 19(7-9):593-600.

187. deFilippi C, Christenson R, Joyce J, Park EA, Wu A, Fitch KV, et al. **Brief Report: Statin Effects on Myocardial Fibrosis Markers in People Living With HIV**. *Journal of acquired immune deficiency syndromes (1999)* 2018; 78(1):105-110.

188. Noguchi K, Tomita H, Kanayama T, Niwa A, Hatano Y, Hoshi M, et al. **Time-course analysis of cardiac and serum galectin-3 in viral myocarditis after an encephalomyocarditis virus inoculation**. *PloS one* 2019; 14(1):e0210971.

189. Nguyen MN, Su Y, Vizi D, Fang L, Ellims AH, Zhao WB, et al. **Mechanisms responsible for increased circulating levels of galectin-3 in cardiomyopathy and heart failure**. *Scientific reports* 2018; 8(1):8213.

190. He B, Nie Q, Wang F, Han Y, Yang B, Sun M, et al. **Role of pyroptosis in atherosclerosis and its therapeutic implications**. *Journal of cellular physiology* 2021; 236(10):7159-7175.

191. Feria MG, Taborda NA, Hernandez JC, Rugeles MT. **HIV replication is associated to inflammasomes activation, IL-1β, IL-18 and caspase-1 expression in GALT and peripheral blood**. *PloS one* 2018; 13(4):e0192845.

192. Lifson JD, Rossio JL, Piatak M, Jr., Parks T, Li L, Kiser R, et al. **Role of CD8(+) lymphocytes in control of simian immunodeficiency virus infection and resistance to rechallenge after transient early antiretroviral treatment**. *Journal of virology* 2001; 75(21):10187-10199.

193. Hansen SG, Ford JC, Lewis MS, Ventura AB, Hughes CM, Coyne-Johnson L, et al. **Profound early control of highly pathogenic SIV by an effector memory T-cell vaccine**. *Nature* 2011; 473(7348):523-527.

194. Lackner AA, Smith MO, Munn RJ, Martfeld DJ, Gardner MB, Marx PA, et al. **Localization of simian immunodeficiency virus in the central nervous system of rhesus monkeys**. *The American journal of pathology* 1991; 139(3):609-621.

195. Sasseville VG, Lackner AA. **Neuropathogenesis of simian immunodeficiency virus infection in macaque monkeys**. *Journal of neurovirology* 1997; 3(1):1-9.

196. Westmoreland SV, Halpern E, Lackner AA. **Simian immunodeficiency virus encephalitis in rhesus macaques is associated with rapid disease progression**. *Journal of neurovirology* 1998; 4(3):260-268.

197. Wang F, Flanagan J, Su N, Wang LC, Bui S, Nielson A, et al. **RNAscope: a novel in situ RNA analysis platform for formalin-fixed, paraffin-embedded tissues**. *The Journal of molecular diagnostics : JMD* 2012; 14(1):22-29.

198. Yuan Z, Wang N, Kang G, Niu W, Li Q, Guo J. **Controlling Multicycle Replication of Live-Attenuated HIV-1 Using an Unnatural Genetic Switch**. *ACS synthetic biology* 2017; 6(4):721-731.

199. Wang LX, Kang G, Kumar P, Lu W, Li Y, Zhou Y, et al. **Humanized-BLT mouse model of Kaposi's sarcoma-associated herpesvirus infection**. *Proceedings of the National Academy of Sciences of the United States of America* 2014; 111(8):3146-3151.

200. Krebs SJ, Ananworanich J. **Immune activation during acute HIV infection and the impact of early antiretroviral therapy**. *Current opinion in HIV and AIDS* 2016; 11(2):163-172.

201. Milting H, Ellinghaus P, Seewald M, Cakar H, Bohms B, Kassner A, et al. **Plasma biomarkers of myocardial fibrosis and remodeling in terminal heart failure patients supported by mechanical circulatory support devices**. *J Heart Lung Transplant* 2008; 27(6):589-596.

202. Keranov S, Dörr O, Jafari L, Liebetrau C, Keller T, Troidl C, et al. **Osteopontin and galectin-3 as biomarkers of maladaptive right ventricular remodeling in pulmonary hypertension**. *Biomarkers in medicine* 2021; 15(12):1021-1034.

203. Kania G, Blyszczuk P, Eriksson U. **Mechanisms of cardiac fibrosis in inflammatory heart disease**. *Trends in cardiovascular medicine* 2009; 19(8):247-252.

204. Shannon RP, Simon MA, Mathier MA, Geng YJ, Mankad S, Lackner AA. **Dilated cardiomyopathy associated with simian AIDS in nonhuman primates**. *Circulation* 2000; 101(2):185-193.

205. Petkov DI, Liu DX, Allers C, Didier PJ, Didier ES, Kuroda MJ. **Characterization of heart macrophages in rhesus macaques as a model to study cardiovascular disease in humans**. *Journal of leukocyte biology* 2019; 106(6):1241-1255.

206. Fischer-Smith T, Bell C, Croul S, Lewis M, Rappaport J. **Monocyte/macrophage trafficking in acquired immunodeficiency syndrome encephalitis: lessons from human and nonhuman primate studies**. *Journal of neurovirology* 2008; 14(4):318-326.

207. Butterfield TR, Landay AL, Anzinger JJ. **Dysfunctional Immunometabolism in HIV Infection: Contributing Factors and Implications for Age-Related Comorbid Diseases**. *Current HIV/AIDS reports* 2020; 17(2):125-137.

208. Wallis ZK, Williams KC. **Monocytes in HIV and SIV Infection and Aging: Implications for Inflamm-Aging and Accelerated Aging**. *Viruses* 2022; 14(2).

209. Kulkarni M, Bowman E, Gabriel J, Amburgy T, Mayne E, Zidar DA, et al. **Altered Monocyte and Endothelial Cell Adhesion Molecule Expression Is Linked to Vascular Inflammation in Human Immunodeficiency Virus Infection**. *Open Forum Infect Dis* 2016; 3(4):ofw224.

210. Pulliam L, Sun B, Rempel H. **Invasive chronic inflammatory monocyte phenotype in subjects with high HIV-1 viral load**. *Journal of neuroimmunology* 2004; 157(1-2):93-98.

211. Fischer-Smith T, Croul S, Sverstiuk AE, Capini C, L'Heureux D, Regulier EG, et al. **CNS invasion by CD14+/CD16+ peripheral blood-derived monocytes in HIV dementia: perivascular accumulation and reservoir of HIV infection**. *Journal of neurovirology* 2001; 7(6):528-541.

212. Williams DW, Eugenin EA, Calderon TM, Berman JW. **Monocyte maturation, HIV susceptibility, and transmigration across the blood brain barrier are critical in HIV neuropathogenesis**. *Journal of leukocyte biology* 2012; 91(3):401-415.

213. Benjamin LA, Bryer A, Emsley HC, Khoo S, Solomon T, Connor MD. **HIV infection and stroke: current perspectives and future directions**. *Lancet Neurol* 2012; 11(10):878-890.

214. Bryant AK, Moore DJ, Burdo TH, Lakritz JR, Gouaux B, Soontornniyomkij V, et al. **Plasma soluble CD163 is associated with postmortem brain pathology in human immunodeficiency virus infection**. *AIDS (London, England)* 2017; 31(7):973-979.

215. Kelly KM, Tarwater PM, Karper JM, Bedja D, Queen SE, Tunin RS, et al. **Diastolic dysfunction is associated with myocardial viral load in simian immunodeficiency virus-infected macaques**. *AIDS (London, England)* 2012; 26(7):815-823.

216. Kelly KM, Tocchetti CG, Lyashkov A, Tarwater PM, Bedja D, Graham DR, et al. **CCR5 inhibition prevents cardiac dysfunction in the SIV/macaque model of HIV**. *Journal of the American Heart Association* 2014; 3(2):e000874.

217. Lane JH, Sasseville VG, Smith MO, Vogel P, Pauley DR, Heyes MP, et al. **Neuroinvasion by simian immunodeficiency virus coincides with increased numbers of perivascular**

macrophages/microglia and intrathecal immune activation. *Journal of neurovirology* 1996; 2(6):423-432.

218. Torre D, Pugliese A. **Interleukin 18 and cardiovascular disease in HIV-1 infection: a partner in crime?** *AIDS reviews* 2010; 12(1):31-39.

219. Nasi M, De Biasi S, Bianchini E, Digaetano M, Pinti M, Gibellini L, et al. **Analysis of inflammasomes and antiviral sensing components reveals decreased expression of NLRX1 in HIV-positive patients assuming efficient antiretroviral therapy**. *AIDS (London, England)* 2015; 29(15):1937-1941.

220. Triantafilou K, Ward CJK, Czubala M, Ferris RG, Koppe E, Haffner C, et al. **Differential recognition of HIV-stimulated IL-1β and IL-18 secretion through NLR and NAIP signalling in monocyte-derived macrophages**. *PLoS pathogens* 2021; 17(4):e1009417.

221. Lenart N, Brough D, Denes A. **Inflammasomes link vascular disease with neuroinflammation and brain disorders**. *Journal of cerebral blood flow and metabolism : official journal of the International Society of Cerebral Blood Flow and Metabolism* 2016; 36(10):1668-1685.

222. Mazaheri-Tehrani E, Mohraz M, Nasi M, Chester J, De Gaetano A, Lo Tartaro D, et al. **NLRP3 and IL-1β Gene Expression Is Elevated in Monocytes From HIV-Treated Patients With Neurocognitive Disorders**. *Journal of acquired immune deficiency syndromes (1999)* 2021; 86(4):496-499.

223. Mullis C, Swartz TH. **NLRP3 Inflammasome Signaling as a Link Between HIV-1 Infection and Atherosclerotic Cardiovascular Disease**. *Frontiers in cardiovascular medicine* 2020; 7:95.

224. Bonsack F, Sukumari-Ramesh S. **Differential Cellular Expression of Galectin-1 and Galectin-3 After Intracerebral Hemorrhage**. *Frontiers in cellular neuroscience* 2019; 13:157.

225. Lalancette-Hébert M, Swarup V, Beaulieu JM, Bohacek I, Abdelhamid E, Weng YC, et al. **Galectin-3 is required for resident microglia activation and proliferation in response to**

ischemic injury. *The Journal of neuroscience : the official journal of the Society for Neuroscience* 2012; 32(30):10383-10395.

226. Tan Y, Zheng Y, Xu D, Sun Z, Yang H, Yin Q. **Galectin-3: a key player in microglia-mediated neuroinflammation and Alzheimer's disease**. *Cell & bioscience* 2021; 11(1):78.

227. Venkatraman A, Hardas S, Patel N, Singh Bajaj N, Arora G, Arora P. **Galectin-3: an emerging biomarker in stroke and cerebrovascular diseases**. *European journal of neurology* 2018; 25(2):238-246.

228. Di Gregoli K, Somerville M, Bianco R, Thomas AC, Frankow A, Newby AC, et al. **Galectin-3 Identifies a Subset of Macrophages With a Potential Beneficial Role in Atherosclerosis**. *Arteriosclerosis, thrombosis, and vascular biology* 2020; 40(6):1491-1509.

229. Hara A, Niwa M, Kanayama T, Noguchi K, Niwa A, Matsuo M, et al. **Galectin-3: A Potential Prognostic and Diagnostic Marker for Heart Disease and Detection of Early Stage Pathology**. *Biomolecules* 2020; 10(9).

230. Li M, Yuan Y, Guo K, Lao Y, Huang X, Feng L. **Value of Galectin-3 in Acute Myocardial Infarction**. *American journal of cardiovascular drugs : drugs, devices, and other interventions* 2020; 20(4):333-342.

231. López B, González A, Querejeta R, Zubillaga E, Larman M, Díez J. **Galectin-3 and histological, molecular and biochemical aspects of myocardial fibrosis in heart failure of hypertensive origin**. *European journal of heart failure* 2015; 17(4):385-392.

232. Becker JT, Kingsley L, Mullen J, Cohen B, Martin E, Miller EN, et al. **Vascular risk factors, HIV serostatus, and cognitive dysfunction in gay and bisexual men**. *Neurology* 2009; 73(16):1292-1299.

233. Manea MM, Comsa M, Minca A, Dragos D, Popa C. **Brain-heart axis--Review Article**. *Journal of medicine and life* 2015; 8(3):266-271.

234. Falcone EL, Mangili A, Skinner S, Alam A, Polak JF, Wanke CA. **Framingham risk score and early markers of atherosclerosis in a cohort of adults infected with HIV**. *Antiviral therapy* 2011; 16(1):1-8.

235. Schulz CA, Mavarani L, Reinsch N, Albayrak-Rena S, Potthoff A, Brockmeyer N, et al. **Prediction of future cardiovascular events by Framingham, SCORE and asCVD risk scores is less accurate in HIV-positive individuals from the HIV-HEART Study compared with the general population**. *HIV medicine* 2021; 22(8):732-741.

236. Haissman JM, Haugaard AK, Knudsen A, Kristoffersen US, Seljeflot I, Pedersen KK, et al. **Marker of Endothelial Dysfunction Asymmetric Dimethylarginine Is Elevated in HIV Infection but Not Associated With Subclinical Atherosclerosis**. *Journal of acquired immune deficiency syndromes (1999)* 2016; 73(5):507-513.

237. Schechter ME, Andrade BB, He T, Richter GH, Tosh KW, Policicchio BB, et al. **Inflammatory monocytes expressing tissue factor drive SIV and HIV coagulopathy**. *Science translational medicine* 2017; 9(405).

238. Funderburg NT, Zidar DA, Shive C, Lioi A, Mudd J, Musselwhite LW, et al. **Shared monocyte subset phenotypes in HIV-1 infection and in uninfected subjects with acute coronary syndrome**. *Blood* 2012; 120(23):4599-4608.

239. Seta Y, Kanda T, Tanaka T, Arai M, Sekiguchi K, Yokoyama T, et al. **Interleukin 18 in acute myocardial infarction**. *Heart (British Cardiac Society)* 2000; 84(6):668.

240. Funderburg NT, Mayne E, Sieg SF, Asaad R, Jiang W, Kalinowska M, et al. **Increased tissue factor expression on circulating monocytes in chronic HIV infection: relationship to in vivo coagulation and immune activation**. *Blood* 2010; 115(2):161-167.

241. Premeaux TA, Javandel S, Hosaka KRJ, Greene M, Therrien N, Allen IE, et al. **Associations Between Plasma Immunomodulatory and Inflammatory Mediators With VACS Index Scores Among Older HIV-Infected Adults on Antiretroviral Therapy**. *Front Immunol* 2020; 11:1321.

242. Shaked I, Hanna DB, Gleißner C, Marsh B, Plants J, Tracy D, et al. **Macrophage inflammatory markers are associated with subclinical carotid artery disease in women with human immunodeficiency virus or hepatitis C virus infection**. *Arteriosclerosis, thrombosis, and vascular biology* 2014; 34(5):1085-1092.

243. Krautter F, Recio C, Hussain MT, Lezama DR, Maione F, Chimen M, et al. **Characterisation of endogenous Galectin-1 and -9 expression in monocyte and macrophage subsets under resting and inflammatory conditions**. *Biomed Pharmacother* 2020; 130:110595.

244. Cassaglia P, Penas F, Betazza C, Fontana Estevez F, Miksztowicz V, Martínez Naya N, et al. **Genetic Deletion of Galectin-3 Alters the Temporal Evolution of Macrophage Infiltration and Healing Affecting the Cardiac Remodeling and Function after Myocardial Infarction in Mice**. *The American journal of pathology* 2020; 190(9):1789-1800.

245. Takahashi N, Sugimoto C, Allers C, Alvarez X, Kim WK, Didier ES, et al. **Shifting Dynamics of Intestinal Macrophages during Simian Immunodeficiency Virus Infection in Adult Rhesus Macaques**. *J Immunol* 2019; 202(9):2682-2689.

246. Cai Y, Sugimoto C, Arainga M, Midkiff CC, Liu DX, Alvarez X, et al. **Preferential Destruction of Interstitial Macrophages over Alveolar Macrophages as a Cause of Pulmonary Disease in Simian Immunodeficiency Virus-Infected Rhesus Macaques**. *J Immunol* 2015; 195(10):4884-4891.

247. Utay NS, Hunt PW. **Role of immune activation in progression to AIDS**. *Current opinion in HIV and AIDS* 2016; 11(2):131-137.

248. Andersen MN, Hønge BL, Jespersen S, Medina C, da Silva Té D, Laursen A, et al. **Soluble Macrophage Mannose Receptor (sCD206/sMR) as a Biomarker in Human Immunodeficiency Virus Infection**. *The Journal of infectious diseases* 2018; 218(8):1291-1295.

249. Moulignier A, Lamirel C, Picard H, Lebrette MG, Amiel C, Hamidi M, et al. **Long-term AIDS-related PCNSL outcomes with HD-MTX and combined antiretroviral therapy**. *Neurology* 2017; 89(8):796-804.

250. Hsue PY, Ribaudo HJ, Deeks SG, Bell T, Ridker PM, Fichtenbaum C, et al. **Safety and Impact of Low-dose Methotrexate on Endothelial Function and Inflammation in Individuals With Treated Human Immunodeficiency Virus: AIDS Clinical Trials Group Study A5314**. *Clin Infect Dis* 2019; 68(11):1877-1886.

251. Stein JH, Yeh E, Weber JM, Korcarz C, Ridker PM, Tawakol A, et al. **Brachial Artery Echogenicity and Grayscale Texture Changes in HIV-Infected Individuals Receiving Low-Dose Methotrexate**. *Arteriosclerosis, thrombosis, and vascular biology* 2018; 38(12):2870-2878.

252. Durstenfeld MS, Hsue PY. **Mechanisms and primary prevention of atherosclerotic cardiovascular disease among people living with HIV**. *Current opinion in HIV and AIDS* 2021; 16(3):177-185.

253. Rosario-Rodríguez LJ, Colón K, Borges-Vélez G, Negrón K, Meléndez LM. **Dimethyl Fumarate Prevents HIV-Induced Lysosomal Dysfunction and Cathepsin B Release from Macrophages**. *Journal of neuroimmune pharmacology : the official journal of the Society on NeuroImmune Pharmacology* 2018; 13(3):345-354.

254. Cross SA, Cook DR, Chi AW, Vance PJ, Kolson LL, Wong BJ, et al. **Dimethyl fumarate, an immune modulator and inducer of the antioxidant response, suppresses HIV replication and macrophage-mediated neurotoxicity: a novel candidate for HIV neuroprotection**. *J Immunol* 2011; 187(10):5015-5025.

255. Kelly KM, Beck SE, Metcalf Pate KA, Queen SE, Dorsey JL, Adams RJ, et al. **Neuroprotective maraviroc monotherapy in simian immunodeficiency virus-infected macaques: reduced replicating and latent SIV in the brain**. *AIDS (London, England)* 2013; 27(18):F21-28.

256. Zink MC, Uhrlaub J, DeWitt J, Voelker T, Bullock B, Mankowski J, et al. **Neuroprotective and anti-human immunodeficiency virus activity of minocycline**. *Jama* 2005; 293(16):2003-2011.

257. Campbell JH, Ratai EM, Autissier P, Nolan DJ, Tse S, Miller AD, et al. **Anti-α4 antibody treatment blocks virus traffic to the brain and gut early, and stabilizes CNS injury late in infection**. *PLoS pathogens* 2014; 10(12):e1004533.

258. Wang X, Das A, Lackner AA, Veazey RS, Pahar B. **Intestinal double-positive CD4+CD8+ T cells of neonatal rhesus macaques are proliferating, activated memory cells and primary targets for SIVMAC251 infection**. *Blood* 2008; 112(13):4981-4990.

259. Williams K, Burdo TH. **Monocyte mobilization, activation markers, and unique macrophage populations in the brain: observations from SIV infected monkeys are informative with regard to pathogenic mechanisms of HIV infection in humans**. *Journal of neuroimmune pharmacology : the official journal of the Society on NeuroImmune Pharmacology* 2012; 7(2):363-371.

260. Shannon RP. **SIV cardiomyopathy in non-human primates**. *Trends in cardiovascular medicine* 2001; 11(6):242-246.

261. Fisher BS, Green RR, Brown RR, Wood MP, Hensley-McBain T, Fisher C, et al. **Liver macrophage-associated inflammation correlates with SIV burden and is substantially reduced following cART**. *PLoS pathogens* 2018; 14(2):e1006871.

262. Schweitzer F, Tarantelli R, Rayens E, Kling HM, Mattila JT, Norris KA. **Monocyte and Alveolar Macrophage Skewing Is Associated with the Development of Pulmonary Arterial Hypertension in a Primate Model of HIV Infection**. *AIDS research and human retroviruses* 2019; 35(1):63-74.

263. Frunza O, Russo I, Saxena A, Shinde AV, Humeres C, Hanif W, et al. **Myocardial Galectin-3 Expression Is Associated with Remodeling of the Pressure-Overloaded Heart and May Delay the Hypertrophic Response without Affecting Survival, Dysfunction, and Cardiac Fibrosis**. *The American journal of pathology* 2016; 186(5):1114-1127.

264. Ghorbani A, Bhambhani V, Christenson RH, Meijers WC, de Boer RA, Levy D, et al. **Longitudinal Change in Galectin-3 and Incident Cardiovascular Outcomes**. *J Am Coll Cardiol* 2018; 72(25):3246-3254.

265. Martínez-Martínez E, Brugnolaro C, Ibarrola J, Ravassa S, Buonafine M, López B, et al. **CT-1 (Cardiotrophin-1)-Gal-3 (Galectin-3) Axis in Cardiac Fibrosis and Inflammation**. *Hypertension* 2019; 73(3):602-611.

266. Hulsmans M, Sam F, Nahrendorf M. **Monocyte and macrophage contributions to cardiac remodeling**. *Journal of molecular and cellular cardiology* 2016; 93:149-155.

267. Ho DD, Bredesen DE, Vinters HV, Daar ES. **The acquired immunodeficiency syndrome (AIDS) dementia complex**. *Annals of internal medicine* 1989; 111(5):400-410.

268. Li Y, Kang G, Duan L, Lu W, Katze MG, Lewis MG, et al. **SIV Infection of Lung Macrophages**. *PloS one* 2015; 10(5):e0125500.

269. Rubiś P, Holcman K, Dziewięcka E, Wiśniowska-Śmiałek S, Karabinowska A, Szymonowicz M, et al. **Relationships between circulating galectin-3, extracellular matrix fibrosis and outcomes in dilated cardiomyopathy**. *Adv Clin Exp Med* 2021; 30(3):245-253.

270. Ekabe CJ, Clinton NA, Kehbila J, Franck NC. **The Role of Inflammasome Activation in Early HIV Infection**. *Journal of immunology research* 2021; 2021:1487287.

271. Walsh JG, Reinke SN, Mamik MK, McKenzie BA, Maingat F, Branton WG, et al. **Rapid inflammasome activation in microglia contributes to brain disease in HIV/AIDS**. *Retrovirology* 2014; 11:35.

272. Bandera A, Masetti M, Fabbiani M, Biasin M, Muscatello A, Squillace N, et al. **The NLRP3 Inflammasome Is Upregulated in HIV-Infected Antiretroviral Therapy-Treated Individuals with Defective Immune Recovery**. *Front Immunol* 2018; 9:214.

273. Mavian C, Ramirez-Mata AS, Dollar JJ, Nolan DJ, Cash M, White K, et al. **Brain tissue transcriptomic analysis of SIV-infected macaques identifies several altered metabolic**

pathways linked to neuropathogenesis and poly (ADP-ribose) polymerases (PARPs) as potential therapeutic targets. *Journal of neurovirology* 2021; 27(1):101-115.

274. Levine AJ, Horvath S, Miller EN, Singer EJ, Shapshak P, Baldwin GC, et al. **Transcriptome analysis of HIV-infected peripheral blood monocytes: gene transcripts and networks associated with neurocognitive functioning**. *Journal of neuroimmunology* 2013; 265(1-2):96-105.

275. Ehinger E, Ghosheh Y, Pramod AB, Lin J, Hanna DB, Mueller K, et al. **Classical monocyte transcriptomes reveal significant anti-inflammatory statin effect in women with chronic HIV**. *Cardiovascular research* 2021; 117(4):1166-1177.

276. Zanni MV, Awadalla M, Toribio M, Robinson J, Stone LA, Cagliero D, et al. **Immune Correlates of Diffuse Myocardial Fibrosis and Diastolic Dysfunction Among Aging Women With Human Immunodeficiency Virus**. *The Journal of infectious diseases* 2020; 221(8):1315-1320.

277. Yadav A, Kossenkov AV, Knecht VR, Showe LC, Ratcliffe SJ, Montaner LJ, et al. **Evidence for Persistent Monocyte and Immune Dysregulation After Prolonged Viral Suppression Despite Normalization of Monocyte Subsets, sCD14 and sCD163 in HIV-Infected Individuals**. *Pathog Immun* 2019; 4(2):324-362.

278. McCausland MR, Juchnowski SM, Zidar DA, Kuritzkes DR, Andrade A, Sieg SF, et al. **Altered Monocyte Phenotype in HIV-1 Infection Tends to Normalize with Integrase-Inhibitor-Based Antiretroviral Therapy**. *PloS one* 2015; 10(10):e0139474.

279. Lorenz DR, Misra V, Gabuzda D. **Transcriptomic analysis of monocytes from HIV-positive men on antiretroviral therapy reveals effects of tobacco smoking on interferon and stress response systems associated with depressive symptoms**. *Hum Genomics* 2019; 13(1):59.

280. Douglas PS, McCallum S, Lu MT, Umbleja T, Fitch KV, Foldyna B, et al. **Ideal cardiovascular health, biomarkers, and coronary artery disease in persons with HIV**. *AIDS (London, England)* 2023; 37(3):423-434.